AN ABSTRACT OF THE DISERTATION OF

Daniel R. Zamzow for the degree of Doctor of Philosophy in Molecular and Cellular Biology presented on June 10, 2014.

Title: Mechanisms that Influence the Posttranslational Modification of the GluN2B Subunit in the Aged Brain

Abstract approved: _____

Kathy R. Magnusson

Memory is essential to everyday life. As we age, deficits in memory become apparent. The toll of age-related cognitive impairment can be devastating to families and costly to society. The NMDA receptor is a molecule in the brain that is instrumental in the formation of memories. The receptor is particularly vulnerable to the effects of aging. Of the fourteen known subunits, the GluN2B subunit has the greatest effect on memory. The subunit also suffers from the greatest loss of expression due to aging. The present study examines the interactions of GluN2B with other proteins and quantifies the changes in posttranslational modification with age.

Co-immunoprecipitation was used to measure the interaction of GluN2B with the scaffolding molecules PSD-95 and GIPC in synaptosomes from the frontal cortex of behaviorally characterized mice of three ages. The interaction between GluN2A and GluN2B was also measured. There were more PSD-95 and GluN2A molecules per GluN2B with age. The increased PSD-95/GluN2B relationship in old mice was associated with poorer memory. The GIPC/GluN2B relationship also correlated with spatial reference memory. The GluN2B/GluN2A relationship indicated an increase in triheteromeric receptors in the aged mouse, but it did not correlate with memory declines during aging. These results suggest that an age-related increase in PSD-95/GluN2B is detrimental to memory.

Young and old mice were behaviorally characterized and homogenates from the frontal cortex and hippocampus were separated by differential centrifugation followed by lysis in Triton X-100. Western blots containing proteins from each cellular fraction were probed

with antibodies for several proteins in the NMDA receptor complex. There was an age-related increase in p1472 in the synaptic fraction from the frontal cortex and an increase in the 115 kDa calpain-mediated cleavage product of GluN2B in the extrasynaptic fraction of old mice with good reference memory. Fyn was increased and p1336 was decreased in the synaptic membranes of poor learners. The percentage of GluN2B, GluN2A, Fyn, and PSD-95 molecules that were palmitoylated increased in an age-dependent manner in the frontal cortex, but not the hippocampus. The thioesterase, APT1, also had an age-related increase in palmitoylation in the frontal cortex. These results suggest that the palmitoylation cycle may be perturbed in the frontal cortex of aged brains and this may influence further processing of the GluN2B subunit.

In the last study we attempted to lower levels of protein palmitoylation in aged mice by lowering systemic levels of palmitate. Xanthohumol is a flavonoid from hops that increases beta-oxidation in the liver thereby decreasing systemic levels of fatty acids. Mice were fed a diet supplemented with xanthohumol and behaviorally characterized in the Morris water maze. There was a small treatment effect on cognitive flexibility in the young mice, but this appeared to be a recovery from the negative effects of a phytoestrogen-deficient diet. Treatment with xanthohumol significantly lowered levels of palmitate in the plasma of old mice, but palmitoyl-CoA and protein palmitoylation was unaffected. These results suggest that there may be some promise in using xanthohumol for the treatment of metabolic syndrome, but it may not be suitable for lowering levels of protein palmitoylation in the brain.

These results presented in this thesis suggest that an age-related increase in palmitoylation of GluN2B and NMDA receptor effector proteins in the brain may affect the function of neurons in the frontal cortex in two ways. First, increased p1472 enhances clustering of GluN2B-containing NMDA receptors on the synaptic membrane, thereby preserving memory in some old mice. Second, an age-related increase in the calpain-mediated cleavage of GluN2B may eventually lead to increased cell death. Interventions that reduce systemic levels of palmitate may not be effective in treating memory deficits. What is needed is a greater understanding of the mechanisms that govern the palmitoylation cycle in brain in order to design more targeted interventions in the future.

Mechanisms that Influence the Posttranslational Modification of the GluN2B Subunit in the Aged Brain

by
Daniel R. Zamzow

A DISSERTATION

submitted to

Oregon State University

in partial fulfillment of
the requirements for the
degree of

Doctor of Philosophy

Presented June 10, 2014
Commencement June 2015

Doctor of Philosophy dissertation of Daniel R. Zamzow presented on June 10, 2014.

APPROVED:

Major Professor , representing Molecular and Cellular Biology Program

Director of the Molecular and Cellular Biology Program

Dean of the Graduate School

I understand that my dissertation will become part of the permanent collection of Oregon State University libraries. My signature below authorizes release of my dissertation to any reader upon request.

Daniel R. Zamzow, Author

ACKNOWLEDGEMENTS

I would like to thank my mentor Kathy for her patience and guidance.

I would like to thank my lab mates, past and present, Siba Das, Brenna Brim, and Valerie Elias for showing me the ropes. Siba for being a good friend and colleague.

I would like to thank my committee members: Fritz Gombart, Pat Chappell, Jane Ishmael and Susan Tornquist.

I would like to thank the great people at LPI for good science and good times.

I would like to especially thank our collaborators: Fritz Gombart, Donald Jump, Chris Depner, Fred Stevens, LeeCole Legette, and Jaewoo Choi.

I want to thank my family for 44 long years of patience.

Most of all I would like to thank my beautiful wife Noreen. She is my center.

CONTRIBUTION OF AUTHORS

Chapter 1: Written by Daniel R Zamzow and edited by Kathy Magnusson

Chapter 2: Conceptualized by Kathy Magnusson. Experiments performed by and manuscript written by Daniel R Zamzow. Manuscript edited by Kathy Magnusson.

Chapter 3: Conceptualized by Kathy Magnusson and Daniel R Zamzow. Experiments performed and manuscript written by Daniel R Zamzow. Manuscript edited by Kathy Magnusson.

Chapter 4: Conceptualized by Daniel R Zamzow. Experiments performed and manuscript written by Daniel R Zamzow. Manuscript edited by Kathy Magnusson.

Chapter 5: Written by Daniel R Zamzow and edited by Kathy Magnusson.

TABLE OF CONTENTS

LIST OF FIGURES

LIST OF TABLES

Chapter 1
Introduction

Memory

The process of memory is one that organizes, encodes, stores, and recovers information. Memory relies on a network of interconnected functions working together to process information. Two general types of memory are declarative and procedural. Declarative memory is explicit and it involves facts, figures, and information for everyday life. It can be brought to mind and declared verbally or thought of as an image. Declarative memory can be divided into episodic memory, which is time and place specific and semantic memory which is mostly facts and general information (Milner et al., 1998). Procedural memory is implicit. It is involved in the development of skills such as typing, driving, or riding a bike. Declarative memory can further be subdivided into short-term or long-term memory. Long-term or reference memory involves the storage and retrieval of large amounts of information on a time scale of hours to years. Short-term memory is the amount of information that can be held in one's mind for a short period of time often limited to less than an hour (Kandel et al., 1986). One of the original ideas behind short-term memory was a capacity limit. The original theory was that a "magic number" of seven plus or minus two was the limit of short-term memory (Miller, 1956). This meant that an individual could only hold 7+/- 2 objects in one's short-term memory at a time. A type of short-term memory is working memory. Working memory is unique from other short-term memories in that it is specific to planning and carrying out a specific behavior (Baddeley, 2000).

Aging affects many types of memory. Memory scores vary by age and sex, with elderly males suffering the greatest declines in all types of memory (Scherr et al., 1988; Singh-Manoux et al., 2012). Short-term memory for simple tasks declines slightly with age(Baddeley et al., 1991), but the changes for more difficult tasks are more pronounced (Scherr et al., 1988). Several aspects of short-term verbal memory begin to decline as early as the fortieth year of life (Singh-Manoux et al., 2012). The delayed non-matching-to-sample (DNMS) task is an assay that tests working memory. There is a steady decline in performance of the DNMS task of working memory with age (Lyons-Warren et al., 2004). Another type of task that tests for executive function is the Wisconsin card sorting task (WCST). This task tests for error rates in working memory. Humans display an age-related impairment in correct answers during the task (Rhodes, 2004). Trace eyeblink conditioning is a task that tests associative learning. Performance in this task is impaired with age in humans (Finkbiner and Woodruff-Pak, 1991). The retrieval of the

contextual details of episodic memories is also impaired with age (Spencer and Raz, 1995). Semantic memory is also affected by age. Verbal fluency and vocabulary are both diminished in the elderly (Singh-Manoux et al., 2012). These studies all demonstrate that many types of memory are affected by the process of aging. In the studies reported in this thesis, I have used a spatial memory assay to test the effects of aging on declarative memory.

1.2 Spatial memory in the animal model

Spatial cognition involves the relationship of one's self to one's surroundings. As humans we are able to call upon our experiences to help us navigate in the world. We can ask specific questions about where we are, where our house is, or where we may have left our keys. Because we possess the ability to use language and symbols, humans are able to employ maps, diagrams, or written or verbal instructions to reach a destination or find an object (Uttal, 1996; Uttal et al., 2006). Testing spatial memory in animals requires a different approach. This approach involves the use of mazes with spatial cues to obtain information over a number of trials and is designated as spatial reference memory (Olton, 1977). A variety of mazes have been employed to test spatial memory in rodents. The T or Y maze, the Barnes circular maze, the radial arm maze, and the Morris water maze have all been used to test spatial memory in rodents (Paul et al., 2009).

Human studies in spatial navigation have demonstrated an age-related decline in spatial memory (Moffat et al., 2001; Driscoll et al., 2005). Similar age-related vulnerabilities in spatial memory are also present in the rodent maze models such as the T-maze, the Barnes circular maze, and the Morris water maze (Barnes et al., 1980; Ingram, 1988; McLay et al., 1999). Of these tests, the Morris water maze has been used quite extensively in the study of aging and spatial memory (Sharma et al., 2010; Gallagher et al., 2011). The maze is a circular pool that varies in size by the type of rodent used (Brandeis et al., 1989). The addition of a water soluble dye makes the water opaque, visually obscuring a platform that is placed in one quadrant of the pool. Visual cues are placed around the rim of the pool and in the area above and around the pool. The animals are gently placed into the pool farthest away from the platform and they are given a certain time frame in which find the hidden platform. The rodent is allowed to "escape" from the pool when it finds the platform and sits on it for at least 30 seconds in order to help it make a spatial map without the distraction of swimming. This process is

repeated by inserting the rodent into the pool at different quadrants. This type of learning is called place learning. The animal's performance is measured in cumulative proximity to the platform. A lower cumulative proximity is a measure for successful spatial learning. After several repetitions the animal's performance improves and they are able to find the platform in less time and usually a more direct route. Young mice generally outperform older mice during the first few days of this task. By the fourth day of testing the old mice have learned the maze well enough to have comparable scores to young mice. After several repetitions of place learning, the animals are allowed to rest for a period of time no less than one hour. During this time it is believed that the memories of the spatial map begin to consolodate. The rodents then participate in a probe trial. The platform is removed and the rodents are allowed to search for the platform for a certain amount of time. The removal of the platform takes away any chance encounters the rodent may have with the platform. If the rodent has learned where the platform should be, their proximity scores will reflect a bias to the quadrant of the platform.

Many different types of spatial memory can be assessed with the Morris water maze. Spatial reference memory is assessed by examining place trial data (Magnusson, 1998a, b). Cognitive flexibility is examined by moving the platform to the opposite quadrant of the pool where the rodents undergo several place trials followed by a probe trial (Magnusson, 2001). Working memory can be tested by moving the platform after each session, where the animals have a naïve trial followed by a delay trial in the same location (Magnusson et al., 2003). Associative memory is assessed by removing all visual cues from around the pool and the room and allowing the animal to find the platform, which is made visible with a flag. This cued task acts as a control for reference memory learning. If the animals fail to reach the platform during cued trials they are removed from the study. Any animals that have cued scores that are outliers are also removed from the study. The cued trial tests for the animal's motivation, mobility, and visual acuity (Magnusson, 2001; Magnusson et al., 2003). The Morris water maze was used exclusively for the studies in this thesis. Reference and reversal (via place and probe trials), working, and cued memory were assessed during the studies.

1.3 Brain regions and spatial memory

Processing of spatial memory is handled in several regions of the brain (Olton, 1977). The frontal lobe is involved primarily in executive functions and working memory (Kessels et al., 2000). The hippocampus is involved in long-term memory (Kandel, 1997).

Animal studies in the Morris water maze have revealed the importance of each brain region in certain aspects of memory. General performance in the Morris water maze declines after the hippocampus is lesioned (Morris et al., 1982; Morris, 1984). Hippocampal lesions interrupts spatial map making, but not the navigational ability of the animal (Pearce et al., 1998). The dorsal hippocampus appears to be more important to spatial learning than the ventral hippocampus (Moser et al., 1993). The hippocampus is important for acquisition, retrieval, and consolidation and storage of information. Applying an antagonist to the α-amino-3-hydroxy-5-methyl-4-isoxazolepropionic acid receptor (AMPAr) in the hippocampus will diminish performance in the Morris water maze if the drug is applied before or after the place trial indicating the need for the hippocampus in acquisition and retention of information (Riedel et al., 1999). Lesions in the prefrontal cortex will interrupt spatial acquisition in rodents (Mogensen et al., 1995). Prefrontal lesions will also interfere with planning in the Morris water maze (Granon and Poucet, 1995). Damage to the prefrontal cortex will result in impaired short-term memory (Horst and Laubach, 2009). The frontal cortex and the hippocampus were examined in the studies in this thesis.

1.4 Memory and glutamate signaling

Memory relies upon the transmission of signals from one neuron to another in the brain. This transmission is achieved when one neuron (presynaptic) emits neurotransmitters that travel across the synaptic cleft to the postsynaptic neuron. The neurotransmitters bind to their target receptors eliciting a signaling cascade in the postsynaptic neuron. Two of the major neurotransmitters are glutamate and gamma-amino butyric acid (GABA). Glutamate is excitatory, while GABA is inhibitory. The polarity of the neuron at rest is maintained by an imbalance of ions between the cytosol and extracellular space. The inside of neurons have a higher K^+ and lower Na^+ and Ca^{++} concentrations than the outside of the cell. When a neuron becomes stimulated with glutamate it depolarizes, activating the cell, thereby initiating a signaling cascade. The inhibitory molecule GABA, however, deactivates the cell by allowing the influx of Cl^- ions (Kandel et al., 2000). Many types of memory rely on excitatory transmission. When a postsynaptic neuron is stimulated by several pulses of excitatory transmission in synchrony the signal becomes enhanced. This enhanced signal is long-lasting and is known as long-term potentiation (LTP) (Cooke and Bliss, 2006). Induction of LTP is considered to be the primary mechanism of learning and memory (Vitureira and Goda, 2013). A long history of

experimental data has established the N-methyl-D-aspartate receptor (NMDAr) as an essential component of LTP induction in many brain regions (Morris, 2013; Nicoll and Roche, 2013).

NMDAr-dependent LTP begins with the depolarization of the postsynaptic neuron. This occurs when stimulus from glutamate causes AMPA receptors to open. AMPA receptors are permeable to both K^+ and Na^+ ions and opening of the pore allows flow of both ions thereby depolarizing the membrane. The NMDAr pore is blocked by magnesium at rest. Depolarization by AMPA receptor stimulation leads to Mg^{++} being expelled from the pore allowing Ca^{++} ions to flow into the postsynaptic neuron (Kandel et al., 2000). Calcium acts as a secondary messenger which activates calmodulin, which in turn activates several protein kinases such as protein kinase A (PKA), protein kinase C (PKC), and calcium/calmodulin dependent kinase 2 (CAMKII) (Lee, 2006). This signaling cascade leads to the phosphorylation of AMPA receptors stimulating insertion into the synaptic membrane and thereby increasing depolarization (Nicoll and Roche, 2013). These NMDAr-mediated events are the essence of LTP. Induction of the NMDAr leads to enhanced downstream signaling which leads to a long-lasting effect leading to LTP.

The long-lasting effects of NMDAr stimulation occur in the maintenance of LTP through late phase LTP. Activation of PKA, CAMKII, and the mitogen-activated protein kinase (MAPK) pathway leads to the synthesis of new proteins by activating cAMP response element binding protein (CREB) (Lee, 2006; Kandel et al., 2014). The primary difference between short-term and long-term memory is the late phase activation of LTP. Protein expression leads to lasting changes in synaptic plasticity, ensuring long-term communication between neurons. Short-term stimulation will affect only posttranslational modification of proteins, limiting any effects to a matter of minutes to hours.

The NMDAr has been well established in initiating LTP. Because LTP is crucial to learning and memory, the NMDAr is a prime candidate for the study of learning and memory. The work completed in this thesis focuses on the elucidation the functional aspects of the NMDAr in learning and memory.

1.5 The NMDA receptor

The NMDA receptor is an ionotropic glutamate receptor that resides primarily on postsynaptic membranes. It is found in nearly every region of the brain, but it is concentrated in the hippocampus and frontal cortex (Nicoll and Malenka, 1999). The receptor is a calcium channel that is permeable to Na^+ and K^+ ions as well. The receptor

is a heterotetramer composed of seven known subunits: GluN1, GluN2A-D, GluN3A-B. The GluN1 subunits are encoded by a single gene that is alternatively spliced to produce 8 different protein products, referred to as splice variants. The GluN2 subunits all have different functions and are concentrated in different brain regions. GluN2B is highly expressed in the frontal cortex and hippocampus of embryonic neurons, but decreases in expression through development. The GluN2A subunit is concentrated in the hippocampus and frontal cortex as well, but conversely levels of expression increase through development. GluN2D is also highly expressed early in development in more caudal regions of the brain, but declines as the brain matures. GluN3A and 3B are highly expressed in motor neurons with GluN3A having higher levels of expression early in development (Bard and Groc, 2011; Collingridge et al., 2013; Paoletti et al., 2013). Several domains in the different subunits govern the function of the NMDA receptor. Extracellular agonist binding sites allow glycine to bind GluN1 subunits and glutamate to bind GluN2 subunits. Activation of the NMDAr requires simultaneous binding of both agonists. An allosteric binding site in the N-terminal domain of GluN2 subunits allows interaction with antagonists such as Zn^{++} and ifenprodil. At rest, the pore of the NMDAr is blocked by Mg^{++}. The pore can also be blocked by the compounds of MK-801 or memantine. The compound NMDA is an agonist that binds the glutamate site, while CPP antagonizes the same site (Paoletti and Neyton, 2007).

The NMDAr is particularly vulnerable to the aging process. Binding to the glutamate site declines more with age in NMDAr than in AMPA receptors. Binding of glutamate, CPP, or NMDA is decreased in the frontal cortex and hippocampus of aged animals. Age-related changes in binding density at the NMDA binding site seem to be more pronounced in the frontal cortex than in the hippocampus in mice, but may be equal in both regions in rats and dogs. Both mRNA and protein expression levels decline with age in each brain region (Magnusson et al., 2010). A more detailed look at the effects of age on the GluN2B subunit will be discussed in the following sections. Aging studies have shown a clear link to the declines of NMDAr binding and expression and poor memory.

1.6 Extrasynaptic NMDAr

NMDAr are able to diffuse laterally within the membrane and travel between synaptic and extrasynaptic sites (Groc and Choquet, 2006; Groc et al., 2006). Extrasynaptic membranes are membranes on dendrites that are not involved in synaptic transmission

(Parsons and Raymond, 2014). Signaling from extrasynaptic sites has very different outcomes than signals from the synapse. Blocking extrasynaptic NMDAr with the drug memantine while stimulating synaptic NMDAr is a tool used to study the effects of receptor localization on downstream signaling. Overall it has been shown that signaling from the synapse provides stimulus for neuroprotection and growth by enhancing antioxidant defense, increasing CREB phosphorylation and brain-derived neurotrophic factor (BDNF) expression, and increasing extracellular signal-regulated kinase 1/2 (ERK1/2) activation (Hardingham and Bading, 2002; Hardingham et al., 2002; Hardingham and Bading, 2010). When signaling is blocked at the synapse, extrasynaptic NMDAr have the opposite effect. Extrasynaptic NMDAr are involved in the pathophysiology of the animal models of Alzheimer's disease, Huntington disease, and stroke (Milnerwood et al., 2010; Dong et al., 2013; Parsons and Raymond, 2014). It is clear that NMDAr signaling from extrasynaptic sites can have detrimental effects on neuronal survival. What is not known is if there is an increase of extrasynaptic NMDAr during aging and if that increase correlates with learning deficits. The studies in this thesis examine extrasynaptic NMDAr in aged mice to see if they correlate with learning deficits.

1.7 The GluN2B subunit

The subunit that has shown the greatest effect on learning and memory is GluN2B. The importance of the GluN2B subunit became clear when a transgenic mouse was created that overexpressed GluN2B. The mice exhibited greater novel object recognition and fear memory than wild-type mice (Tang et al., 1999). Follow-up studies produced transgenic mice that overexpressed the GluN2B subunit specifically in either the frontal cortex or hippocampus. Transgenic mice overexpressing GluN2B in the frontal cortex had significantly better working memory than wild-type mice (Cui et al., 2011). Transgenic mice overexpressing GluN2B in the hippocampus performed better in the Morris water maze and in novel object recognition than wild-type mice (Wang et al., 2009). Conversely, transgenic GluN2B knockout mice had impaired suckling response leading to death shortly after birth (Kutsuwada et al., 1996). Interestingly, the application of the GluN2B-specific antagonist ifenprodil had no effect on spatial memory in rats in the Morris water maze (Guscott et al., 2003). There was, however, a significant effect of the application of either ifenprodil or Ro-25-6981 on fear learning (Rodrigues et al., 2001; Dalton et al., 2008). The GluN2B subunit promotes LTP, while the GluN2A subunit

promotes long-term depression (LTD) (Yashiro and Philpot, 2008). The differences in LTP and LTD are frequency dependent. LTP occurs when a large stimulation from glutamate occurs during a short time leading to a large influx of Ca^{++} enhancing downstream signaling. LTD, however, occurs when there is a weaker stimulation over a longer period of time which leads to a blunted signal downstream (Malenka and Bear, 2004). The developmental shift from GluN2B to GluN2A subunits leads to a greater number of triheteromeric receptors (GluN1/GluN2A/GluN2B) which increases the incidence of LTD in the adult mouse (Rauner and Kohr, 2011).

The GluN2B subunit, compared to other NMDAr subunits, has the greatest decline in expression with age. In C57BL/6 mice there is a significant decline in mRNA expression in the frontal cortex and parts of the hippocampus (Magnusson, 2000, 2001; Ontl et al., 2004; Magnusson et al., 2006). There are also significant declines in protein expression in the hippocampus and frontal cortex (Magnusson et al., 2002; Ontl et al., 2004; Magnusson et al., 2007; Zhao et al., 2009). The most significant decline in protein expression occurs in the frontal cortex (Zhao et al., 2009). There is also a significant age-related decline in expression of the GluN2B subunit in monkeys and rats (Sonntag et al., 2000; Clayton and Browning, 2001; Clayton et al., 2002; Bai et al., 2004; Dyall et al., 2007; Shi et al., 2007; Coultrap et al., 2008). Increasing the expression of GluN2B in the brains of aged mice improves spatial learning. A viral vector containing the GluN2B transcript was injected into either the hippocampus or frontal cortex of old mice. Spatial learning in the Morris water maze was improved in mice treated with the vector in the frontal cortex or the hippocampus (Brim et al., 2013).

These data indicate the importance of the GluN2B subunit in learning and memory. The subunit is vulnerable to decline due to aging. The memory of old mice can be rescued with the application of GluN2B. The fact that application of a GluN2B-specific antagonist had no effect on spatial learning points to the complexity of cellular dynamics that goes beyond expression level. I have focused my thesis on the understanding of how GluN2B's interaction with other proteins in the aged brain might affect learning.

1.8 The NMDA receptor complex

The C-termini of NMDAr subunits are able to bind to several signaling molecules (Husi et al., 2000). The molecules affect localization, trafficking, posttranslational modification, and function of the receptor. NMDAr are assembled in the endoplasmic reticulum (ER) and trafficked to the dendrites on vesicles (Stephenson et al., 2008). Synapse-

associated protein 97 (SAP97) and calcium/calmodulin-dependent serine protein kinase (CASK) work in concert to guide the receptor to Golgi outposts near dendrites or receptors can follow the normal secretory pathway (Jeyifous et al., 2009). Vesicles containing the receptor then fuse with membranes with the aid of a protein complex containing the kinesin motor KIF-17, mLin-10, and mLin-7 (Bard and Groc, 2011). From there the receptor can diffuse through the membrane to the synaptic, perisynaptic, extrasynaptic sites (Groc and Choquet, 2006; Groc et al., 2009). The scaffolding protein, postsynaptic density protein 95 (PSD-95), enriches the NMDAr on the postsynaptic membrane (Elias and Nicoll, 2007; Xu, 2011; Zheng et al., 2011). PSD-95 binds to GluN1, GluN2A, and GluN2B (Zheng et al., 2011). While binding of PSD-95 to the NMDAr can enhance clustering on postsynaptic membranes, it is not essential to the function of the receptor (Passafaro et al., 1999; Washbourne et al., 2002). PSD-95 preferentially binds to the ESDV motif on the GluN2B C-terminus through its PDZ domain, but recent evidence has shown that it can also bind to a PSDP motif via its SH3 domain (Cousins and Stephenson, 2012). Fyn is a member of the Src-family protein kinase (PTK) that phosphorylates tyrosines on GluN2A and GluN2B (Trepanier et al., 2012). Fyn can bind to PSD-95 thereby increasing its efficiency in phosphorylating GluN2A (Tezuka et al., 1999). The protein phosphorylase striatal-enriched phosphatase 61 (STEP61) binds to and dephosphorylates phosphotyrosine residues on GluN2B (Braithwaite et al., 2006). Calpains bind to and cleave the C-terminus from GluN2 subunits (Guttmann et al., 2001). Another member of the membrane-associated guanylate kinases (MAGUK) family that binds to NMDAr subunits is GAIP-interacting protein, C-terminus (GIPC). GIPC has been shown to preferentially bind to NMDAr on extrasynaptic membranes (Yi et al., 2007).

There is currently very little information of the effects of aging on the aforementioned NMDAr complex proteins. There have been conflicting reports as to the expression of PSD-95 in the aged brain. Synaptosomes from the hippocampus of male Fisher 344X Brown Norway rats had an age-related reduction in PSD-95 protein levels (VanGuilder et al., 2011). In old male Wistar rats there was an increase in immunohistochemistry staining of PSD-95 in the CA1, CA3 and dentate gyrus of the hippocampus for good and bad learners, with bad learners having the most PSD-95 (Nyffeler et al., 2007). STEP61 becomes upregulated in a mouse model of Alzheimer's disease (Kurup et al., 2010). Expression of Calpain 1 is increased in the hippocampus of aged rats (Hajieva et al.,

2009). Although members of the NMDAr complex are important to the operation of the receptor, very little is known about the effects of aging on NMDAr complex proteins. In the studies in this thesis I examined proteins from the NMDAr in young and old brains to ascertain if expression or localization was linked to memory performance in mice.

1.9 Posttranslational modification of GluN2B

The GluN2B subunit can be modified by phosphorylation of tyrosine and serine residues on the C-terminus. To date, six residues have been identified as bona fide sites of phosphorylation: Y1252, Y1336, Y1472, S1303, S1323, and S1480 (Lee, 2006). The tyrosine residues are all phosphorylated by Fyn (Trepanier et al., 2012), serines 1303 and 1323 are phosphorylated by protein kinase C (PKC) (Liao et al., 2001), serine 1303 is phosphorylated by CaMKII (Strack et al., 2000), and serine 1480 is phosphorylated by casein kinase 2 (CK2) (Chung et al., 2004). Phosphorylation of S1303 and S1323 by PKC potentiates NMDAr currents while phosphorylation of S1303 by CaMKII initiates the dissociation of the CaMKII/GluN2B complex (Liao et al., 2001; Liu et al., 2006). There is no known function for p1252, but exposure to hypoxic ischemia will increase levels of p1252 (Knox et al., 2013). The other phosphorylation sites have been well characterized and have implications to this thesis.

Phosphorylation of Y1472 by Fyn deters the binding of the clathrin adapter protein AP2 preventing endocytosis and allowing PSD-95 to bind to the GluN2B subunit (Lavezzari et al., 2003). Mutation of a tyrosine to a phenylalanine at 1472 does not affect the binding of PSD-95 to the GluN2B subunit, therefore p1472 enhances synaptic enrichment of GluN2B-containing receptors by inhibiting endocytosis rather than promote the interaction with PSD-95. GluN2B subunits that are phosphorylated on Y1336 are found predominantly on extrasynaptic membranes (Goebel-Goody et al., 2009). There are a greater number of p1336 subunits found on extrasynaptic membranes early in development than in adulthood (Jiang et al., 2011). Phosphorylation of Y1336 is also a signal for calpain-mediated cleavage of the C-terminus of the GluN2B subunit (Wu et al., 2007). Interestingly, stimulation of the NMDAr will cause the dephosphorylation of p1472, but not p1336 (Ai et al., 2013). Phosphorylation of S1480 is dependent on activation of the NMDAr (Chung et al., 2004; Sanz-Clemente et al., 2010; Sanz-Clemente et al., 2013). Stimulation of the NMDAr will activate CK2, which in concert with CaMKII, phosphorylates S1480 deterring the binding of PSD-95 with GluN2B (Sanz-Clemente et al., 2010; Sanz-Clemente et al., 2013). This leads to rapid internalization of the receptor

and deactivation of the signal.

STEP61 is a phosphatase that dephosphorylates p1336 and p1472 (Braithwaite et al., 2006). Knocking out the gene for STEP61 in mice increases p1472 and enhances memory in the radial arm water maze (Venkitaramani et al., 2011). Interestingly, Fyn knockout mice preserved their spatial memory (Huerta et al., 1996). Levels of p1472 seem to remain steady with age in the rat hippocampus, but increased levels are associated with increased LTP (Coultrap et al., 2008). It is unclear whether the blueberry-induced increase in p1472 enhances memory.

At the molecular level, phosphorylation of GluN2B subunits is essential for proper function. What is not known is how each phosphorylation event contributes to learning and memory. Very little is known about posttranslational modification of the GluN2B subunit in the aged brain. The studies in this thesis examine posttranslational modification of the GluN2B subunit in the age brain.

1.10 Protein palmitoylation

Protein palmitoylation is a posttranslational modification whereby a 16 carbon palmitate is covalently bound to the free sulfhydryl of a cysteine. Palmitate needs to be activated to palmitoyl-CoA in order to be a substrate for palmitoylation (Linder and Deschenes, 2007). Many neuronal proteins involved in synaptic plasticity are palmitoylated (Fukata and Fukata, 2010). Proteins are palmitoylated by palmitoyl acyltransferases (PAT) otherwise known as DHHC enzymes (Greaves and Chamberlain, 2011). Conversely, proteins are depalmitoylated by acyl-protein thioesterases (Conibear and Davis, 2010). A palmitoylation/depalmitoylaton cycle allows for the modulation of signal strength and the recycling of proteins, saving the energy needed for *de novo* synthesis. While many proteins in neuronal cells utilize palmitoylation to enhance their function (el-Husseini Ael and Bredt, 2002; Fukata and Fukata, 2010), some instances of protein palmitoylation do not promote neuronal growth or survival. Infantile neuronal ceroid lipofuscinosis (INCL) is caused by a deficiency in palmitoyl protein thioesterase-1. One of the hallmarks of the disease is an overabundance of palmitoylated vesicular fusion proteins. This diminished level of depalmitoylation does not allow the vesicular proteins to detach from the vesicular membrane after exocytosis to be recycled and used in fresh vesicles (Kim et al., 2008). The AMPA receptor also uses palmitoylation as a negative feedback modulator. When the GluR1-4 subunits of the AMPA receptor are palmitoylated the receptor cannot be inserted into the synaptic membrane. Only through NMDAr-

stimulated depalmitoylation will AMPA receptors be inserted into the synaptic membrane (Hayashi et al., 2005). In pancreatic beta cells excessive protein palmitoylation leads to ER stress and apoptosis (Baldwin et al., 2012). It is clear that unchecked protein palmitoylation can have detrimental effects on cell survival and growth.

Several of the NMDAr complex proteins are palmitoylated. The GluN2 subunits, Fyn, and PSD-95 are all palmitoylated (El-Husseini Ael et al., 2002; Hayashi et al., 2009; Sato et al., 2009). Palmitoylation of the GluN2 subunits enhances interaction with Fyn, increasing p1472 on the GluN2B subunit and deterring internalization of the receptor (Hayashi et al., 2009). Palmitoylation of PSD-95 clusters the protein on synaptic membranes (El-Husseini Ael et al., 2002; Noritake et al., 2009). It is not necessary, however, for PSD-95 to be palmitoylated in order to be found on synaptic membranes (Topinka and Bredt, 1998). Fyn undergoes two lipid modifications: myristoylation and palmitoylation. Mutated Fyn proteins lacking the cysteine needed for palmitoylation have slightly decreased plasma membrane localization (Sato et al., 2009).

Two APT enzymes have been so far identified. APT1 and APT2 have been shown to depalmitoylate certain proteins. APT1 is able to depalmitoylate H-Ras, Synaptosomal-Associated Protein 23 (SNAP23), and the alpha subunit of G-proteins, while APT2 specifically targets growth-associated protein 43 (GAP43) (Kong et al., 2013). Interestingly, both proteins are themselves palmitoylated, with APT1 alone able to depalmitoylate both proteins. Recent evidence indicates that APT1 is mostly cytosolic, but acts as a gatekeeper for protein palmitoylation by residing on the Golgi apparatus to depalmitoylate excess numbers of palmitoylated proteins on the Golgi apparatus (Vartak et al., 2014). It is interesting to note that like the AMPA receptor, both GluN2 subunits and PSD-95 undergo depalmitoylation upon activation of the NMDAr (El-Husseini Ael et al., 2002; Hayashi et al., 2009). This suggests a direct connection between the NMDAr and APT1 activation.

The amyloid precursor protein (APP) is palmitoylated and levels of palmitoylation increase with age (Bhattacharyya et al., 2013). Palmitoylation of APP increases interaction with beta secretase, which may increase production of the neurotoxic Aβ peptide. Because palmitoylation is essential to the function of the NMDAr and its effector proteins I focused on examining the age-related changes in protein palmitoylation to see if they might influence learning and memory.

1.11 Summary

The NMDAr is pivotal in LTP and learning and memory (Morris, 2013; Nicoll and Roche, 2013). The NMDAr is also vulnerable to the effects of aging (Magnusson et al., 2010). Of the NMDAr subunits, GluN2B has displayed the greatest effect on memory. Overexpression of the subunit in mice results in improved learning scores over wild-type mice (Tang et al., 1999; Wang et al., 2009; Cui et al., 2011). Among the NMDAr subunits, GluN2B shows the greatest decline with age in the frontal cortex (Ontl et al., 2004; Magnusson et al., 2007; Zhao et al., 2009). There are also significant age-related declines in the hippocampus (Magnusson et al., 2002). Increasing expression levels of GluN2B in either the hippocampus or frontal cortex in aged mice improved spatial memory (Brim et al., 2013). I have focused the studies in this thesis on GluN2B because of the great effect it has on spatial memory and because it is particularly vulnerable to decline with age.

Subcellular fractionation of homogenates from the hippocampus or the frontal cortex revealed a steady decline of GluN2B expression with age in nearly every fraction (Zhao et al., 2009). There was, however, an apparent increase in GluN2B expression in the light membrane fraction from the frontal cortex alone (unpublished data). This pilot data indicated that the localization of GluN2B-containing NMDAr might be different in the frontal cortex than in the hippocampus. This suggested a mechanism of control that was more involved than simply expression of the protein. It is this reason that I focused on the frontal cortex for the first study. The chapter 2 study used behaviorally tested animals from three age groups in the Morris water maze. In this study I used subcellular fractionation to isolate membranes from synaptosomes as previously described (Dunah and Standaert, 2001). GluN2B-containing NMDAr were enriched with a co-immunoprecipitation assay. The proteins that were co-immunoprecipitated were chosen for analysis based on their known association with GluN2B-containg receptors on either synaptic (PSD-95) or extrasynaptic (GIPC) membranes (Yi et al., 2007; Zheng et al., 2011). We found an age-related increase of the association of GluN2B with PSD-95. The phosphorylation of Y1472 on GluN2B allows PSD-95 to bind versus AP-2 and palmitoylation of GluN2B enhances p1472 via Fyn (Lavezzari et al., 2003; Hayashi et al., 2009). This information coupled with results from our first study lead us to the hypothesis that the posttranslational modification of the GluN2B subunit might be affected by the aging process. In the chapter 3 study, I tested this theory by using differential centrifugation coupled with Triton X-100 solublization of membranes into synaptic and

peri-/extrasynaptic fractions. Both the hippocampus and frontal cortex from behaviorally characterized young and old mice were examined. Expression levels of several of the NMDAr complex and three phospho-GluN2B proteins were examined. A second batch of behaviorally characterized young and old mice was used to test the palmitoylation status of NMDAr complex proteins in both the hippocampus and frontal cortex. Our results indicated that the palmitoylation status of NMDAr complex proteins increased with age in the frontal cortex alone and correlated with poorer learning in age mice.

We then theorized that increased levels of palmitoylation might be due to higher levels of the fatty acid palmitate in aged mice. Evidence has suggested that increased levels of palmitate in the brains of mice are associated with poor performance in the Morris water maze (Yetimler et al., 2012). The rate of acyl-CoA synthesis in the brains of rodents is increased with age (Terracina et al., 1992). Together, these data suggested that lowering plasma palmitate levels might decrease protein palmitoylation and improve learning in old mice. In chapter 4 we tested our theory by using a flavonoid known to decrease plasma fatty acids by increasing beta-oxydation in the liver, xanthohumol (Kirkwood et al., 2013; Legette et al., 2013). We fed a diet supplemented with xanthohumol to young and old mice for 2 months. After behavioral characterization in the Morris water maze, we examined palmitate, palmitoyl-CoA, and palmitoylated proteins from the frontal cortex and hippocampus.

The results of the studies in this thesis will examine the localization of GluN2B subunits and effector proteins in the aged brain. It will show how posttranslational modifications of the GluN2B subunit in the aged brain are associated with good or bad memory. Finally, the results will show if an intervention aimed at reducing systemic levels of palmitate can affect learning and memory in the aged mouse.

An increase in the association of GluN2B containing NMDA receptors with membrane scaffolding proteins was related to memory declines during aging

Daniel R Zamzow, Valerie Elias, Michelle Shumaker, Cameron Larson, Kathy R Magnusson

The Journal of Neuroscience

1121 14th Street, NW, Suite 1010, Washington, DC 20005

24 July 2013, 33(30): 12300-12305

Abstract

The *N*-methyl-D-aspartate (NMDA) receptor is an important component of spatial working and reference memory. The receptor is a heterotetramer composed of a family of related subunits. The GluN2B subunit (GluN2B) of the NMDA receptor appears to be essential for some forms of memory and is particularly vulnerable to change with age in both the hippocampus and cerebral cortex. GluN2B expression is particularly reduced in frontal cortex synaptic membranes. The current study examined the relationship between spatial cognition and protein-protein interactions of GluN2B-containing NMDA receptors in frontal cortex crude synaptosomes from 3, 12 and 26 month old C57BL/6 mice. Aged mice showed a significant decline in spatial reference memory and reversal learning from both young and middle-aged mice. Co-immunoprecipitation of GluN2B subunits revealed an age-related increase in the ratio of both postsynaptic density-95 (PSD-95) and the GluN2A subunit to the GluN2B subunit. Higher ratios of PSD-95/GluN2B and GAIP-interacting protein, C terminus (GIPC)/GluN2B were associated with poorer learning index scores across all ages. There was a significant correlation between GIPC/GluN2B and PSD-95/GluN2B ratios, but PSD-95/GluN2B and GluN2A/GluN2B ratios did not show a relationship. These results suggest that there were more triheteromeric (GluN2B/GluN2A/GluN1) NMDA receptors in older mice than in young adults, but this did not appear to impact spatial reference memory. Instead, an increased association of GluN2B-containing NMDA receptors with synaptic scaffolding proteins in aged animals may have contributed to the age-related memory declines.

Introduction

One of the hallmarks of aging is cognitive decline. Spatial memory, the detailed recollection of one's surroundings, is critical for navigating through everyday life and exhibits a significant decline with age (Gallagher, Burwell et al. 1993). Age-related spatial memory impairments in rodents are similar to those seen in humans and, as such, rodents have provided a suitable model for testing (Barnes, 1979).

The *N*-methyl-D-aspartate (NMDA) receptor is an ionotropic glutamate receptor that is essential for spatial memory tasks (Morris et al., 1986). The NMDA receptor is believed to be a tetramer consisting of several different subunits: GluN1, GluN2A-D, and GluN3A-B. Developmentally, GluN1, GluN2B and GluN3A subunits all decrease with age to adulthood, while GluN2A and GluN3B subunits increase during development (Low and Wee, 2010). The NMDA subunit that may be the most essential for learning and memory

is the GluN2B subunit. Transgenic mice that overexpressed the GluN2B subunit in the cortex or hippocampus showed a significant improvement in several forms of memory (Tang et al., 1999; Cui et al., 2011). Conversely, injections of the GluN2B subunit-specific antagonist, ifenprodil, or siRNA directed against the GluN2B subunit resulted in significant impairment of fear memory (Zhao et al., 2005).

The NMDA receptor is particularly vulnerable to change during aging, showing a decrease in binding density in the cerebral cortex and hippocampus (Muller et al., 1994). Decreases in NMDA receptor binding in the frontal cortex and hippocampus of aged animals are associated with poorer spatial memory (Scheuer et al., 1995). The greatest effects due to age on the NMDA receptor are evident in both mRNA and protein expression of GluN2B subunits in the cerebral cortex and hippocampus (Magnusson, 2000; Magnusson et al., 2002). However, aged mice also show a greater decline in protein expression of GluN2B in the synaptic membrane than in the tissue as a whole in the frontal cortex (Zhao et al., 2009), suggesting an additional effect of aging beyond subunit production.

PSD-95 is a member of the membrane associated guanylate kinase (MAGUK) family of proteins, which act as scaffolding molecules in glutamatergic synapses (Xu, 2011). NMDA receptors are concentrated and held at synapses by PSD-95 (Roche et al., 2001; Xu, 2011). Like the GluN2B subunit, protein expression of PSD-95 is diminished with age in the hippocampus of rats (VanGuilder et al., 2010). Though less characterized in neurons as compared to other MAGUK proteins, GAIP-interacting protein, C-terminus (GIPC) has been shown to interact with GluN2-containing NMDA receptors preferentially on extrasynaptic membranes (Yi et al., 2007). In the current study, we assessed the spatial reference memory of C57BL/6 mice of three different ages and quantified the interaction of GluN2B subunit with associated proteins in the frontal cortex.

Methods

Animals

A total of 304 male C57BL/6 mice from three age groups (3, 12 and 26 months of age) were used for the study. The older two ages were obtained from National Institute on Aging, NIH. Young mice were purchased from JAX mice (Bar Harbor, MA), which stocks the NIH colony. They were fed *ad libitum* and housed under 12/12 h light/dark cycle. Animals were randomly divided into two behavioral groups; naïve and behaviorally tested, with 48-56 animals in each age/behavioral group. Animals in the behaviorally

tested group were subjected to a learning experience with the use of the Morris water maze during the 12 h light cycle, as described below. Animals in the naïve group were housed for the same amount of time as the behaviorally tested animals. After the behavioral testing, all animals were euthanized by exposure to CO_2 and decapitated. The brains were harvested, frozen in dry ice and stored at −80ºC.

Behavioral testing

Spatial reference memory, cognitive flexibility and associative memory (cued control task) were tested with the use of the Morris water maze as previously described (Das et al., 2012). Briefly, for the first two days, mice were acclimated to the water maze, followed by 2 days of testing for spatial reference memory, 1 day of reversal training to test cognitive flexibility and 1 day of associative memory testing (cued control task). Place and probe trials were conducted in the presence and absence of the platform, respectively. There was a 1 hour rest period after every 4 place trials and 2 minute inter-trial intervals between the other place trials.

Tissue subfractionation and lysis

Biochemical fractionation of the frontal cortex (rostral 4 mm of cortex) was performed as previously described (Dunah and Standaert, 2001), with a few modifications. Briefly, tissue was homogenized on ice with a Dounce homogenizer in TE buffer (10mM Tris–HCl, pH 7.4, 1mM EDTA, 1mM EGTA) plus 320mM sucrose and protease inhibitor cocktail (Sigma). Homogenate was centrifuged at 4°C 1000 x g for 10 min and the resulting pellet (P1) was discarded. The supernatant (S1) was centrifuged at 4°C 10600 x g for 20 min to produce the crude synaptosome pellet, P2. The P2 was resuspended in 150μl of DOC buffer (50 mM Tris-HCl, pH 9.0, 1% sodium deoxycholate and protease inhibitor cocktail) and lysed at 37°C for 45 min followed by addition of IP buffer (50 mM Tris-HCl, pH 7.4, 1mM EDTA, 1mM EGTA, 150 mM NaCl ,1% Triton X-100 and protein inhibitor cocktail) and incubated while rotating at 4°C. The total lysate was precleared with 100 µl of 50:50 Protein A/G agarose bead slurry in IP buffer for 1 hr while rotating at 4°C. Protein determinations were made with Bio-Rad DC Protein Assay (Bio-Rad Laboratories). In order to have enough protein for 3 precipitation replicates, 4 lysed samples of like age and behavioral group were pooled based on similarity of learning index (see data analysis) for N=11-14.

Immunoprecipitation

A total of 500 μg of lysed P2 was diluted in IP buffer to 500μl. Diluted samples were

incubated with 5 μl of GluN2B antibody (NeuroMab) while rotating for 36 hrs at 4°C and precipitated by incubation with Protein A/G agarose beads (Santa Cruz) for 2 hrs at 4°C. Precipitated proteins were released from the beads by heating to 95°C for 5 min in Laemmli sample buffer.

Western blot

Sodium dodecyl sulfate–poly acrylamide gel electrophoresis (7.5%) was used for Western blotting as described previously (Zhao et al., 2009). Each gel contained 4 different μg loads (1.5, 3, 6 and 12μg/well) of standards obtained from crude synaptosomes prepared from combined caudal cortices from all naïve young animals. Protein samples from different age/treatment groups were loaded on each gel and analyzed in triplicate. Proteins were transferred to PVDF membranes and incubated overnight at 4°C in one of the following primary antibodies: GluN2B (Millipore), GluN2A or GIPC (Santa Cruz), PSD-95 (ThermoScientific), or GAPDH (Calbiochem). Membranes were rinsed and incubated in fluorescence-based secondary antibody (Rockland Immunochemicals). Bands were visualized by scanning in the LI-COR Odyssey imager.

Data analysis

Data for behavioral testing were analyzed as previously described (Das et al., 2012). Cumulative proximity measures, which reflect search distance from the platform, were used for the place, reversal and cued trials and average proximity and learning index (calculated for probe trials 0-2), which reflects development of a spatial bias, were used for probe trials (Gallagher et al., 1993). Repeated measures ANOVAs and Fisher's protected LSD were performed using data from individual animals. Brain tissue from four animals, with similar learning index scores (Fig. 2.1E), were combined for protein assessment. Behavioral data was averaged for each combination of 4 animals to provide a single value for use in correlational analysis with the protein results. Protein blots were analyzed using Li-Cor Odyssey software. Integrated intensity measures were obtained using median background subtraction method. A standard curve was obtained using a linear fit with Prism 4.0 software (GraphPad Software Inc.) from integrated intensity values for known loads of caudal cortex. Sample values were interpolated from the standard curve as caudal cortex equivalents. Because the GIPC in the crude synaptosomes was not measurable in the standard loads, GAPDH was used to create a standard curve to calculate total GIPC coimmunoprecipated with GluN2B. Each protein

coimmunoprecipitated with GluN2B was expressed as a ratio of protein/GluN2B. Statistical analyses for both behavioral trials and protein expression were done with analysis of variance (ANOVA) followed by Fisher's protected least significant difference using Statview software (SAS Institute). Post-hoc analyses of differences between each age group were planned based on previous studies of NMDA receptor aging. Pearson's correlation coefficients were calculated to assess the relationships between different protein precipitation ratios and reference memory (learning index).

Results

Behavioral testing

There was a significant effect of age on cumulative proximity in blocks of 2 place trials for spatial reference ($F_{(2,157)}$=52.2, p<.0001) and reversal ($F_{(2,157)}$=11.3, p<.0001; Fig. 2.1A,B) learning trials. The 26-month-old mice had significantly higher cumulative proximities in both spatial learning and reversal trials than both 3- and 12-month-old mice (p≤ 0.0007; Fig. 2.1A,B). High proximity scores indicate more time spent away from the platform. There was a significant effect of age on average proximity in probe trials 0-2 ($F_{(2,157)}$=48.7, p<.0001; Fig. 2.1C) and learning index scores ($F_{(2,157)}$=47; p<.0001; Fig. 2.1D) for spatial reference memory, with each older age group having significantly higher scores than each younger (p<.0001). The distribution of learning index scores for the groups of four animals that were combined for protein analysis is shown in Fig. 2.1E. There was no significant effect of age on cumulative proximity in the cued trials ((F2,157)=2.2, p=.12; Fig. 2.1F).

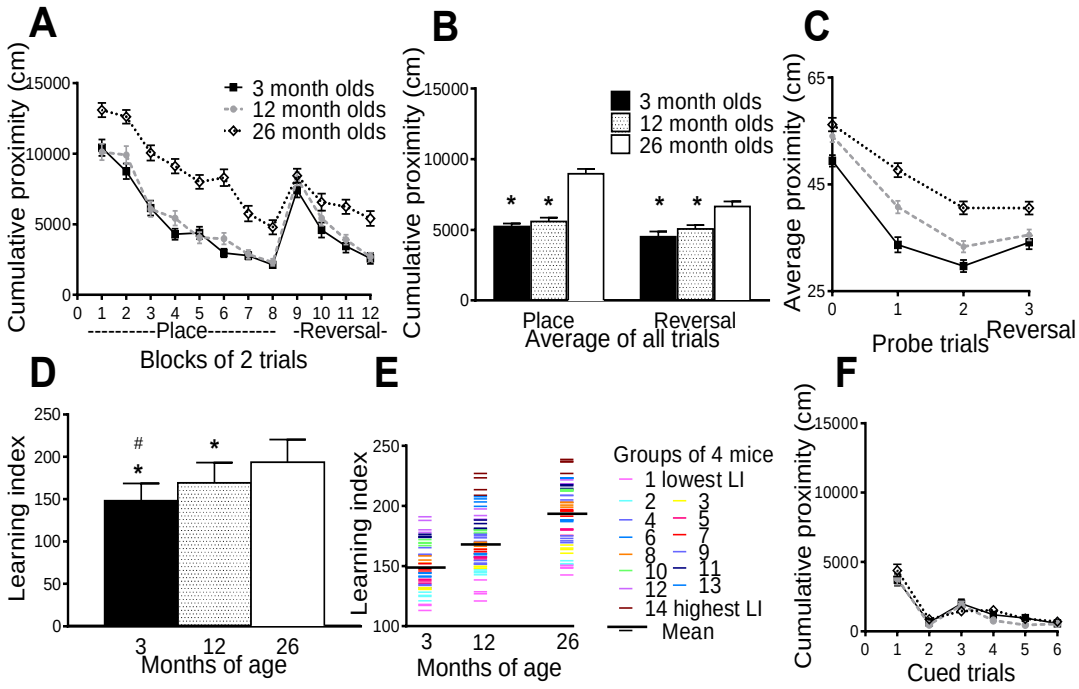

Figure 2.1. Effects of age on performance in memory tasks. A-C) Performance for three ages, averaged across individual mice, for blocks of 2 place and reversal trials (A) and averaged trials (B) for spatial reference memory and cognitive flexibility, respectively; probe trials (C) and learning index scores derived from probe trials (D) for spatial reference memory, and cued control trials (F) in the water maze. E) Distribution of learning index scores for individual mice within the groups of 4 mice that were combined for protein analysis. Each group is represented by a different color. $p < .05$ for difference from 12 (#) and 26 (*) month olds. N = 48-56. Data = mean ± SEM.

Age-related changes in protein associations with GluN2B

In order to determine whether GluN2B-containing NMDA receptors have a different membrane localization in aged mice, GluN2B antibodies were used to co-immunprecipitate PSD-95, GIPC, and GluN2A from crude frontal cortex synaptosomal preparations of 3-, 12- and 26-month old mice (Fig. 2.2A). The behaviorally tested and naïve animals did not differ significantly in the relative amount of each protein co-immunoprecipitated with GluN2B (p=.46-.97; data not shown), therefore we concentrated only on animals that were behaviorally characterized for this report. The amount of GluN2B precipitated from frontal cortex lysates showed a near-significant overall effect of age ($F_{(2,34)}$=2.847,p=.07; Fig. 2.2B). There was significantly less GluN2B precipitated from the 26-month-old mice than the 3 month olds (p = .02; Fig. 2.2B). There was a significant

main effect of age on the ratio of PSD-95/GluN2B ($F_{(2,31)}$=8.994,p=.0007;Fig. 2.2C) and a near-significant main effect of age on the GluN2A/GluN2B ratio ($F_{(2,31)}$=2.64,p=.08;Fig. 2.2D), but not

for GIPC/GluN2B ($F_{(2,34)}$=.832,p=.44;Fig. 2.2E). There was a significantly higher ratio of PSD-95/GluN2B in the 26-month-old mice as compared to both the 3 and 12 month olds (p = .0003;Fig. 2.2C). Analysis of GluN2A/GluN2B ratios showed a significant increase with age between 3- and 26-month old mice (p=.03;Fig. 2.2D).

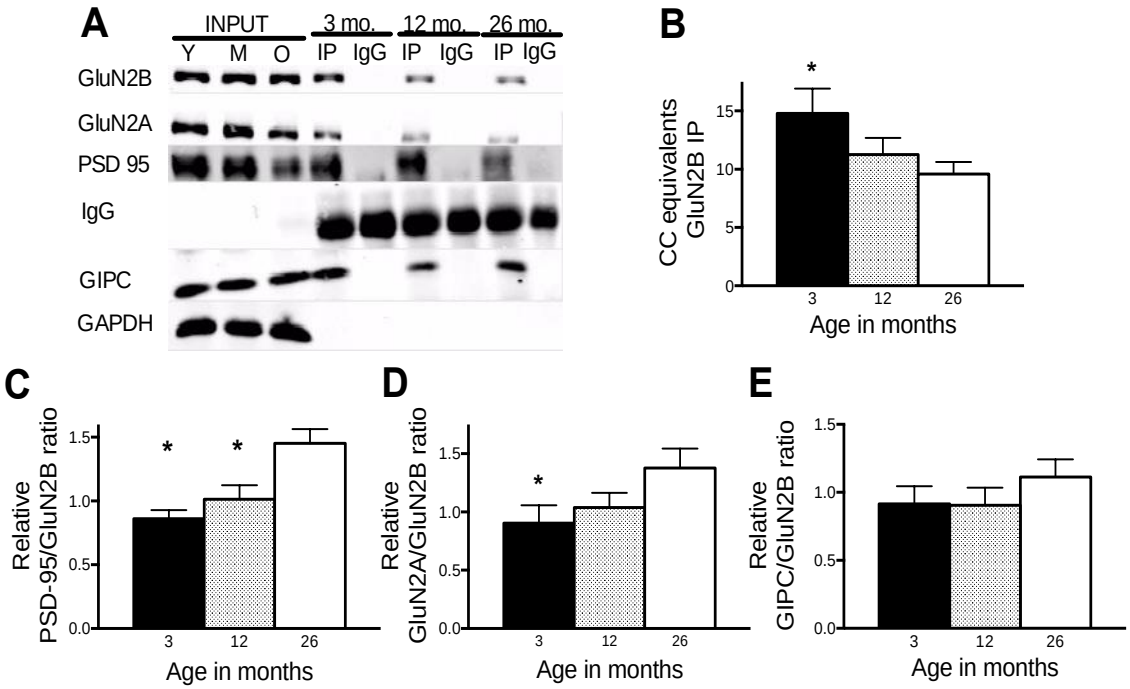

Figure 2.2. Significant changes in PSD-95/GluN2B and GluN2A/GluN2B relative ratios with age. A) Representative blot of proteins co-immunoprecipitated with GluN2B subunit. B) Amount of GluN2B subunit immunoprecipitated declined significantly with age. (C-E) There were significant age-related increases in PSD-95 (C) and GluN2A (D) when co-IP with GluN2B subunit, but not with GIPC (E; p=0.38). Y=young, M=middle age, O=old. Input= 10% of IP lysate. IP is GluN2B subunit immunoprecipitated proteins. IgG is nonspecific mouse IgG control. * p< .05 for difference from 26 month olds. N=11-14. Data = mean ± SEM.

Relationships between protein associations and memory

Pearson's correlation coefficients were calculated for the learning index scores in all three age groups and the ratios of proteins co-immunoprecipitated with GluN2B from combined brains. We were able to replicate past work by significantly correlating the amount of GluN2B precipitated with learning index scores across all ages (p<.0001;Fig. 2.3A)(Magnusson et al., 2007). Lower amounts of GluN2B precipitated were associated

with higher (poorer) learning index scores (Fig. 2.3A). Correlational analysis of PSD-95/GluN2B ratios to learning index scores revealed that a significantly greater number of PSD-95 proteins interact with GluN2B in animals with higher learning index scores across all ages (p=.001;Fig. 2.3B). Although there was no significant increase in the GIPC/GluN2B ratio with age, there was a significant correlation between the protein ratio and learning index scores across all ages (p=.003;Fig. 2.3C). Higher GIPC/GluN2B ratios were associated with higher learning index scores. Because PSD-95 preferentially binds to GluN2A (Xu, 2011), we tested the hypothesis that increased association of PSD-95 with age might be due to an increase in triheteromeric (GluN1/GluN2A/GluN2B) NMDA receptors.

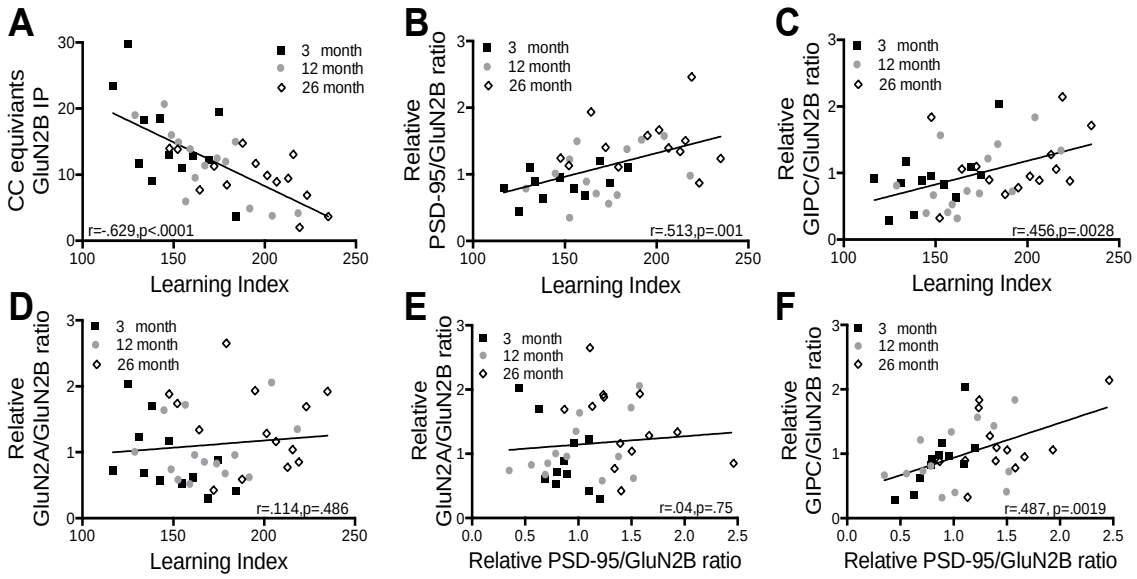

Figure 2.3. Correlation of GluN2B subunit complex proteins with spatial reference memory task. Significant correlations between learning indices and relative amounts of GluN2B immunoprecipitated (A) or the ratios of PSD-95/GluN2B (B) or GIPC/GluN2B (C) co-immunoprecipitated. GluN2A/GluN2B ratios did not correlate with learning index (D) or PSD-95/GluN2B ratios (E). (F) GIPC/GluN2B ratios correlated positively with PSD-95/GluN2B ratios N=11-14. Data points are combinations of 4 brains within each of three age groups. r=Pearson correlation coefficient.

There was no significant correlation between learning index scores and GluN2A/GluN2B ratios (p=.48;Fig. 2.3D). This suggested that although the GluN2A/GluN2B ratios increased with age, the age-related memory deficits were related more to the relationship between PSD-95 and GluN2B, not between PSD-95 and GluN2A. To test this idea, we analyzed the correlation between GluN2A/GluN2B and PSD-95/GluN2B and found no significance (p=.56; Fig. 2.3E). We then looked at the correlation between GIPC/GluN2B and PSD-95/GluN2B. There was a significant positive correlation between the two ratios in combined brains across all ages (p=.0019; Fig. 2.3F).

Discussion

In this study we demonstrated that GluN2B and PSD-95 precipitated together to a greater degree in aged mice than in young mice. This increased interaction was significantly correlated with poorer performance in a spatial reference memory task, as assessed by the Morris water maze. We also found that an increased association of GIPC and GluN2B was related to a reduction in spatial reference memory across all ages. Finally, although the GluN2A/GluN2B ratio increased with age, suggesting that there was an increase in triheteromeric receptors with increased age, there was no relationship to spatial reference memory.

The GluN2A/GluN2B ratio increased significantly with age between the young and old mice, suggesting that there was an increase in triheteromeric receptors in the synaptic environment of aged mice. This is consistent with electrophysiological results from oocytes injected with mRNA from the frontal cortex of young or old mice; increased sensitivity to Mg^{++} and a switch to more low affinity ifenprodil sites in old mice fits with a shift to increased GluN2A association with GluN2B (Kuehl-Kovarik et al., 2000). An increase in triheteromeric receptors could also account for the greater decline in GluN2B seen in the synaptic membrane than the tissue as a whole in previous work (Zhao et al., 2009). Recent evidence indicates that triheteromeric receptors predominate in the hippocampus of young adult mice (Rauner and Kohr, 2011). Our data suggested that, rather than just having a loss of GluN2B-containing NMDA receptors during aging in the frontal cortex, there was an increase in prevalence of triheteromeric receptors across

adult aging (Fig. 2.4a,e). GluN2A is less mobile in synapses than GluN2B and is found mostly at the PSD, while GluN2B is often extrasynaptic (Barria and Malinow, 2002; Groc et al., 2006). The presence of both subunits may mean that triheteromeric receptors can be localized to extrasynaptic, as well as, synaptic membranes in aged animals (Fig. 2.4a,e), which could also contribute to age-related declines in GluN2B subunits in the synaptic membrane (Zhao et al., 2009).

There was no significant relationship between GluN2A/GluN2B ratios and spatial reference memory. Nor was there a correlation between GluN2A/GluN2B and PSD-95/GluN2B ratios, suggesting that there was an additional increased PSD-95/GluN2B interaction that was not accounted for by PSD-95 binding GluN2A. Although PSD-95 is predominantly localized near the synaptic membrane (Xu, 2011), this increased association of GluN2B with PSD-95 did not enhance spatial reference memory. A new report has found an additional binding site for PSD-95 on GluN2A and GluN2B C-terminal tails and implies that the ratio of PSD-95 to GluN2 subunit may not be 1:1, but, because PSD-95 can dimerize, could be as high as 4:1 (Cousins and Stephenson, 2012). In the hippocampus, a 40% loss of synaptic GluN2B expression associated with aging is not matched by the 15% loss in PSD-95 expression, suggesting a greater effect of aging on the NMDA subunit (Magnusson et al., 2002; VanGuilder et al., 2010). The age-related decline in GluN2B expression in the synaptic membrane in frontal cortex may result in more molecules of PSD-95 binding to each GluN2B subunit than is seen in younger animals (Fig. 2.4b). PSD-95 is also able to cluster 2-amino-3-hydroxy-5-methyl-4-isoxazole proprionic acid (AMPA) receptors via the scaffolding protein Stargazin, but there is evidence that Stargazin preferentially binds PSD-93 while PSD-95 has a higher affinity for GluN2A (Stiffler et al., 2006; Elias and Nicoll, 2007). The increased association of PSD-95 to NMDA receptors may alter AMPA receptor clustering during aging, however, PSD-93 may act in a compensatory manner.

Data has shown that PSD-95 is able to concentrate NMDA receptors at the synapse (Roche et al., 2001). However, NMDA receptors are able to cluster on new synapses without PSD-95 (Washbourne et al., 2002), and blocking the ability of PSD-95 to cluster has no effect on NMDA receptor localization at synapses (Passafaro et al., 1999). Similarly, the synaptic localization of NMDA receptors was unaffected in PSD-95 mutant mice that displayed deficits in synaptic plasticity and spatial learning (Migaud et al., 1998). PSD-95 can enhance NMDA receptor clustering, but it seems that it is not

necessary for proper localization of receptors, so it is not clear that the ability of PSD-95 to concentrate NMDA receptors to the synapse is directly responsible for the memory declines during aging.

Higher GIPC/GluN2B ratios showed a relationship with poorer learning across all ages. GIPC is a scaffolding protein that binds via its PDZ region to GluN2-containing NMDA receptors preferentially on extrasynaptic membranes (Yi et al., 2007). Our results indicated that memory declines during aging may be related to an age-related increase in the proportion of the GluN2B-containing NMDA receptors that remain in old animals that were associated with surface membranes, both in and around synapses. Our data also showed that GIPC/GluN2B and PSD-95/GluN2B ratios positively correlated across all ages, which may mean that there was a common mechanism influencing the alterations in association of GluN2B with these two scaffolding proteins. Recent evidence that PSD-95 can localize with NMDA receptors on extrasynaptic membranes (Fan et al., 2012) might explain this relationship (Fig. 2.4f).

Another potential mechanism could be a decrease in normal cycling of the receptors off of the membrane, resulting in a decrease in the population of internalized receptors for breakdown or recycling (Fig. 2.4c). An increased number of PSD-95 molecules per GluN2B, as mentioned above, or altered phosphorylation status (Goebel-Goody et al., 2009) might increase stabilization of receptors in the membrane. Preliminary work in our lab (unpublished observation) showed that a greater percentage of GluN2A, GluN2B and PSD-95 proteins are palmitoylated in aged frontal cortex than in young. Palmitoylation stabilizes NMDA and AMPA receptors in the synaptic membrane and depalmitoylation is necessary to cycle the receptors off the membrane (Baekkeskov and Kanaani, 2009; Hayashi et al., 2009; Noritake et al., 2009). An increased number of palmitoylated proteins could explain an age-related increase in association of remaining GluN2B-containing NMDA receptors with the surface membrane (Fig. 2.4d).

In summary, there appeared to be an increase in triheteromeric receptors during aging, but this did not appear to influence spatial reference memory. Age-related memory declines were more related to an increased association of GluN2B-containing NMDA receptors with membrane scaffolding proteins.

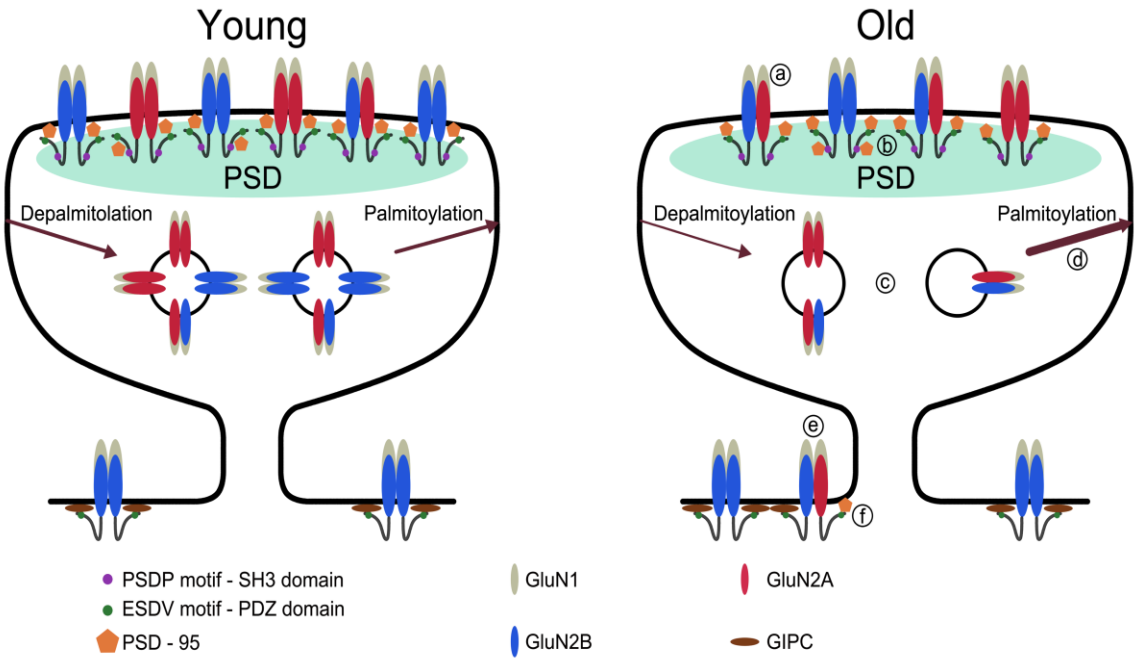

Figure 2.4. Potential mechanisms of age-related changes in glutamatergic synapses in the frontal cortex. Declines in synaptic membrane expression of GluN2B subunits (Zhao et al., 2009) and an increase in PSD-95/GluN2B ratio in aged frontal cortex associated with poor memory could be related to: a) an increase in triheteromeric NMDA receptors, b) an increase in the number of PSD-95 molecules per GluN2 subunit, and/or c) decreased cycling of receptors off of the membrane, which may be influenced by increased palmitoylation of subunits and PSD-95 (d). Synaptic membrane decreases in GluN2B subunits and high GIPC/GluN2B ratios in frontal cortex being associated with high PSD-95/GluN2B ratios and poor memory could be caused by: e) GluN2B-containing NMDA receptors being more mobile than those with GluN2A, which may allow triheteromeric receptors to traffic to extrasynaptic membranes where they interact with GIPC and/or f) PSD-95 being aberrantly located in the extrasynaptic membrane in the poorest old learners.

Chapter 3

Posttranslational modifications of GluN2B in aged mice

Formatted for submission to The Journal of Neuroscience

Abstract

The N-methyl-D-aspartate receptor (NMDAr) is particularly vulnerable to the effects of aging. The GluN2B subunit of the NMDAr, compared to other NMDAr subunits, suffers the greatest losses of expression in the aging brain, especially in the frontal cortex. One protein from the NMDAr complex, the scaffolding protein PSD-95, has an increased interaction with GluN2B in the aged frontal cortex, which correlates with poorer learning. In this study we explored some of the mechanisms that may promote differences in the NMDAr complex in the frontal cortex of aged animals. Two ages of mice, 3 and 24 month, were behaviorally tested in the Morris water maze. The frontal cortex and hippocampus from each mouse were subjected to differential centrifugation followed by solubilization in Triton X-100. Proteins from Triton insoluble membranes, Triton soluble membranes, and intracellular membranes/cytosol were examined by Western blot. Levels of GluN2B phosphotyrosine 1472 were increased in the Triton insoluble membranes from the frontal cortex of old mice with good reference memory. At the same time levels of GluN2B phosphotyrosine 1336 remained steady. The 115 kDa GluN2B cleavage product was found with greater intensity on Triton soluble membranes from the frontal cortex of old mice with good reference memory. The percentage of GluN2A, GluN2B, Fyn, PSD-95, and APT1 that were palmitoylated had an age-related increase in the frontal cortex, but not the hippocampus. These data suggest that there may be a perturbation in the palmitoylation cycle in the frontal cortex of aged mice, leading to deviations in NMDAr localization.

Introduction

A vulnerability of the aging process is cognitive decline. Signs of memory decline may begin around 50 years of age and some aspects of cognition begin to decline around 40 years of age (Scherr et al., 1988; Singh-Manoux et al., 2012). Spatial memory, the detailed recollection of one's surroundings, is critical for navigating through everyday life and exhibits a significant decline with age (Gallagher, Burwell et al. 1993) . Age-related spatial memory impairments affect many mammalian species, therefore rodents have served as an appropriate model for cognitive aging (Gallagher et al., 2011).

The *N*-methyl-D-aspartate receptor (NMDAr) is an ionotropic glutamate receptor that is essential for spatial memory tasks (Morris et al., 1986). The NMDAr is particularly vulnerable to change during aging (Magnusson et al., 2010). Protein expression levels of NMDAr subunits decline with age in the hippocampus and frontal cortex (Magnusson et

al., 2002; Magnusson et al., 2007; Das and Magnusson, 2011). The GluN2B subunit expression declines significantly in most cellular fractions in the hippocampus of aged mice but there is a more pronounced aging effect in the synaptic membrane, than in the tissue as a whole, in the frontal cortex (Zhao et al., 2009). Recent evidence shows that there is an increased interaction between GluN2B subunits and postsynaptic density protein 95 (PSD-95), suggesting an additional effect of aging beyond subunit production (Zamzow et al., 2013).

The NMDAr interacts with many different proteins (Husi et al., 2000). NMDArs are concentrated and held at synapses by PSD-95 (Roche et al., 2001; Xu, 2011). The Src kinase, Fyn, phosphorylates tyrosines 1336 and 1472 on GluN2B which influences localization of GluN2B-containing receptors and long-term potentiation (LTP) (Nakazawa et al., 2001; Goebel-Goody et al., 2009). Striatal-enriched protein tyrosine phosphatase (STEP) dephosphorylates tyrosines 1336 and 1472 on the GluN2B subunit and inhibition of STEP enhances NMDAr current (Pelkey et al., 2002; Lee, 2006). Calpain also influences members of the NMDAr complex, like GluN2B, PSD-95, and STEP, by calcium-induced cleavage, leading to deactivation and altered localization of the proteins (Nguyen et al., 1999; Lu et al., 2000; Guttmann et al., 2001).

Protein palmitoylation is a posttranslational modification that is an important regulator of synaptic plasticity (Fukata and Fukata, 2010). The NMDAr subunits GluN2A and GluN2B are both palmitoylated (Hayashi et al., 2009). Palmitoylation of the NMDAr subunits GluN2A and GluN2B affects localization of the receptor by enhancing access of the Src kinase, Fyn, to its substrate on the C-terminus of the GluN2B subunit (Hayashi et al., 2009). Fyn and PSD-95 are also palmitoylated, which enriches each protein on synaptic membranes (El-Husseini Ael et al., 2002; Sato et al., 2009).

What is not currently known is the effect age has on post-translational modification of NMDAr complex proteins. In the current study, we assessed the spatial reference memory of C57BL/6 mice of two different ages, separated synaptic membranes by subcellular fractionation, and quantified protein expression and post-translational modifications.

Materials and Methods

Animals

A total of 35 male C57BL/6 mice from two age groups (3-5 and 24 months of age) were

used for this study. The 18 mice in the older age group were obtained from National Institute on Aging, NIH. Nineteen young mice were purchased from JAX mice (Bar Harbor, MA), which stocks the NIH colony. They were fed *ad libitum* and housed with a 12/12 h light/dark cycle. Twenty four mice (12 young (3 months old), 12 old) in study 1 were fed a standard chow diet (LabDiet) and 13 mice (7 young (5 months old), 6 old) in study 2, which were controls from a separate study, were fed the defined AIN-93G diet. After the behavioral testing, all animals were euthanized by exposure to CO_2 and decapitated. The brains were harvested, frozen in dry ice and stored at -80^{o}C.

Behavioral testing

Spatial reference memory, cognitive flexibility and associative memory (cued control task) were tested with the use of the Morris water maze as previously described (Das et al., 2012). Study 1 mice were tested for only 2 days of reference memory, while study 2 had an additional day. Briefly, for the first two days, mice were acclimated to the water maze, followed by 2 days of testing for spatial reference memory, 1 day of reversal training to test cognitive flexibility and 1 day of associative memory testing (cued control task). Reference memory consisted of 8 place trials per day and probe trials at the end of each day. A naive probe trial was performed at the beginning of the first day of memory testing. The platform was kept in the same quadrant for each place trial. Place trials consisted of a maximum of 60 seconds in the water searching for the platform, 30 seconds on the platform and 2 minutes of cage rest. If a mouse failed to find the platform within the designated 60 second swim time, it was led to the platform by the experimenter. Probe trials were performed to assess the animal's ability to show a bias for the platform location. During the probe trial, the platform was removed and the mouse was allowed to search in the water for 30 seconds. After 2-3 days of place trials, a reversal task was performed in order to assess cognitive flexibility. The platform was placed in the opposite quadrant in the tank and place and probe trials performed similar to the reference memory task.

After 3 days of reference memory and one day of reversals, the study 2 mice were tested for spatial working memory as previously described (Das and Magnusson, 2011). The task consisted of two sessions per day for 7 days. The platform positions were changed between each session. Each session consisted of 4 trials. The first trial was a naïve trial in which the mouse was allowed to search for the platform position for a maximum of 60 seconds, after which the mouse was allowed to remain on the platform

for 30 seconds, followed by cage rest for 10 minutes (delay period). In the second trial the mouse was placed in the water at a different entry point from the naïve trial and allowed to search for the platform for a maximum of 60 seconds. The mouse was again allowed to stay on the platform for 30 s and allowed to rest in the cage for 2 minutes. The mouse was placed into the water 2 more times at 2 different entry points and allowed to find the platform for 60 s. They spent 30 s on the platform and rested in the cage for 2 minutes between trials. Mice were then placed into their cages until the next session, which started about 3 h from the beginning of the first session. If the mouse failed to find the platform within the designated 60 s for any of the trials, it was led to the platform by the experimenter. The entry points within one session were randomly assigned for each trial. Working memory was assessed between naïve and delay trials. Cued trials were designed to test motivation, visual acuity, and physical ability for the task. The mice performed 6 cued trials. The positions of entry and the platform positions varied between trials. The platform was kept submerged, but was marked by a 20.3 cm support with a flag. The mice were allowed to search for the platform for 60 seconds. The animal's movements in the water maze were tracked and analyzed with the SMART tracking system (San Diego Instruments, San Diego, CA).

Tissue processing for cell subfractionation

Biochemical fractionation of the frontal cortex (rostral 4 mm of cortex) and hippocampus was performed on 23 mice (11 young, 12 old; study 1) as previously described (Dunah and Standaert, 2001), with a few modifications. Briefly, tissue was homogenized on ice with a Dounce homogenizer in TE buffer (10mM Tris–HCl, pH 7.4, 1mM EDTA, 1mM EGTA) plus 320mM sucrose and protease inhibitor cocktail (Sigma). Homogenate was centrifuged at 4°C 1000 x g for 10 min and the resulting pellet (P1) was discarded. The supernatant (S1) was centrifuged at 4°C 12000 x g for 20 min in an Eppendorf centrifuge to produce the crude synaptosome pellet (P2) and the supernatant cytosolic and microsomal fraction (S2). The P2 fraction was then solubilized in Triton X-100 (Sigma) and fractionated as previously described (Milnerwood et al., 2010). The P2 pellet was resuspended with 300µl Triton buffer (10 mM Tris-HCl, 100mM NaCl, 0.5 % Triton, pH7.2) and rotated slowly (15min, 4°C), followed by centrifugation (12,000*g,* 20min, 4°C). The supernatant (triton-soluble fraction) containing non-PSD membranes was retained. The P2 pellet was resuspended in 150µl SDS buffer (10mM Tris-HCl, 150mM NaCl, 1% Triton-X, 1% deoxycholic acid, 1% SDS, 1mM DTT, pH7.5), followed by gentle rotation

(1h, 4°C) and centrifugation (10,000*g*, 15min, 4°C). The pellet was discarded and the supernatant (triton insoluble PSD fraction) retained. Microsomal and cytosolic (S2), PSD (TxP), and non-PSD (TxS) samples were stored at -80°C.

Tissue processing for Acyl-biotinyl exchange

In order to quantify levels of protein palmitoylation, proteins were subjected to the acyl-biotinyl exchange method as previously described (Wan et al., 2007). The frontal cortices and hippocampi from study 2 mice (5 young, 6 old) were homogenized on ice in a Dounce homogenizer with 500 μl of buffer LB(50 mM Tris-HCl, pH 7.4, 150 mM NaCl, 5 mM ethylenediaminetetraacetic acid (EDTA), protease inhibitor cocktail (Sigma)) and 10 mM N-ethylmaleimide (NEM). Homogenization involved 12 strokes from each of 2 pestles of increasing sizes in homogenization buffer. Aliquots were taken from each sample to analyze total fatty acid transporter proteins. After homogenization Triton X-100 was added to a final concentration of 1.7% and the mixture incubated with rotation at 4°C for 2 hours. Excess NEM was stripped and proteins were precipitated with three sequential chloroform:methanol (1:3, v/v) precipitations. Precipitated proteins were solubilized in 300 μl of 4SB(50 mM Tris-HCl, pH 7.4, 150 mM NaCl, 5 mM (EDTA), 4% sodium dodecyl lsulfate (SDS)), and diluted with 1.2 ml of +HA buffer (0.7 M hydroxylamine, pH 7.4, 0.4 mM N-[6-(Biotinamido)hexyl]-3'-(2'-pyridyldithio)propionamide (HPDP-biotin) (Pierce, Rockford,IL), 0.2% Triton X-100, 150 mM NaCl, protease inhibitor cocktail) or 1.2 ml of –HA buffer (50 mM Tris-HCl, pH 7.4, 0.4 mM HPDP-biotin, 150 mM NaCl, 0.2% Triton X-100). The mixtures were incubated with rotation at room temperature for 2 hours, followed by 3 sequential chloroform:methanol (1:3, v/v) precipitations. Precipitated proteins were solubilized in 150 μl of 2SB buffer (50 mM Tris-HCl, pH 7.4, 2% SDS, 5 mM EDTA, 150 mM NaCl, protease inhibitor cocktail) and diluted in 2.8 ml of buffer LB + 0.2% Triton X-100. Proteins were precipitated from the mixture by incubation with 60 μl of Streptavidin-agarose (Pierce) for 2 hours at room temperature with rotation. Beads were pelleted, washed 3 times in LB, and proteins were eluted by boiling the beads in 150 μl of LB + 10% β-mercaptoethanol.

Western blot

Sodium dodecyl sulfate–poly acrylamide gel electrophoresis (10%) was used for Western blotting as described previously (Zhao et al., 2009). Each gel contained 4 different μg loads (2, 4, 8 and 16 μg/well) of standards, obtained from homogenate

prepared by combining caudal cortices from all young animals. Protein samples from representatives of each different age group were loaded on each gel and analyzed in triplicate. Proteins were transferred to PVDF membranes, blocked in Odyssey blocking buffer (LiCor, Lincoln, NE): Tris-buffered saline (TBS) (1:1, v/v) and incubated at 4°C in primary antibodies, membranes rinsed 3 times with TBS-T, and incubated in fluorescence-based secondary antibody. Bands were visualized by scanning in the LI-COR Odyssey imager. See Table 3.1 for antibody dilutions and sources.

Table 3.1. Antibody dilutions and sources for Western blots

GluN2B	1:1000	Millipore		GIPC	1:250	Santa Cruz
p1472	1:1000	Phosphosolutions		Calpain 1	1:250	Santa Cruz
p1336	1:1000	Phosphosolutions		Calpain 2	1:250	Santa Cruz
p1480	1:1000	Phosphosolutions		CD36	1:250	Santa Cruz
PSD-95	1:1000	Thermoscientific		ACSL6	1:250	Santa Cruz
STEP	1:1000	Millipore		FATP1	1:250	Santa Cruz
APT1	1:1000	Abcam		Actin	1:250	Santa Cruz
GluN2A	1:250	Santa Cruz		Flotillin	1:250	Santa Cruz
Fyn	1:250	Santa Cruz		Secondary	1:5000	Rockland

Data analysis

Data for behavioral testing were analyzed as previously described (Das et al., 2012). Cumulative proximity measures, which reflect search distance from the platform, were used for the place, reversal and cued trials and average proximity measures were used for probe trials (Gallagher et al., 1993). Based on reference memory acquisition performance, the old mice were divided into the categories of "Reference memory-Good" (RG) and "Reference memory-Bad" (RB) learners as previously described (Lee et al., 1994; Rowe et al., 2007; Yetimler et al., 2012) with some modification. The criteria for "reference-bad" old learners was established by selecting old mice with average 2 day reference scores that were 2 standard deviations above the mean of the young mice, while "reference-good" old learners were within the same 2 standard deviation window (Fig. 3.1A). A total of three young mice (1 from group 1 and 2 from group 2) were also identified as RB learners, using the same criteria. They were removed from further consideration because of the low N for young RB within each study. Protein blots were

analyzed using Li-Cor Odyssey software. Integrated intensity measures were obtained using median background subtraction method. A standard curve was obtained using a linear fit with Excel (Microsoft) from integrated intensity values for known loads of caudal cortex. Sample values were interpolated from the standard curve as caudal cortex equivalents. Each protein was normalized to beta-actin within each sample of total protein. Because the relative percentage of Flotillin molecules that are palmitoylated does not change with age (Bhattacharyya et al., 2013), all proteins precipitated through ABE were normalized to Flotillin. Statistical analyses for behavioral trials and protein expression using data from individual animals, were done with analysis of variance (ANOVA) followed by Fisher's protected least significant difference (PLSD) using Statview software (SAS Institute).

Results

STUDY 1

Behavioral analysis

Performance for spatial learning and flexibility were evaluated for young and old mice in the Morris water maze in two separate study groups. Comparison of study 1 & 2 for 2 day reference place learning ($F_{(1,28)}$=2.0, p=.17) yielded no significant differences between study groups, so the combined data is presented in Fig. 3.1A. Because there were no significant study differences in reference place learning and a significant number of good and bad learners could be identified among the old mice, the protein data was examined based on reference place learning.

An examination of reference scores showed a significant overall effect of age ($F_{(1,32)}$=20.48, p<.0001; Fig. 3.1A). Based on acquisition in the reference memory task, the old mice were divided into the categories of "Reference memory-Good" (RG) and "Reference memory-Bad" (RB) (see Methods). After dividing the old mice into the categories of RG and RB, the overall differences among the study 1 groups remained significant ($F_{(2,20)}$=17.87, p<.0001; Fig. 3.1B). Significant differences in learning scores were evident between young and RB (p<.0001), between young and RG (p=.004), and between RG and RB (p=.0005) in reference memory trials across both days. There was an overall effect of reference memory status for reversal trials ($F_{(2,20)}$=5.37, p=.01; Fig. 3.1D) with significant between group effects for young and RG (p=.003). An overall effect of reference memory status was evident for the reversal probe trial ($F_{(2,20)}$=5.78, p=.01; Fig. 3.1D) with between group effects for young and RG (p=.002). There was no

significant overall effect of reference memory status for probe trials ($F_{(2,20)}$=2.33, p=.12: Fig. 3.1C) or cued trials ($F_{(2,20)}$=.48, p=.62; Fig. 3.1E).

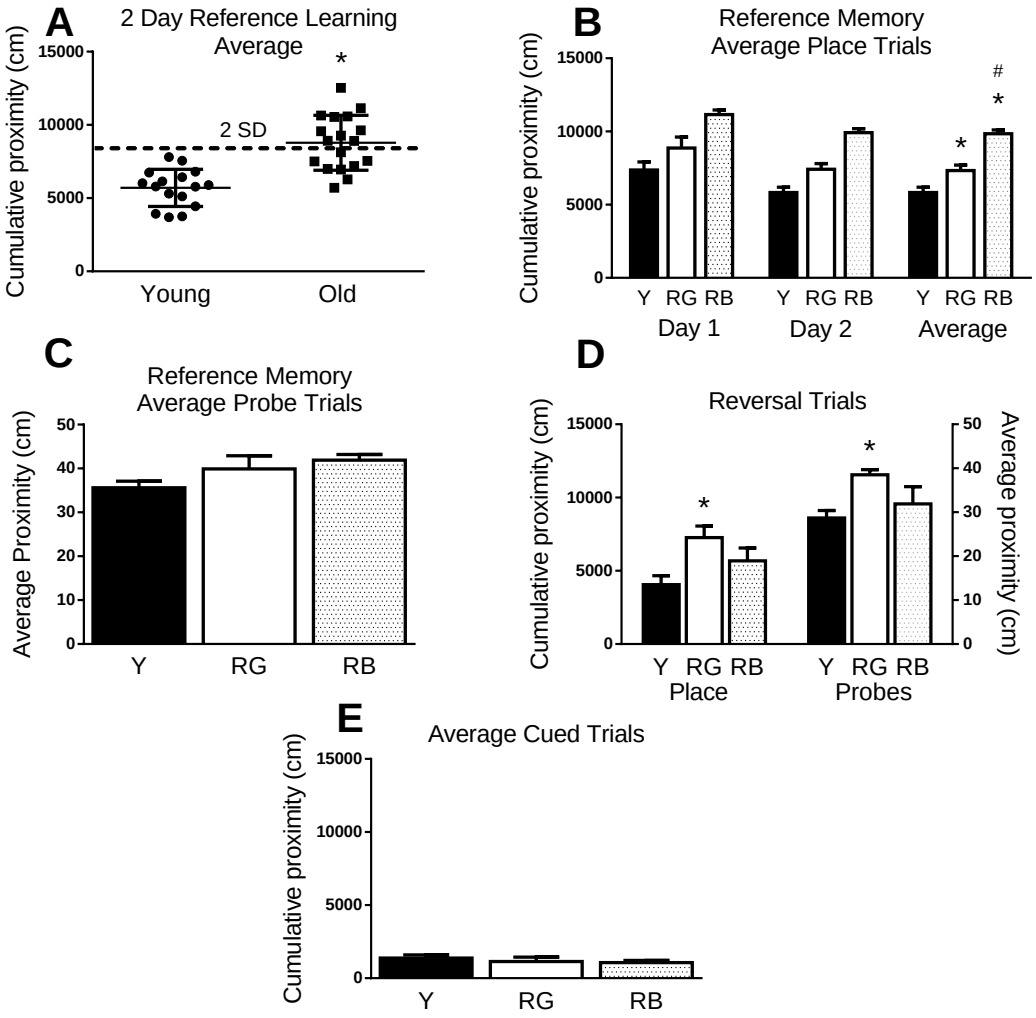

Figure 3.1. Behavioral testing. Aged mice have significantly poorer reference memory than young mice. A) Study 1 & 2 combined: Old mice were separated based on acquisition of reference memory in place trials; bad old learners were >2 standard deviations (SD) above the young mean. B-E) Study 1 only: Significant differences in reference memory acquisition (B), but not probe trials (C). D) Significant differences were seen in averaged place and probe reversal trials. E) No significance differences were seen in cued trials. * for difference of p<.05 from young. # for difference of p<.05 from RG. NOVA and Fisher's PLSD). N=5-11. Data=mean +/- SEM. Y=young. RG= old Reference memory-Good. RB= old Reference memory-Bad.

Age-related changes in GluN2 proteins

A previous study in our lab showed an age-related increase in the association of PSD-95 with GluN2B-containing NMDArs (Zamzow et al., 2013). PSD-95 is normally enriched on synaptic membranes, but it can also be found on extrasynaptic membranes in the mouse model of Huntington's disease (Zheng et al., 2011; Fan et al., 2012). GluN2B-containing NMDArs are very mobile, moving easily between synaptic and extrasynaptic membranes (Groc et al., 2006; Parsons and Raymond, 2014). We hypothesized that there may be an aging effect on the membrane localization of NMDArs and their effector proteins

To test our theory we employed differential centrifugation of brain homogenates followed by membrane solublization in 0.5% Triton X-100. Because the synaptic membrane is insoluble in non-ionic detergents, exposure to a low concentration of Triton X-100 is an effective way to separate synaptic from peri- and extrasynaptic membranes (Goebel-Goody et al., 2009; Milnerwood et al., 2010). We examined proteins from three synaptosomal fractions from the hippocampus and frontal cortex of young and aged mice: synaptic membranes (TxP), peri/extrasynaptic membranes (TxS) and cytosol/microsomes (S2). To test for the proper separation of the fractions, a representative western blot was probed for proteins known to reside on detergent-resistant synaptic membranes (PSD-95) or detergent-soluble membranes (p97ATPase), including endoplasmic reticulum and Golgi apparatus (Jiang et al., 2011)(Fig. 3.2A).

There was a significant reference memory status effect on GluN2B subunits in the synaptic membranes (TxP) of frontal cortex synaptosomes ($F_{(2,20)}$=5.5, p=.012; Fig. 3.2B,C). Significant decreases in GluN2B subunit expression were found between young and both RG (p=.025) and RB (p=.007). There were no significant age-related differences in GluN2B subunit expression in the TxS and S2 fractions from the frontal cortex or any of the fractions from the hippocampus (p=.17-.99; Fiig3.2B,C). The GluN2A subunit did not show any significant age-related differences in any fraction or brain region (p=.16-.62; Fig. 3.2B,D).

Phosphorylation by Fyn kinase of tyrosines 1336 and 1472 on the C-terminus of the GluN2B subunit has profound effects on the localization of the subunit. Phosphotyrosine 1472 (p1472) inhibits binding of the GluN2B subunit with the clathrin adaptor protein AP-2, allowing PSD-95 to bind instead and keeping the GluN2B subunit at the synapse (Prybylowski et al., 2005). Conversely, phosphotyrosine 1336 (p1336) can be found on the GluN2B subunit localized to extrasynaptic membranes (Goebel-Goody et al., 2009; Jiang et al., 2011).

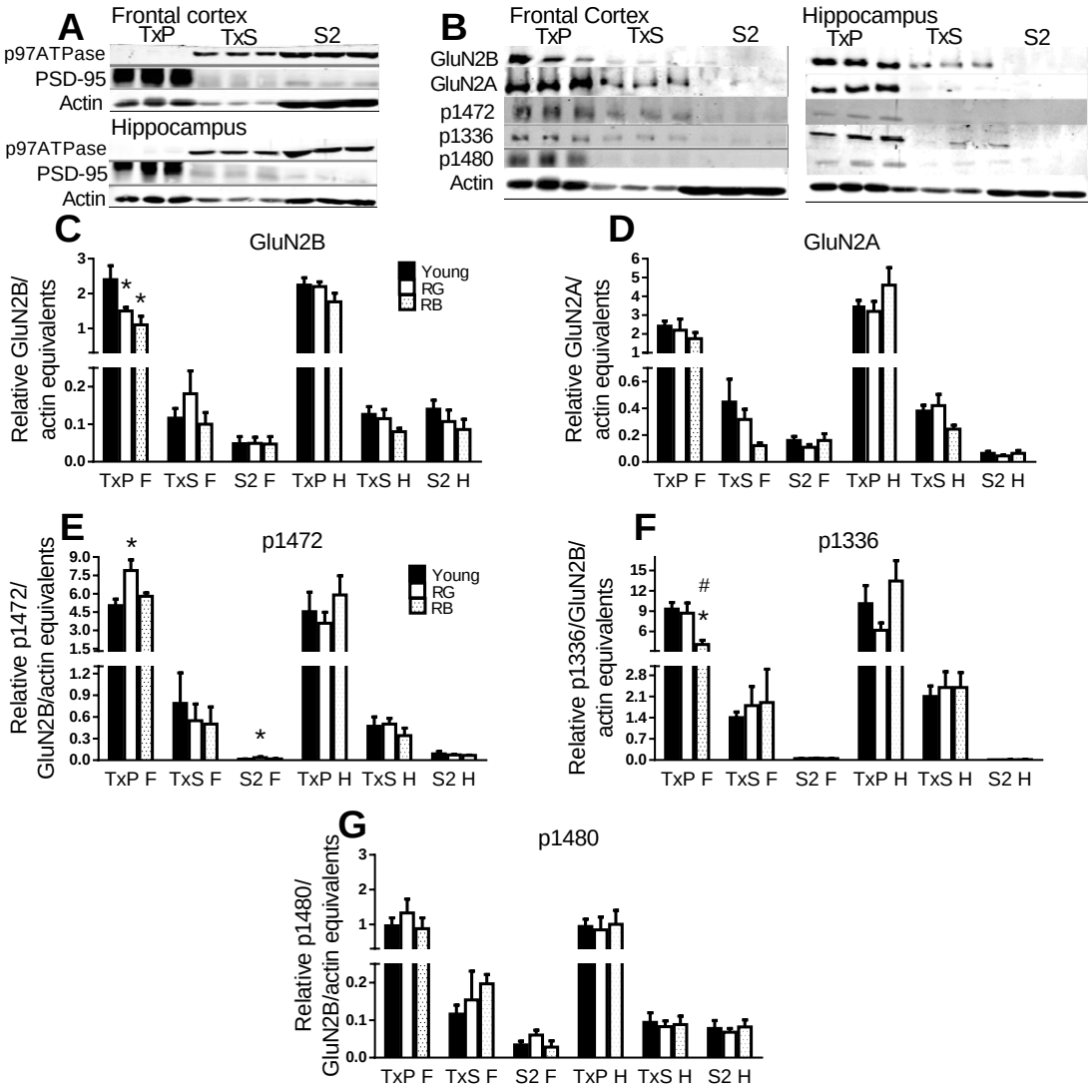

Figure 3.2 GluN2 subunits. Representative blots for Triton X-100 membrane solubilization (A) and GluN2 proteins (B). Order of lanes within each fraction from left to right is young, RG, and RB. Significant differences in reference memory status for GluN2B (C), p1472 (E), and p1336 (F). No significant differences in GluN2A (D) or p1480 (G). * indicates p<.05 for difference from young. # indicates p<.05 for difference from RG (ANOVA and Fisher's PLSD). N=3-11. Data= mean +/- SEM. RG= old Reference memory-Good. RB= old Reference memory-Bad.

We probed all synaptosomal fractions with antibodies specific to p1336 and p1472. There was an overall effect of reference memory status on p1472 levels in the TxP fraction from the frontal cortex ($F_{(2,20)}$=5.7, p=.01; Fig. 3.2B,E), with a significant increase

between young and RG (p=.003). There were no significant overall effects of reference memory status on p1472 in the TxS fraction of the frontal cortex or in any of the fractions from the hippocampus (p=.10-.84; Fig. 3.2B,E). There was a significant increase in p1472 in the S2 fraction of the frontal cortex in RG, as compared to young (p=.04; Fig. 3.2B,E). We next examined the levels of p1336 in all fractions. There was an overall effect of reference memory status in the TxP fraction of the frontal cortex ($F_{(2,19)}$=3.87, p=.039; Fig. 3.2B,F), with a significant decrease between young and RB (p=.01) and between RG and RB (p=.036). Examination of the remaining fractions from both brain regions revealed no significant reference memory status differences in p1336 (p=.23-.83).

The GluN2B subunit can also be phosphorylated on serine 1480. Activation of the NMDAr causes casein kinase 2 to phosphorylate serine 1480 (p1480), which disrupts the binding of GluN2B with PSD-95 (Sanz-Clemente et al., 2013). We used p1480 as a proxy to ask whether the increased level of p1472 in the frontal cortex synaptic membranes was due to decreased activation of the NMDAr. There were no significant differences in p1480 with age, brain region, or synaptosomal fraction (p=.23-.95; Fig. 3.2B,G), suggesting that the increased p1472 signal may not be entirely due to decreased activation of the NMDAr.

Scaffolding proteins and GluN2B phosphorylation

The GluN2B subunit shows an age-related increase in association with PSD-95 and there is an association between the binding of GluN2B to GAIP interacting protein, C terminus(GIPC) and poor memory in aged animals (Zamzow et al., 2013). In young mice, there is an increased association of NMDArs with Fyn, which is mediated by PSD-95(Tezuka et al., 1999; Trepanier et al., 2012). Striatal-enriched protein phosphatase (STEP61) is also a part of the NMDAr complex and is involved with dephosphorylating p1472 (Braithwaite et al., 2006). We probed the cellular fractions with antibodies to PSD-95, GIPC, Fyn, and STEP to ascertain if there were any changes in expression or cellular localization associated with reference memory status.

Expression levels of PSD-95 did not decline with age or reference memory status in the synaptic fractions from the frontal cortex or the hippocampus. There were no significant differences in PSD-95 expression due to reference memory status in any of the cellular fractions (p=.33-.89; Fig.3.3A,B). The TxP fraction in the frontal cortex had a significant reference memory status-related increase in GIPC ($F_{(2,16)}$=4.56, p=.026; Fig. 3.3C), with

a significant increase between young and RG (p=.011). The remaining fractions of the frontal cortex, as well as all fractions of the hippocampus saw no significant differences in GIPC, based on reference memory status (p=.44-.66; Fig. 3.3A,C).

There was a significant reference memory status-related increase in synaptic Fyn in the frontal cortex ($F_{(2,20)}$=5.36, p=.013) and a near significant overall effect in the hippocampus ($F_{(2,20)}$=3.2, p=.06; Fig. 3.3A,D). The increase in synaptic Fyn between young and RB in both the frontal cortex (p=.005) and hippocampus (p=.02) was significant. There was also a significant reference memory status effect in the S2 fraction from the hippocampus ($F_{(2,20)}$=4.88, p=.02; Fig. 3.3A,D), with a significant increase between the young and the RG (p=.006). There were no other significant overall effects in any of the other fractions (p=.23-.33).

Because the amount of Fyn increased similarly with age in both the frontal cortex and the hippocampus, it seemed that Fyn expression could not explain the brain region differences in GluN2B phosphorylation states in old mice. Since STEP61 is known to dephosphorylate phosphotyrosine residues on GluN2B, we looked at the expression levels of STEP61 in the cellular fractions. There were no significant overall reference memory status-related effects on any of the cellular fractions in either brain region for STEP61 (p=.23-.78; Fig. 3.3A,E). An alternatively spliced isoform, STEP46, is able to bind to the GluN2B subunit and affect phosphorylation of tyrosine 1472 (Snyder et al., 2005), therefore we analyzed the relative expression levels of STEP46 in all cellular fractions. There were no significant effects of reference memory status in the cellular fractions from the frontal cortex (p=.56-.71), however there was a slight, but significant effect on STEP46 in the S2 fraction from the hippocampus ($F_{(2,20)}$=3.5, p=.05; Fig. 3.3A,F). A significant increase in STEP46 was seen between the young and RG (p=.016). These data suggest that the increase in p1472 in the frontal cortex of RG learners may not be due to the expression levels of Fyn, STEP, or PSD-95.

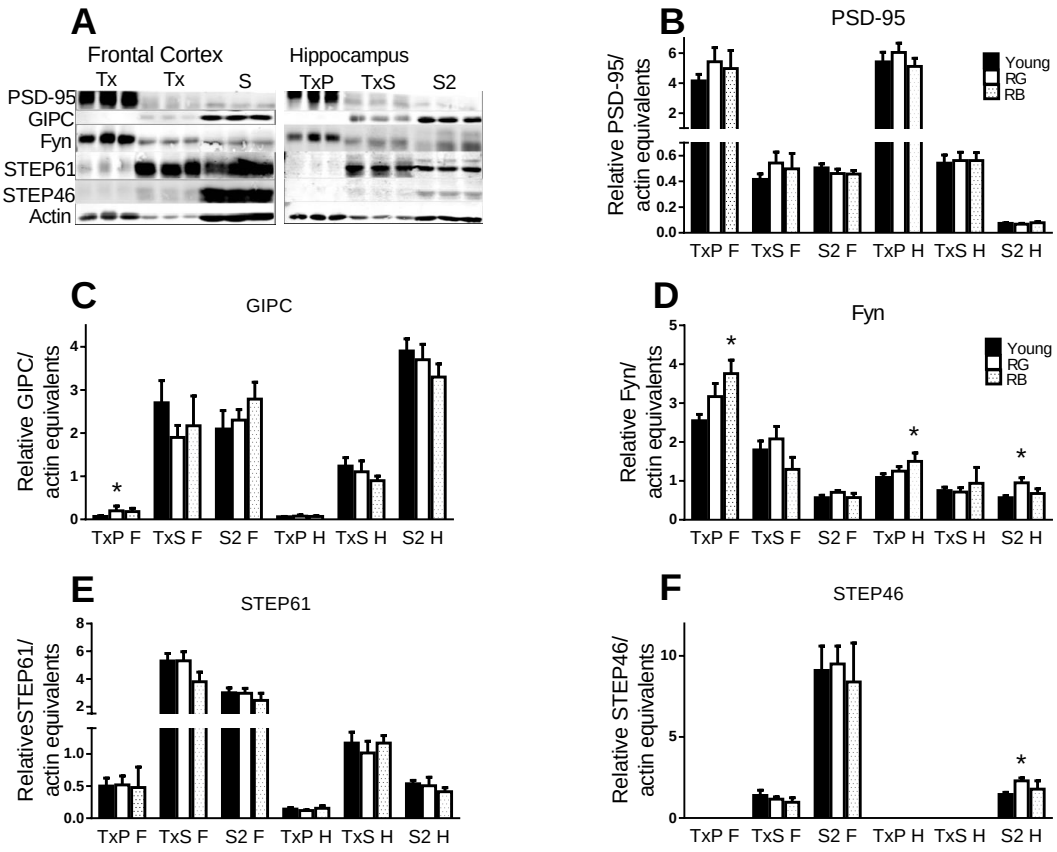

Figure 3.3. Scaffolding, kinase, and phosphatase. Representative blot of proteins (A). Order of lanes within each fraction from left to right is young, RG, and RB. No changes were seen in PSD-95 (B) or STEP61 (E). Significant increases were seen for GIPC in the synaptic membrane of frontal cortex from old good reference learners (C). Fyn was increased in old bad reference memory mice in the synaptic membrane of both brain regions. Significant increases were also seen in Fyn expression in the cytosol of old good reference learners (D). STEP46 expression was increased in hippocampal cytosol from old good reference learners. (F). * indicates $p<.05$ difference from young and # indicates $p<.05$ for difference from RG (ANOVA and Fisher's PLSD). N=3-11. Data= mean +/- SEM. RG= old Reference memory-Good. RB= old Reference memory-Bad.

Calpain cleavage

The GluN2 subunits are proteolytically cleaved by calpain in a calcium-dependent manner (Guttmann et al., 2001). The cleavage event on GluN2B is triggered by p1336, leading to a population of truncated GluN2B subunits residing on extrasynaptic membranes (Wu et al., 2007). We assessed the role that calpain cleavage may have in localizing NMDArs to extrasynaptic membranes. There was a near significant effect of reference memory status ($F_{(2,20)}$=2.96, p=.074; Fig. 3.4A,B) on cleavage of the GluN2B subunit in the frontal cortex TxS fraction. RG exhibited significantly more cleavage of GluN2B than young (p=.041) and near significantly more than RB (p=.056). There was, however, no effect of reference memory status in the TxS fraction from the hippocampus (p=.60). Because both PSD-95 and STEP61 also undergo cleavage by calpain (Nguyen et al., 1999; Lu et al., 2000) we wished to see if calpain cleavage in aged animals was limited to only the frontal cortex for other proteins. There was no significant effect of reference memory status on the cleavage product of STEP61, STEP33, in either the frontal cortex (p=.89; Fig. 3.4A,C) or the hippocampus (p=.78) in the S2 fractions. There was a significant effect of reference memory status on the 50kDa calpain cleavage product of PSD-95 in the S2 fraction of the frontal cortex ($F_{(2,20)}$=15.46, p<.0001; Fig. 3.4A,D) and in the hippocampus ($F_{(2,20)}$=5.05, p=.0168). RG exhibited more PSD-95 cleavage than both young (p<.0001) and RB (p=.027) and RB had more than young (p=.028) in the frontal cortex (Fig. 3.4A,D). RG also had significantly more PSD-95 cleavage than young in the hippocampus S2 fraction (Fig. 3.4A,D).

Two isoforms of calpain predominate in the brain, μ-calpain (calpain 1) and m-calpain (calpain 2) (Wu and Lynch, 2006). Both proteins undergo autolysis, with calpain 1 producing a 55 kDa fragment, while calpain 2 produces 3 fragments of 55, 40, and 30 kDa (Nath et al., 1996; Li et al., 2004; Huang et al., 2010). We probed all cellular fractions to test whether the increased calpain-mediated cleavage of GluN2B subunits in the frontal cortex might be due to higher expression and/or higher activation of calpains. There was no reference memory status-mediated difference in calpain 1 expression in the S2 fraction of the frontal cortex (p=.97). There was a near significant main effect of reference memory status in the TxS ($F_{(2,20)}$=3.35, p=.056) and S2 ($F_{(2,20)}$=3.45, p=.051; Fig. 3.4A,E) fractions from the hippocampus. The RB had significantly less calpain 1 than RG in both TxS (p=.02) and S2 (p=.02) hippocampal fractions (Fig. 3.4A,E). There was no significant effect of reference memory status on calpain 2 expression in any

cellular fraction of either frontal cortex or hippocampus (p=.34-.45; Fig. 3.4A,G). There were significant reference memory status effects on the 55 kDa autolysis cleavage product of calpain 1 in the S2 fractions from the frontal cortex ($F_{(2,20)}$=13.83, p=.0002) and the hippocampus ($F_{(2,20)}$=6.8, p=.006). RG had significantly higher calpain1 cleavage product than young in both frontal cortex (p= <.0001) and hippocampus (p=.002) and RB had higher expression than young in frontal cortex in S2 fractions (p=.005; Fig. 3.4A,F). A look at autolysis cleavage products of calpain 2 revealed an interesting distinction between the frontal cortex and the hippocampus. The 40 kDa cleavage product was found primarily in cellular fractions from the frontal cortex, while the 55 kDa cleavage product was found in the hippocampus (Fig. 3.4A,H). There was no reference memory status effect on levels of the 40 kDa cleavage product in the S2 fraction from the frontal cortex (p=.42). A significant reference memory status effect was present in the TxS ($F_{(2,20)}$=8.61, p=.002) and the S2 ($F_{(2,20)}$=33.82, p<.0001; Fig. 3.4A,H) fractions for the 55 kDa cleavage product from the hippocampus. Both RG (p=.02) and RB (p=.0007) had significantly higher levels of calpain 2 cleavage 55 products in hippocampal TxS fractions (Fig. 3.4A,H). Hippocampal S2 fractions showed increases in RB from both young and RG (p<.0001) for the 55kDa cleavage of calpain 2 (Fig. 3.4A,H).

These data indicate that while calpain expression does not change dramatically in the old mice, the activities of the enzymes increased greatly in older mice. This amplified calpain activity does not, however, explain a lack of difference between young and old in the levels of cleaved GluN2B subunits in the TxS fraction from the hippocampus.

Figure 3.4 Calpain activity. Calpain activity is increased in both the hippocampus and frontal cortex. Representative blot of proteins (A). Order of lanes within each fraction from left to right is young, RG, and RB. Calpain cleavage increased with age for GluN2B(B) and PSD-95(D), but not STEP(C). Calpain 1 decreased slightly in the hippocampus of old mice with poor reference memory (E), but calpain 2 was unchanged (G). Increased autolysis activity of calpain 1 (F) and calpain 2 (H) in the aged brain. * indicates $p<.05$ for difference from young; # indicates $p<.05$ for difference from RG (ANOVA and Fisher's PLSD). N=3-11. Data= mean +/- SEM. RG= old Reference memory-Good. RB= old Reference memory-Bad.

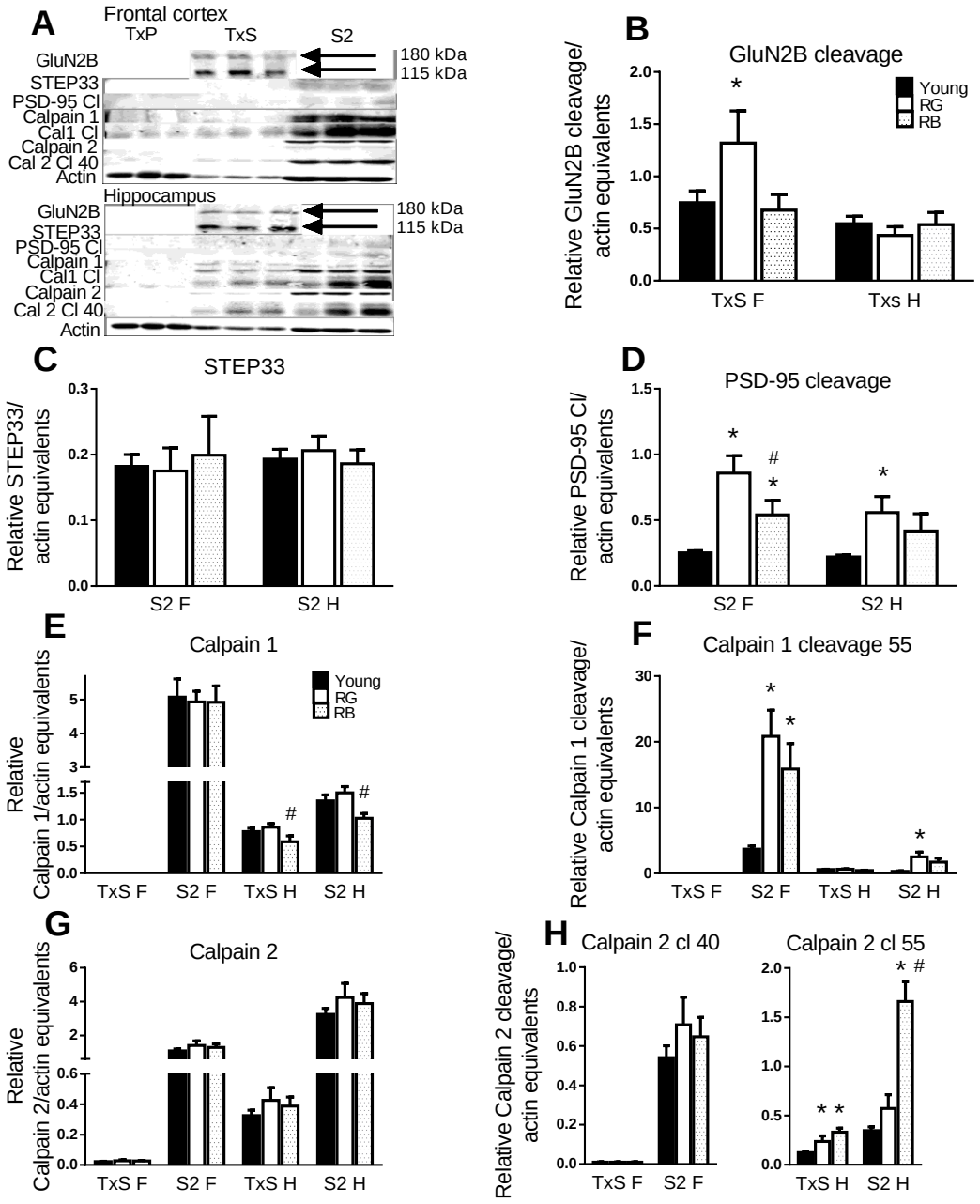
A
Frontal cortex
TxP
TxS
S2
GluN2B
STEP33
PSD-95 Cl
Calpain 1
Cal1 Cl
Calpain 2
Cal 2 Cl 40
Actin
180 kDa
115 kDa
Hippocampus
B
GluN2B cleavage
Relative GluN2B cleavage/ actin equivalents
Young
RG
RB
TxS F
Txs H
C
STEP33
Relative STEP33/ actin equivalents
S2 F
S2 H
D
PSD-95 cleavage
Relative PSD-95 Cl/ actin equivalents
E
Calpain 1
Relative Calpain 1/actin equivalents
F
Calpain 1 cleavage 55
Relative Calpain 1 cleavage/ actin equivalents
G
Calpain 2
Relative Calpain 2/actin equivalents
H
Calpain 2 cl 40
Calpain 2 cl 55
Relative Calpain 2 cleavage/ actin equivalents

Figure 3.4

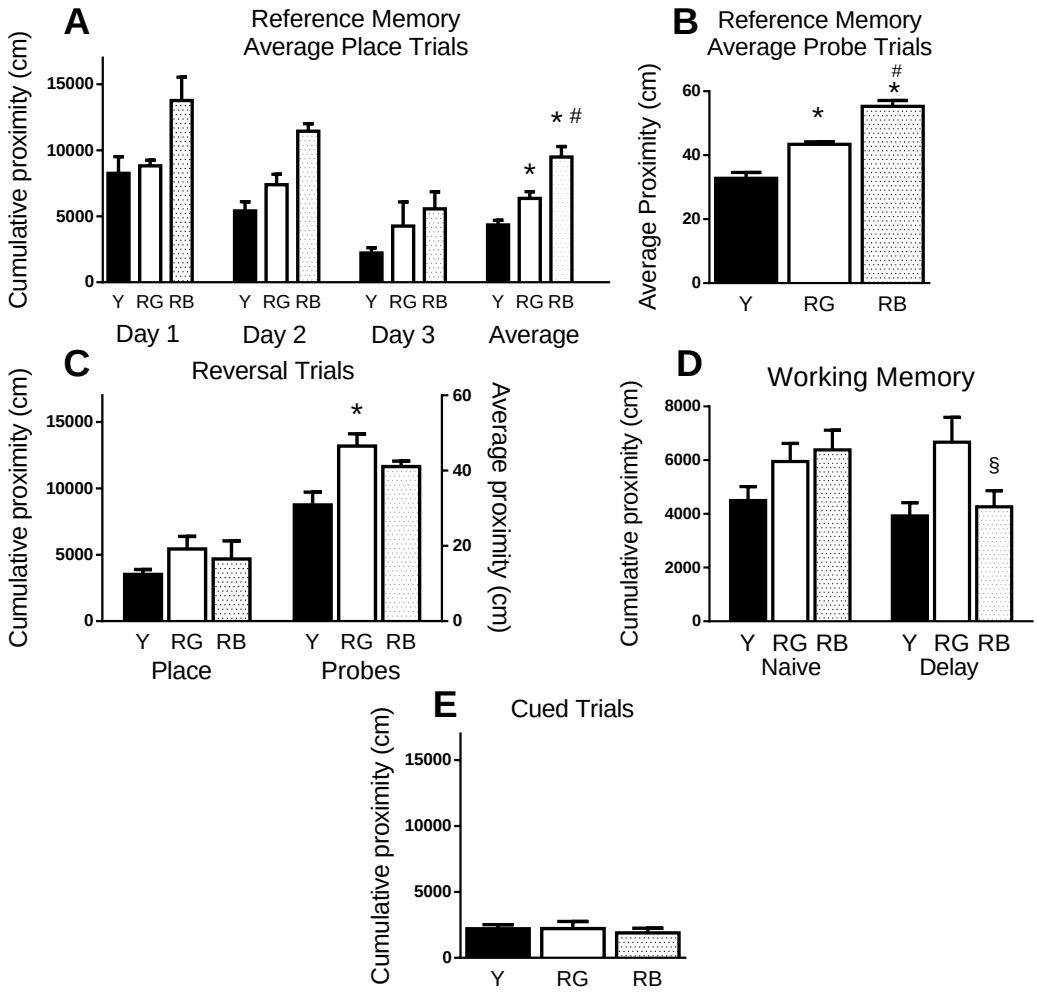

Figure 3.5. Behavioral data from study 2. Aged mice have significantly poorer reference memory than young mice. A)Significant differences in reference memory, B) probe trials, and C) reversal probe trials, but not reversal place trials D) Significant differences between naïve and delay trial for RB. E) No significance differences were seen in cued trials. * for difference of p<.05 from young. # for difference of p<.05 from RG. § for difference of p<.05 from naïve trial of same group(ANOVA and Fisher's PLSD). N=3-5. Data=mean +/- SEM. Y=young. RG= old Reference memory-Good. RB= old Reference memory-Bad.

STUDY 2

Behavioral analysis

Study 2 mice were subjected to 3 days of reference memory place trials. There was an overall effect of reference memory status ($F_{(2,8)}$=15.34,p=.001; Fig. 3.5A). Significantly lower cumulative proximities were evident in young, as compared to both RG (p=.025) and RG and RB (p=.04), and on day 2 between young and RG (p=.0003) and RB (p=.0001) but RG also had lower proximities than RB (p=.04) across all place trials (Fig. 3.5A). There was a significant effect of reference memory status on probe trials ($F_{(2,8)}$=40.16,p<.0001; Fig. 3.5B), with significant differences between each group across all probe trials (p=.003; Fig. 3.5B). The pattern of relationships between groups was similar between study 1 an 2 probe trials, but with respect to significant differences, the reference memory probes in study 2 better mimicked the place trials than in study 1. Reversal trials yielded no overall effect of reference memory status ($F_{(2,8)}$=1.49, p=.28; Fig 3.5C). There was, however, a significant reference memory status effect in the reversal probe trial ($F_{(2,8)}$=.6.29, p=.02; Fig. 3.5C), with RG exhibiting higher average proximity than young (p=.01), similar to the results seen in study 1 (Fig. 3.1D). Study 2 mice were subjected to 7 days of working memory. An overall effect of reference memory status was found when comparing naïve and delay trials ($F_{(2,8)}$=8.915, p=.0025; Fig. 3.5D). A closer look revealed no significant differences between trials for young (p=.9473) or RG (p=.5337), however the RB mice performed significantly better in the delay trial vs the naïve trial (p=.0287). There was no significant effect of reference memory status on cumulative proximity in the cued trials ($F_{(2,8)}$=.20, p=.82; Fig. 3.5E)

GluN2 subunits have increased palmitoylation with age

Posttranslational modification by palmitoylation occurs on GluN2A and GluN2B subunits as well as PSD-95 and Fyn (Hayashi et al., 2009; Noritake et al., 2009; Sato et al., 2009). PSD-95 is a soluble protein that requires palmitoylation to cluster on postsynaptic membranes (El-Husseini Ael et al., 2002). Likewise, palmitoylation of Fyn localizes the protein to detergent resistant membranes (Sato et al., 2009). More importantly, palmitoylation of the GluN2B subunit enhances its interaction with Fyn, thereby increasing phosphorylation of tyrosine 1472. We asked if the increased p1472 seen in the TxP fraction of frontal cortex of old mice with good reference memory was driven by a change in the palmitoylation levels of GluN2B subunits. We used the acyl-biotin exchange method to precipitate acylated proteins from whole cell lysates of the frontal cortex and hippocampus.

The GluN2A ($F_{(2,8)}$=19.05, p=.0009) and GluN2B ($F_{(2,8)}$=10.26, p=.006; Fig. 3.6A,B) subunits had significant reference memory status effects on palmitoylation in frontal cortex lysates. PSD-95 ($F_{(2,8)}$=50.66, p<.0001) and Fyn ($F_{(2,8)}$=5.21, p=.03; Fig. 3.6A,C) also exhibited significant effects in the frontal cortex. In each case, both the RG and RB had higher levels of palmitoylation than the young (p<.001 to .05; Fig. 3.6). Interestingly, there was no significant reference memory status effect on the relative palmitoylation levels of proteins in the hippocampus (p=.54-.82; Fig. 3.6).

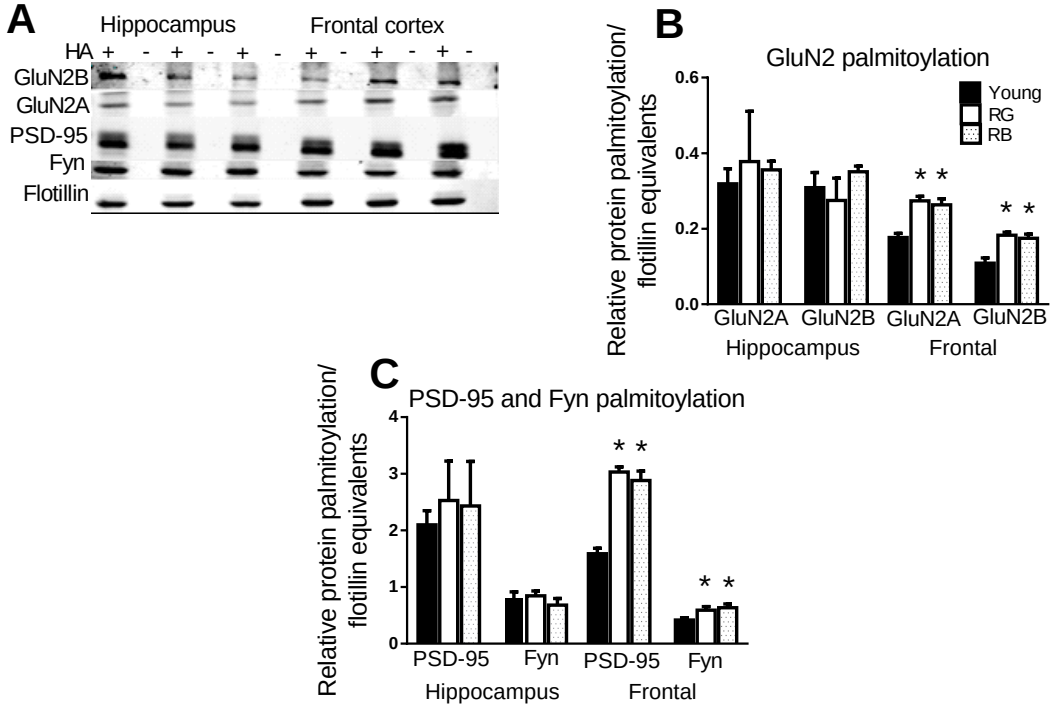

Figure 3.6. Protein palmitoylation. Age-related increase in palmitoylation in frontal cortex. Representative blot of proteins precipitated by ABE (A). Order of lanes within each fraction are from left to right young, RG, and RB. There was an age-related increase in palmitoylation in the frontal cortex for GluN2 subunits (B) as well as PSD-95 and Fyn (C). * indicates p<.05 for difference from young (ANOVA and Fisher's PLSD). N=3-5. Data= mean +/- SEM. RG= old Reference memory-Good. RB= old Reference memory-Bad. HA= hydroxylamine treated.

Fatty acid transporters unchanged with age

The substrate for protein palmitoylation is palmitoyl-CoA (Greaves and Chamberlain, 2011). Palmitoyl-CoA molecules in the brain are formed by esterifying palmitate that has crossed the blood-brain barrier. The manner in which most palmitate molecules are transported into brain cells is still not settled (Schwenk et al., 2010), but several proteins

have been identified that are involved in transporting and esterifying palmitate in the brain. Palmitate can be transported across the blood-brain barrier by the fatty acid transport proteins, fatty acid transport protein 1 (FATP 1) and fatty acid translocase (CD36) (Mitchell et al., 2011). Palmitate is esterified in the brain by long-chain acyl-CoA synthetase 6 (ACSL6) (Van Horn et al., 2005). Up-regulation of these proteins might lead to increased palmitoyl-CoA, thereby driving an increase in protein palmitoylation.

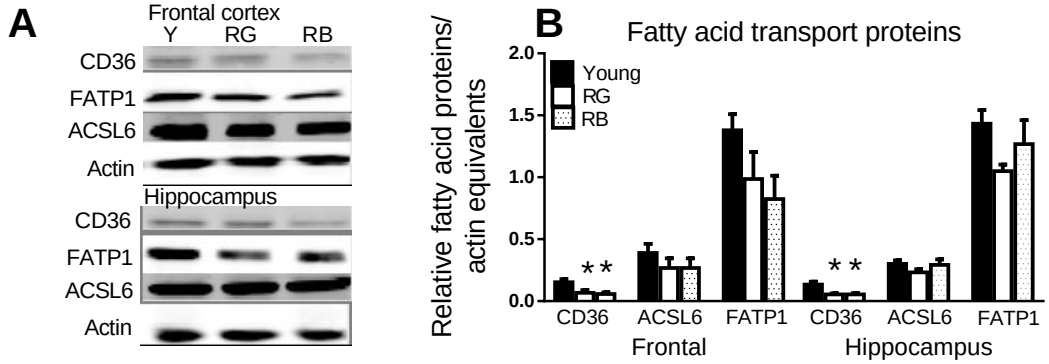

Figure 3.7 Fatty acid transport proteins. Fatty acid transport proteins remain unchanged with age. Representative blot of proteins (A). CD36 expression decreases with age, but not ACSL6 or FATP1 (B). * indicates p<.05 for difference from young. (ANOVA and Fisher's PLSD). N=3-5. Data= mean =/- SEM. RG= old Reference memory-Good. RB= old Reference memory-Bad.

We examined expression levels of CD36, FATP1, and ACSL6 in whole cell lysates from the frontal cortex and hippocampus. There was a modest, but significant effect of reference memory status on CD36 in the frontal cortex ($F_{(2,8)}$=5.53, p=.03) and hippocampus ($F_{(2,8)}$=5.77, p=.02; Fig. 3.7A,B). Both RG (p=.02-.03) and RB (p=.02) had lower CD36 expression than young in both regions. There was no significant reference memory status effect in the frontal cortex or hippocampus on the expression of ACSL6 (p=.36-.44) or FATP1 (p=.09-.16). These data suggest that increased protein palmitoylation levels in the frontal cortex might not be related to fatty acid transporter expression.

APT1 increased palmitoylation with age

A cycle of palmitoylation and depalmitoylation of proteins is orchestrated by palmitoyl acyltransferases (PAT) that palmitoylate proteins and acyl-protein thioesterases (APT) that depalmitoylate proteins (Linder and Deschenes, 2007). The function of many of the PAT is degenerate, but to date only two APT have been found in brain tissue (Conibear

and Davis, 2010; Greaves and Chamberlain, 2011). Recent evidence indicates that the thioesterases APT1 and APT2 are palmitoylated and both enzymes become depalmitoylated by APT1 (Kong et al., 2013). We focused on APT1 because of the broad range ability to control its own palmitoylation as well as the depalmitoylation of other proteins.

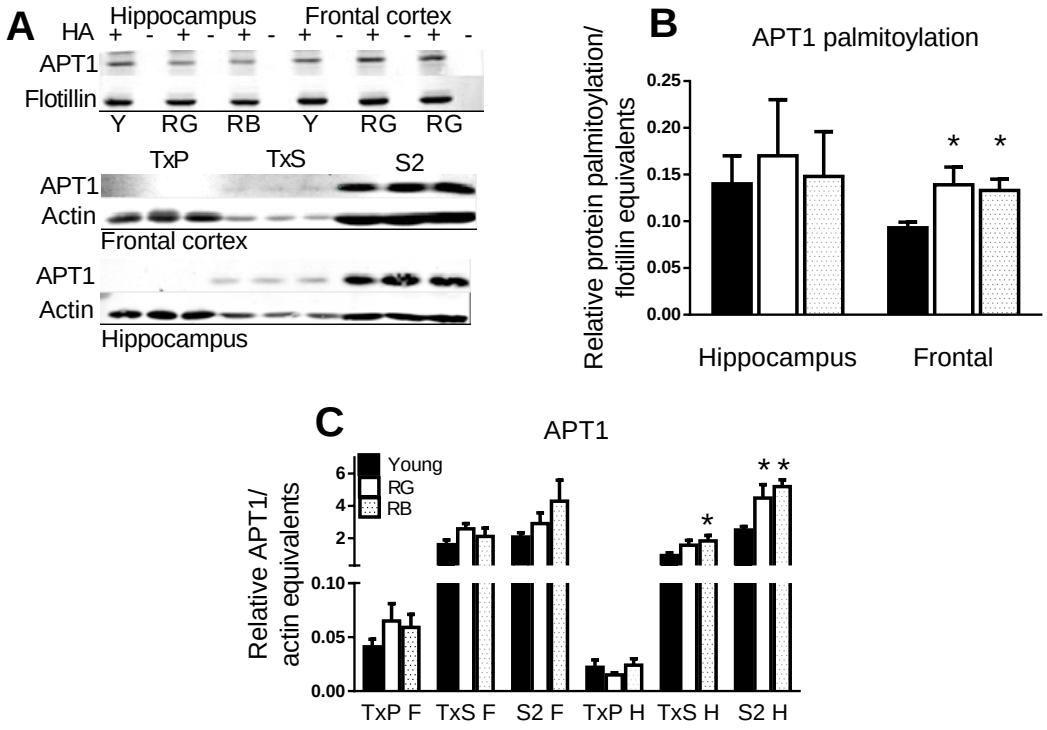

Figure 3.8. APT1 palmitoylation and localization. Representative blot (A). Palmitoylation of APT1 increased with age in frontal cortex, but not in the hippocampus from study 2. Order of lanes from left to right are young, RG, and RB. (B). APT1 expression increased in the TxS and S2 fractions from hippocampus of old mice from study 1 (C). * indicates p<.05 for difference from young (ANOVA and Fisher's PLSD). N=3-11. Data = mean +/- SEM. RG= old Reference memory-Good. RB= old Reference memory-Bad.

We found a significant reference memory status effect on the palmitoylation status of APT1 in the frontal cortex ($F_{(2,8)}$=5.541, p=.03; Fig. 3.8A,B), but not the hippocampus (p=.88). Both RG (p=.02) and RB (p=.03) had higher palmitoylated APT1 expression than young in the frontal cortex (Fig. 3.8B). We next examined the cellular localization of APT1, using the brain tissue from study 1. There was no effect of reference memory status on the cellular fractions from the frontal cortex (p=.13-.26; Fig. 3.7A,C). There was a significant effect on the TxS ($F_{(2,20)}$=3.84, p=.03) and S2 ($F_{(2,17)}$=6.24, p=.009; Fig.

3.8A,C) fractions from the hippocampus, but no effect was found in the TxP fraction (p=.58). RB had significantly higher APT1 in the hippocampal TxS (p=.02) fraction than young and both RB (p=.007) and RG (p=.01) had higher levels in the hippocampal S2 fraction than young (Fig. 3.8C).

Discussion

In this study, there was a significant decline in spatial memory with age, but the old mice could be subdivided based on good and bad acquisition of reference memory. The better spatial learning, however, appeared to be at a cost to cognitive flexibility and working memory in the old. Expression of GluN2B declined with age in TxP from frontal cortex, but p1472 in TxP and calpain cleavage products of GluN2B in the TxS fraction from frontal cortex increased only in old mice with good reference memory. Expression of Fyn increased in TxP from frontal cortex and hippocampus primarily in old mice with the worst memory. Palmitoylaton of several NMDAr complex proteins increased in an age-dependent manner. Finally, the acyl-protein thioesterase, APT1, showed increased palmitoylation with age in the frontal cortex and increased expression in the TxS and S2 fractions from the hippocampus.

The localization of GluN2B on synaptic membranes declined with age and reference memory status in the frontal cortex, but not the hippocampus. At the same time, the levels of p1472 increased in the TxP from the frontal cortex of old mice with good reference memory, while levels in the hippocampus remained steady with age and reference memory status. The phosphorylation of tyrosine 1472 appears to remain steady with age in the hippocampus of rats as well (Coultrap et al., 2008). Phosphorylation of tyrosine 1472 enhances synaptic membrane localization by preventing the clathrin adaptor protein AP-2 from binding to GluN2B and internalizing the NMDAr (Lavezzari et al., 2003). Triheteromeric GluN2A/GluN2B containing NMDAr predominate in the adult hippocampus (Rauner and Kohr, 2011). Data from our lab suggests that triheteromeric NMDArs increase with age in the frontal cortex (Zamzow et al., 2013). The kinetics of the triheteromeric NMDAr are governed mostly by GluN2A (Tovar et al., 2013). Increasing the expression of GluN2B in the frontal cortex promotes long-term potentiation and enhanced memory (Cui et al., 2011; Brim et al., 2013). It may be that the increased p1472 found in the frontal cortex of old mice with good reference memory is found on GluN2B/GluN1 receptors, giving an adaptive advantage over aged mice with poor memory.

The levels of p1336 declined significantly in the TxP fraction from frontal cortex of old mice with bad reference memory. At the same time, levels of p1472 in the TxP fraction from frontal cortex of old mice with bad reference memory remained similar to young mice. Recent evidence suggests that activation of the NMDAr does not affect p1472 and p1336 similarly. Activation of NMDAr causes a decrease in synaptic p1472, while p1336 remains unchanged (Ai et al., 2013). What is not known is if a decrease in NMDAr activation would lead to a change in p1336. It may be that old mice with bad reference memory suffer from a lack of NMDAr activation, keeping p1472 levels similar to young mice, while p1336 levels are decreased.

There were significant increases in Fyn levels in Txp from frontal cortex and hippocampus and in hippocampal TxS fractions from bad learners. The pattern of Fyn expression levels in the hippocampus roughly matches the pattern of p1472 and p1336 expression in the TxP, with the RB group having a numerical increase in all instances. The same cannot be said for the frontal cortex. The highest levels of Fyn in the TxP were in the RB group, but the highest levels of p1472 were in the RG group and the RB group had the lowest levels of p1336. This indicates that increased expression of Fyn cannot be the sole contributor to differential phosphorylation of the GluN2B subunit. Mice that overexpress Fyn have higher levels of p1472, but not p1336 (Knox et al., 2013). Fyn, PSD-95, and STEP61 all have their activity governed by phosphorylation (Braithwaite et al., 2006; Zhang et al., 2011; Trepanier et al., 2012). There may be an aging effect on the phosphorylation status of these proteins which alters their activity.

There were no significant group differences in levels of PSD-95 or STEP61 in any fractions from the frontal cortex or hippocampus. There was a small, but significant increase in expression of STEP46, an alternatively spliced isoform, in the S2 fraction from the hippocampus. STEP46 can bind to GluN2B, possibly to dephosphorylate p1472 (Snyder et al., 2005). STEP46 may have had an effect on phosphorylation of GluN2B in the hippocampus, but we were unable to detect any significant differences. There was a significant increase in GIPC in the TxP from the frontal cortex, with a greater amount found in the old good learners. Previous data from our lab found that poor memory correlated with GluN2B/GIPC association (Zamzow et al., 2013). GIPC is also able to bind to GluN1 and GluN2A subunits via its PDZ domain (Yi et al., 2007). The ESDV motif of GluN2B may be more available for GIPC to bind in old mice with poor reference memory. An increased presence of GIPC in the TxP from the frontal cortex suggests that

trafficking is perturbed, possibly due to increased residence time of NMDArs on synaptic membranes.

The relative levels of protein palmitoylation increased in an age-dependent manner in the frontal cortex, but not the hippocampus of mice. GluN2A, GluN2B, Fyn, and PSD-95 all had age-related increases in palmitoylation regardless of reference memory status. Palmitoylation of the C-terminus of GluN2 subunits promotes phosphorylation of tyrosine residues, specifically p1472 on GluN2B (Hayashi et al., 2009). We saw a significant rise in p1472 in the TxP from the frontal cortex for old mice with good reference memory, while levels of p1336 remained similar to young. It is not known if p1336 is affected by palmitoylation of GluN2B. The C-terminus of the GluN2B subunit undergoes calpain-mediated cleavage initiated by p1336 (Wu et al., 2007). We found that the 115 kDa GluN2B cleavage product was located in the TxS fraction, indicating a peri-/extrasynaptic localization. There was a significant group-related increase in cleaved GluN2B only in the TxS from the frontal cortex. This suggests that there is increase p1336 in the frontal cortex of aged mice with good reference memory. Because calpain cleavage of GluN2B subunits is fairly rapid (Guttmann et al., 2001), it may be that subunits with p1336 are unable to accumulate on synaptic membranes. It is interesting to note that calpain activity was increased in the frontal cortex and hippocampus, as witnessed by the calpain autolysis and PSD-95 cleavage products. The increased activity did not affect hippocampal GluN2B, which further supports the idea that increased palmitoylation in the frontal cortex may influence the modification of GluN2B subunits.

PSD-95 palmitoylation was significantly increased in an age-dependent manner. Palmitoylation of PSD-95 clusters the protein on synaptic membranes (El-Husseini Ael et al., 2002). Our data, however, showed no change in PSD-95 levels in the TxP from either the frontal cortex or hippocampus. Data indicates that mutating the N-terminal cysteine residues responsible for the palmitoylation of PSD-95 does not eliminate association with the synaptic membrane (Topinka and Bredt, 1998). In normal hippocampal neurons, the half-life of palmitate on PSD-95 is roughly 2 hours, but the half-life of the PSD-95 protein is 30 hours (El-Husseini Ael et al., 2002). This indicates dynamic cycling of PSD-95 on and off of synaptic membranes. The increased palmitoylation of PSD-95 in the frontal cortex of aged mice may indicate a perturbation in the palmitoylation cycle but not a change in localization.

In order to explain the increased palmitoylation of proteins in the frontal cortex of aged mice we examined fatty acid transport proteins, with the assumption that up-regulation of these transporters may be responsible for increased substrate for palmitoylation. We found no increase in expression in either the frontal cortex or hippocampus. We then focused on the depalmitoylating enzyme, APT1. There was an age-related increase in palmitoylation of APT1 in the frontal cortex, but not the hippocampus. APT1 expression increased significantly in aged mice in the TxS and S2 fractions from the hippocampus. Recent evidence has found that APT1 acts like a gatekeeper by residing on the Golgi apparatus to control excess palmitoylation of proteins, including APT1 (Vartak et al., 2014). Increased palmitoylation of APT1 would indicate that dynamic shuttling on and off of Golgi membranes may be diminished with age in the frontal cortex. Stimulation of the NMDAr is responsible for the rapid depalmitoylation of GluN2 subunits (Hayashi et al., 2009), PSD-95 (El-Husseini Ael et al., 2002), and the α-Amino-3-hydroxy-5-methyl-4-isoxazolepropionic acid receptor (AMPAr) (Hayashi et al., 2005). This suggests a link between the NMDAr and APT1.

In this study, we found that the posttranslational modification of GluN2B subunits was perturbed with age. Increased phosphorylation, calpain-mediated cleavage, and palmitoylation were evident in only the frontal cortex. Increased palmitoylation of APT1 in the frontal cortex suggested that the palmitoylation cycle may be disrupted in the aged brain. Further analysis of the link between APT1 and the NMDAr may elucidate the mechanism of activation of APT1.

Chapter 4
Xanthohumol treatment lowers plasma palmitate in aged mice

Formatted for submission to Behavioral Brain Research

Abstract

The protein palmitoylation cycle has been shown to be important for protein signaling and synaptic plasticity. Data from our lab showed a change in the palmitoylation status of certain proteins with age. A greater percentage of the NMDA receptor subunits GluN2A and GluN2B, along with Fyn and PSD95 proteins, were palmitoylated in the old mice. The higher level of protein palmitoylation was also associated with poorer learning scores. Xanthohumol is a prenylated flavonoid that has been shown to increase beta-oxidation in the livers of rodents, decreasing circulating free fatty acids in the serum. What is not known is whether the application of xanthohumol could influence the palmitoylation status of proteins. In this study, young and old mice were fed a diet supplemented with xanthohumol for 8 weeks. Spatial memory was assessed with the Morris water maze and protein palmitoylation quantified. The young xanthohumol-treated mice showed a significant improvement in cognitive flexibility. However, this appeared to be associated with the young control mice, on a defined, phytoestrogen-deficient diet, performing worse than normal and xanthohumol reversing this effect. The old mice receiving xanthohumol did not significantly improve their learning scores. Xanthohumol treatment was unable to affect the palmitoylation of NMDA receptor subunits and associated proteins assessed in this study. This evidence suggests that xanthohumol may play a role in improving cognitive ability when there is a phytoestrogen deficiency, but it may be ineffective in adjusting the palmitoylation status of neuronal proteins in aged individuals.

Introduction

Memory is a process that is vulnerable to degradation with the advancement of age. Indeed, many adults start to experience deficits in memory around 50 years of age and some aspects of cognition begin to decline around 40 years of age (Scherr et al., 1988; Singh-Manoux et al., 2012). Cognitive decline related to aging affects many mammalian species, from humans to primates to rodents, therefore rodents have served as an appropriate model for cognitive aging (Gallagher et al., 2011).

Although there is a clear loss of cognitive function with increased age, normal aging is not associated with gross morphological changes in the brain. Studies have demonstrated that there appears to be no significant change in neuron cell number in the prefrontal cortex or hippocampus of humans (West et al., 1994; Pakkenberg and Gundersen, 1997), primates (Gazzaley et al., 1997; Keuker et al., 2003), or rodents

(Rapp and Gallagher, 1996; Merrill et al., 2001). Similarly, the extent of dendritic branching shows no significant age-related decline in the hippocampus of humans (Flood et al., 1987; Hanks and Flood, 1991), primates (Flood, 1993), or rodents (Turner and Deupree, 1991). Recent evidence suggests that the morphology of hippocampal synaptosomes and synaptic vesicles may not be altered with increased age (VanGuilder et al., 2010). Areas of the prefrontal cortex, however, may be vulnerable to dendritic loss with age in humans (de Brabander et al., 1998) and rodents (Markham and Juraska, 2002), suggesting a potential difference in the modes of age-related decline in neuronal function in the prefrontal cortex and hippocampus.

While the morphology of neurons may not be greatly altered with age, the expression of many synaptic proteins is significantly affected by aging (Xiong and Chen, 2010). Specifically, the GluN2B subunit of the NMDA receptor and the scaffolding protein PSD-95 are particularly vulnerable to decline with increased age in the hippocampus of rodents (VanGuilder et al., 2011; Magnusson, 2012). Recent evidence suggests that the relationship between PSD-95 and GluN2B may be altered during aging in the frontal cortices of mice (Zamzow et al., 2013). Data from our lab (Zamzow et al., 2012) suggested that age-induced alterations in protein-protein interactions might be due to increased palmitoylation of those proteins, which may have led to the decline in spatial memory.

Protein palmitoylation is a post-translational modification whereby a 16 carbon fatty acid, palmitate, is covalently bound to a free sulfhydryl on the cysteine of a protein via a labile thioester bond. Palmitoyl-CoA, the esterified biologically active form of palmitate, serves as the substrate for palmitoyltransferase enzymes. Protein palmitoylation is an important regulator of synaptic plasticity (Fukata and Fukata, 2010). The NMDA receptor subunits GluN2A and GluN2B are both palmitoylated under normal conditions (Hayashi et al., 2009). Palmitoylation of these NMDA receptor subunits affects localization of the receptor by enhancing access of the Src kinase, Fyn, to its substrate on the C-terminus of the GluN2B subunit (Hayashi et al., 2009). Fyn and PSD-95 are also palmitoylated, which enriches each protein on synaptic membranes (El-Husseini Ael et al., 2002; Sato et al., 2009). Interestingly, depalmitoylation of PSD-95 is required for internalization of AMPA receptors, but not NMDA receptors (El-Husseini Ael et al., 2002). However, it may be that a global increase in the percentage of neuronal proteins that are palmitoylated could lead to significant perturbations in trafficking and localization of NMDA receptors.

A consequence of aging in humans and rodents is a redistribution of fat deposition from adipose tissue to muscle and liver, leading to metabolic syndrome in many elderly (Tchkonia et al., 2010). Cellular metabolism undergoes an age-associated increase in lipogenesis (Kuhla et al., 2011). Evidence also indicates that the lipid composition of the brain in rodents and humans changes with age. In humans, there is a small, but significant increase in the levels of palmitate in erythrocytes, which is matched in the cerebral cortex (Carver et al., 2001). In mice, palmitate shifts more towards phosphatidylcholine (PC) membranes and the turnover rate decreases during aging (Ando et al., 2002). Manipulations of fatty acids can affect memory. Mice fed a high fat diet performed much worse in the Morris water maze than control mice (Pancani et al., 2013). These studies indicate that aging results in perturbed fatty acid metabolism and the presence of increased fat can lead to poorer spatial memory. This led us to hypothesize that fatty acid changes during aging could contribute to the increase in palmitoylated proteins in aged individuals.

Xanthohumol is a prenylated chalconoid present in hops (Stevens and Page, 2004). The compound has been used to successfully lower body weight and fasting glucose in a rat model of obesity, Zucker fa/fa (Legette et al., 2013). Xanthohumol appears to increase beta-oxidation of fatty acids in the liver and reduce overall cellular oxidative stress (Kirkwood et al., 2013). What is not known is whether xanthohumol could specifically reduce total plasma palmitate and/or palmitoylation of proteins important to synaptic plasticity in an aged rodent.

We also addressed whether steady-state palmitoyl-CoA pools may be influencing the age-related increase in palmitoylated proteins in the frontal cortex of mice and whether these could be altered by Xanthohumol. The goal of this study was to increase beta-oxidation in the livers of old mice with a dietary supplement, xanthohumol. The hypothesis tested was that supplementation would decrease the systemic levels of palmitate, which could lower the steady-state levels of palmitoyl-CoA and palmitoylation in the brain and lead to better spatial memory performance in old mice.

Materials and Methods

Animals

A total of 55 male C57BL/6 mice from two age groups (3 and 24 months of age) were used for the study. The older age group was obtained from National Institute on Aging,

NIH. Young mice were purchased from JAX mice (Bar Harbor, MA), which stocks the NIH colony. They were fed *ad libitum* and housed with a 12/12 h light/dark cycle. After the behavioral testing, all animals were euthanized by exposure to CO_2 and decapitated. Blood was collected in heparin-treated vials (BD Bioscience, San Jose, CA) and stored on ice until further processed. The brains and livers were harvested, frozen in dry ice and stored at −80^{o}C.

Treatment

A total of 49 mice (24 young, 25 old) were fed a diet with or without xanthohumol for a duration of 8 weeks. Xanthohumol was emulsified by mixing 547 mg of xanthohumol powder (gifted from ABInBev) with a solution consisting of 12.6 g oleic acid, 14 g propylene glycol, and 14 g Tween 80 (OPT). A modified diet (Dyets, Inc, Bethlehem, PA) was made by mixing 20 g of either OPT or xanthohumol emulsion with 1 kg of modified AIN-93G defined diet. The AIN-93G formula was made free of soy isoflavones by substituting corn oil for soybean oil.

Six additional mice (3 young, 3 old), separate from the spatial memory study, were treated with xanthohumol via gavage in order to measure xanthohumol concentrations in the cerebral cortex. Xanthohumol was emulsified in OPT to a final concentration of 1.4 mg xanthohumol/100 μl of OPT for old mice and 1 mg/100 μl OPT for the young mice. The mice were gavaged once daily with 100 μl of xanthohumol/OPT emulsion for a total of 5 days. All animals were euthanized by exposure to CO_2 and decapitated, with the brain immediately harvested, frozen on dry ice, and stored at -80°C until further processed.

Behavioral testing

Spatial reference memory, cognitive flexibility and associative memory (cued control task) were tested with the use of the Morris water maze as previously described (Das et al., 2012). Briefly, for the first two days, mice were acclimated to the water maze, followed by 4 days of testing for spatial reference memory, 1 day of reversal training to test cognitive flexibility and 1 day of associative memory testing (cued control task). Reference memory consisted of 8 place trials per day and probe trials at the end of each day. A naive probe trial was performed at the beginning of the first day of memory testing. The platform was kept in the same quadrant for each place trial. Place trials consisted of a maximum of 60 seconds in the water searching for the platform, 30 seconds on the platform and 2 minutes of cage rest. If a mouse failed to find the platform

within the designated 60 second swim time, it was led to the platform by the experimenter. Probe trials were performed to assess the animal's ability to show a bias for the platform location. During the probe trial, the platform was removed and the mouse was allowed to search in the water for 30 seconds. After 4 days of place trials, a reversal task was performed in order to assess cognitive flexibility. The platform was placed in the opposite quadrant in the tank, but there were 8 place and 1 probe trial, similar to the reference memory task. Cued trials were designed to test motivation, visual acuity, and physical ability for the task. The mice performed 6 cued trials. The positions of entry and the platform positions varied between trials. The platform was kept submerged, but was marked by a 20.3 cm support with a flag. The mice were allowed to search for the platform for 60 seconds. The animal's movements in the water maze were tracked and analyzed with the SMART tracking system (San Diego Instruments, San Diego, CA).

Tissue processing

The rostral 4 mm of the frontal cortex and the hippocampi from each brain were dissected. The remaining caudal cortex was reserved for xanthohumol assays and protein standards. The frontal cortices and hippocampi were homogenized on ice in a Dounce homogenizer with 500 μl of homogenization buffer. The homogenization buffer consisted of 10mM ammonium acetate (pH 5.3) with 1.0 nM 17:0 CoA internal standard (Avanti Polar Lipids, Alabaster, AL) and 10 mM N-ethylmaleimide (NEM). Homogenization involved 12 strokes from each of 2 pestles of increasing sizes in homogenization buffer, followed by addition of 1.0 ml of chloroform:methanol, (1:2, v/v) and 10 more strokes from the larger pestle. An additional 1.5 ml of chloroform:methanol (1:2, v/v) was added to the homogenate. The mixture was vortexed and centrifuged at 4500xg for 15 minutes in a hanging bucket Beckman J2-HC centrifuge . The top layer, containing acyl-CoA; lower organic layer, and protein interface were all separated. The acyl-CoA and organic layers were purged with nitrogen and stored at -80°C until further processed. The protein pellet was resuspended in 4SB buffer (50 mM Tris-HCl, pH 7.4, 150 mM NaCl, 5 mM ethylenediaminetetraacetic acid (EDTA), 4% sodium dodecyl lsulfate (SDS),10 mM NEM, and protease inhibitor cocktail (Sigma, Saint Louis, MO)) and aliquots were saved and stored at -80°C until further processed.

Blood samples were centrifuged at 1000g for 10 minutes in a tabletop Eppendorf 5415C centrifuge . The plasma was removed and stored at -80°C until further processed.

Approximately 200 mg of liver tissue was weighed from each mouse and homogenized in 1.0 ml of ice cold methanol:water (90:10, v/v). Whole cortices (450-500 mg) from gavaged mice were homogenized in 2.0 ml of ice cold methanol:water (90:10, v/v). Samples were centrifuged at 4000g for 10 minutes in a tabletop centrifuge. The supernatant was removed and stored at -80°C until further processed.

Acyl-biotinyl exchange

In order to quantify levels of protein palmitoylation, proteins were subjected to the acyl-biotinyl exchange method as previously described (Wan et al., 2007). Briefly, protein lysates from the separation described above were thawed and mixed with rotation at 4°C overnight. Excess NEM was stripped and proteins were precipitated with three sequential chloroform:methanol (1:3, v/v) precipitations. Precipitated proteins were solubilized in 300 μl of 4SB and diluted with 1.2 ml of +HA buffer (0.7 M hydroxylamine, pH 7.4, 0.4 mM N-[6-(Biotinamido)hexyl]-3'-(2'-pyridyldithio)propionamide (HPDP-biotin) (Pierce, Rockford,IL), 0.2% Triton X-100, 150 mM NaCl, protease inhibitor cocktail) or 1.2 ml of –HA buffer (50 mM Tris-HCl, pH 7.4, 0.4 mM HPDP-biotin, 150 mM NaCl, 0.2% Triton X-100). The mixtures were incubated with rotation at room temperature for 2 hours, followed by 3 sequential chloroform:methanol (1:3, v/v) precipitations. Precipitated proteins were solubilized in 150 μl of 2SB buffer (50 mM Tris-HCl, pH 7.4, 2% SDS, 5 mM EDTA, 150 mM NaCl, protease inhibitor cocktail) and diluted in 2.8 ml of buffer LB (50 mM Tris-HCl, pH 7.4, 150 mM NaCl, 5 mM EDTA, protease inhibitor cocktail, 0.2% Triton X-100). Proteins were precipitated from the mixture by incubation with 60 μl of Streptavidin-agarose (Pierce) for 2 hours at room temperature with rotation. Beads were pelleted, washed 3 times in LB, and proteins were eluted by boiling the beads in 150 μl of LB + 10% β-mercaptoethanol.

Xanthohumol analysis

Aliquots of plasma, liver, and brain extractions from each mouse were subjected to enzymatic hydrolysis as previously described (Legette et al., 2012; Legette et al., 2014). Briefly, 20 μl of extract was mixed with 380 μl 0.1M sodium acetate, pH 4.7; 10 μl internal standard 4,2 dihydroxychalcone, and 600 U of *Helix pomatia* sulfatase/glucuronidase. Samples were incubated at 37°C for 2 hours, followed by vortexing, and centrifugation at 12000 g for 2 minutes in a tabletop centrifuge. Samples were extracted with Whatman filter paper 8X45 mm and the paper was dried overnight in a vacuum desiccator over Drierite. Dry paper strips were extracted with 500 μl of

acidified methanol (0.1% formic acid in methanol) for 30 minutes at room temperature. Liquid chromatography with tandem mass spectrometry (LC-MS/MS) was performed on an Applied Biosystems 4000 QTRAP hybrid linear ion trap-triple quadrupole instrument (AB Sciex, Framingham, MA) operated at a source temperature of 600°C with a needle voltage of -4500 kV. Nitrogen was used as the source gas, curtain gas, and collision gas. Selected reaction monitoring (SRM) experiments were conducted at collision energies ranging from -25 to -40 eV. Chromatographic separations of xanthohumol and its metabolites were carried out on a 2X50mm Zorbax 300SB C8 column (Agilent, Santa Clara, CA). The elution gradient consisted of 25–60% solvent B (0.1% formic acid in acetonitrile) in solvent A (aqueous 0.1% formic acid) for 2.6 minutes at a flow rate of 0.5 ml/minute after an initial 1.4 minutes at 25% solvent B. The column was washed with 100% solvent B for 1.4 minutes and re-equilibrated at 25% solvent B for 9 minutes prior to each injection. Concentrations were calculated using the internal calibration method and Analyst Software (Analyst 1.5, AB Sciex).

Fatty acid analysis

Aliquots of plasma were treated as previously described (Zehethofer et al., 2008). Briefly, 20 μl of plasma was mixed with 2 μl of internal free fatty acid standard 19:1 (final conc, 2 μM; NuChek, Waterville,MN). The plasma/standard mixtures were added to 100 μL of a solvent mixture (methanol: n-hexane: phosphoric acid (2M), (40:10:1, v/v)) and vortexed. After 5 minutes, 140 μl of n-hexane and 60 μl of water were added, vortexed and centrifuged for 5 minutes at 12000g in a tabletop centrifuge. The organic supernatant was transferred to another vial, dried under a nitrogen stream, and reconstituted in 100 μl of acetonitrile.

The organic layers extracted from the frontal cortices and hippocampi were dried under nitrogen and reconstituted in 1 ml of chloroform:methanol (2:1, v/v). A 500 μl aliquot of reconstituted organic extracts was combined with 10 μl of internal free fatty acid standard 19:1 (final concentration 10 μM; NuChek) and subjected to base hydrolysis by adding 1 ml of 1M KOH in methanol:water (7:3, v/v) and incubated for 5 minutes at 50^{o}C. The mixture was vigorously shaken, and then 1 ml of hexane (pH adjusted to 3 with 5M HCl) was added and vortexed again. The upper hexane layer was transferred to a 1 ml vial, dried under nitrogen, and reconstituted in 1 ml of acetonitrile.

Ultra high-pressure liquid chromatography was performed on a Shimadzu Nexera system (Shimadzu, Kyoto, Japan) coupled to a hybrid quadruple-time of flight (TOF)

mass spectrometer (MS) AB SCIEX Triple TOF 5600. Chromatographic separations were carried out on an ACQUITY UPLC HSS T3 column (100 × 2.1 mm, 1.8 μm, Waters, Milford, MA). Mobile phases consisted of water (A) and acetonitrile (B), both with 0.1% acetic acid. The elution gradient was as follows: 0 minute, 60% B; 3.5 minute, 90% B with a 0.3 ml/minute flow rate; 10 minute, 100% B; 13.5 minute, 60% B with a 0.6 ml/minute flow rate. The column temperature was held at 45°C, and the injection volume was 10 μL. The instrument was operated at a source temperature of 500°C and IonSpray voltage of -4500 kV. The instrument was set in negative ion mode and the information-dependent MS/MS acquisition mode, with the collision energy set at -45 V and a collision energy spread of 10 V. TOF MS acquisition time was 0.25 seconds, and MS/MS acquisition time was 0.1 seconds. The scan range was 70–1200 *m*/*z* for TOF MS and 50–1200*m*/*z* for MS/MS. Ion source gas 1 and 2 and curtain gas (all nitrogen) were set at 45, 50, and 35, respectively. Quantitation of analyte peaks was carried out with Peakview software (Ab Sciex).

Acyl-CoA analysis

Acyl-CoA molecules were extracted from frontal cortices and hippocampi separately as previously described (Kasuya et al., 2009). Briefly, acyl-CoA samples were washed twice with 2 ml of 10 mM ammonium acetate (pH 5.3): chloroform (1:1, v/v). The top aqueous layers from each wash were removed, combined, and dried under nitrogen. The acyl-CoA extracts were reconstituted in 100 μl of 10 mM ammonium acetate (pH 5.3).

LC-MS/MS was carried out on an Applied Biosystems 4000 QTRAP hybrid linear ion trap-triple quadrupole instrument (AB Sciex) operated at a source temperature of 550°C with a needle voltage of **-**5200 kV. Chromatographic separations were carried out on XTerra MS C8 column (2.1 x 50 mm, 2.5 μm, Waters) at a temperature of 40°C. The mobile phases consisted of (A)10 mM ammonium formate (pH 5.5) and (B) acetonitrile. The elution gradient was as follows: 0 minute, 20% B; 2.8 minute, 45% B; 3 minute, 25% B; 4 minute, 65% B; 9 minute, 90% B; 9.1 minute, 100% B; 12.1 minute, 20% B with a flow rate of 0.3 ml/minute. Multiple reaction monitoring was carried out in the positive ion mode. Concentrations were calculated using the internal calibration method and Analyst Software (Analyst 1.5, AB Sciex).

Western blot

Sodium dodecyl sulfate–poly acrylamide gel electrophoresis (10%) was used for Western blotting as described previously (Zhao et al., 2009). Each gel contained 4 different μg loads (2, 4, 8 and 16 μg/well) of standards, obtained from homogenate prepared by combining caudal cortices from all naïve young animals. Protein samples from representatives of each different age/treatment group were loaded on each gel and analyzed in triplicate. Proteins were transferred to PVDF membranes, blocked in Odyssey blocking buffer (LiCor, Lincoln, NE): Tris-buffered saline (TBS) (1:1, v/v) and incubated at 4°C in one of the following primary antibodies (diluted in blocking buffer): GluN2B (Millipore, Billerica, MA; 1:1000 dilution), GluN2A (Santa Cruz, Santa Cruz, CA ; 1:250), Fyn (Santa Cruz; 1:250), PSD-95 (ThermoScientific, Waltham, MA; 1:1000), Flotillin (Santa Cruz; 1:250) or GAPDH (Calbiochem, Millipore, 1:10000). Membranes were rinsed three times with TBS-T and incubated in fluorescence-based secondary antibody (Rockland Immunochemicals, Gibertsville, PA; 1:5000) diluted in blocking buffer. Bands were visualized by scanning in the LI-COR Odyssey imager.

Data analysis

Data for behavioral testing were analyzed as previously described (Das et al., 2012). Cumulative proximity measures, which reflect search distance from the platform, were used for the place, reversal and cued trials and average proximity measures were used for probe trials (Gallagher et al., 1993). In order to establish a lab standard to compare to the controls in this study, we averaged reference memory performances from days 1 & 2 for control young (N=59) and old (N=70 from two previous studies in the lab ((Zamzow et al., 2013) and unpublished data), in which animals were maintained on a chow diet and had undergone behavioral testing for reference memory similar to the present study for at least 2 days. Protein blots were analyzed using Li-Cor Odyssey software. Integrated intensity measures were obtained using median background subtraction method. A standard curve was obtained using a linear fit with Excel (Microsoft) from integrated intensity values for known loads of caudal cortex. Sample values were interpolated from the standard curve as caudal cortex equivalents. Each protein was normalized to GAPDH within each sample of total protein. Because the relative percentage of Flotillin molecules that are palmitoylated does not change with age (Bhattacharyya et al., 2013), all proteins precipitated through ABE were normalized to Flotillin. Statistical analyses for behavioral trials, protein expression, xanthohumol, acyl Co-A and fatty acids using data

from individual animals, were done with analysis of variance (ANOVA) followed by Fisher's protected least significant difference (PLSD) using Statview software (SAS Institute). Based on previous findings from our lab that showed differential associations of frontal and hippocampal NMDA receptors with different phases of learning in place trials (Das et al., 2012; Brim et al., 2013), we also examined each day of reference memory testing separately.

Results

Xanthohumol distribution and effects

The average daily food intake for an adult male C57BL/6 mouse has previously been documented to be around 4 g/day (Bachmanov et al., 2002). Accordingly, the amount of xanthohumol administered in the diet was calculated to be 1 mg xanthohumol/4 g of diet or approximately 30 mg xanthohumol/kg body weight/day. Previous data had shown that fatty acid metabolism, body weight, and glucose were significantly altered in Zucker fa/fa rats when fed 16.9 mg xanthohumol/kg body weight (Legette et al., 2013). Therefore, a daily dose approximating 30 mg/kg body weight was expected to significantly alter the fatty acid metabolism in the test mice.

Dietary consumption was monitored biweekly in all groups. The average dietary intake was approximately 2.7 g of diet/day for each of the 4 groups (Fig. 4.1A). Dietary intake was not significantly affected by age ($F_{(1,43)}$=.004, p=.95) or treatment ($F_{(1,43)}$=.08, p=.78). However, the lower than expected intake reduced the estimated xanthohumol dosage to about 20 mg/kg/day. The mice were also weighed biweekly and the total change in body weight over the 8 weeks of treatment was documented for each animal (Fig. 4.1B). There was no significant effect of treatment ($F_{(1,43)}$=.35, p =.56), however there was a significant difference between ages ($F_{(1,43)}$=8.6, p=.005) with respect to total weight gain (Fig. 4.1B), with young gaining more weight than old.

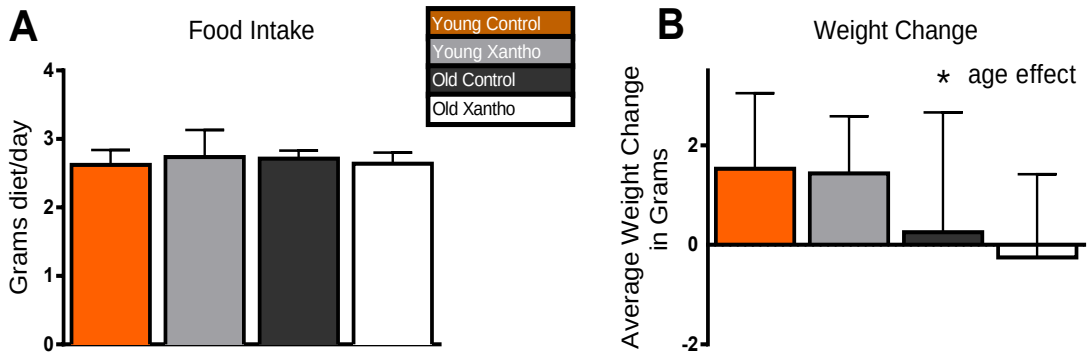

Figure 4.1. Dietary intake and body weight change of xanthohumol-treated mice. The average daily food intake did not vary by age or treatment (A). There was an aging effect, but not a treatment effect in weight change during the study (ANOVA and Fisher's PLSD). (B). Data = mean +/- SEM. N=12-13.

The concentration of xanthohumol in wet tissue extracts of liver, plasma, and brain were measured with HPLC-MS/MS. There was a non-significant increase in xanthohumol concentration in the liver ($F_{(1,19)}$= 2.18, p=.17; Fig. 4.2A). Old and young mice differed little in plasma concentration ($F_{(1,14)}$=.12, p = .73; Fig. 4.2B) in the long-term feeding study. The initial attempts to quantify xanthohumol in the brains of behaviorally-tested mice were limited to caudal cortical regions without the frontal cortex and hippocampus that were used for the rest of the analyses. The limited tissue, coupled with a lower than expected dosage of xanthohumol, provided a signal that was too low to quantify. In order to determine if xanthohumol was able to cross the blood-brain barrier, 3 young and 3 old mice were gavaged with xanthohumol emulsion (40mg/kg) for five days. Xanthohumol was extracted from the whole cortex, including hippocampus, of each mouse. There was no significant effect of age on xanthohumol concentration in the cortex ($F_{(1,5)}$=.685, p =.45; Fig 3.2C). Although only a small percentage of the plasma xanthohumol concentration was found in the cortices of the mice (Fig. 4B,C), the compound was able to cross the blood-brain barrier in quantifiable amounts.

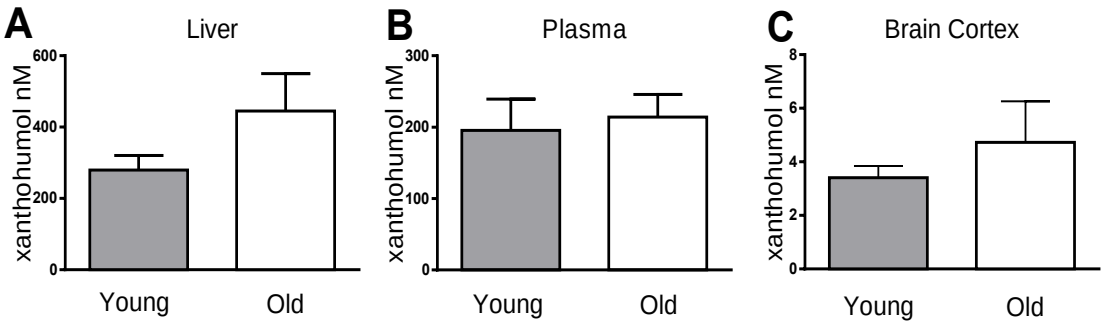

Figure 4.2. Xanthohumol tissue concentrations. Concentrations of xanthohumol were examined by HPLC-MS/MS in the (A) liver, (B) plasma, and (C) cortex of young and old treated mice. There were no significant difference between ages (ANOVA and Fisher's PLSD). Data = mean +/- SEM. N =3-8.

Behavioral testing

The spatial memory and cognitive flexibility of the mice was assessed over 5 days in the Morris water maze. The first four days, the mice searched for the hidden platform in the same quadrant of the maze and then were tasked with finding the platform in the opposite quadrant on the fifth day. There was a near significant overall effect of age ($F_{(1,45)}$=3.66, p=.06) , but no effect of treatment ($F_{(1,45))}$=1.9, p=.18) across four days of reference memory. Analysis of each day of platform trials for reference memory showed a significant effect of age during the fourth ($F_{(1,45)}$=6.27, p=.016) day of testing and a near-significant effect of age on the first day ($F_{(1,45)}$=3.44 p=.07), with old mice having higher cumulative proximity to the platform, indicating that they spent more time searching further from the platform than the young mice (Fig. 4.3A). There was a near significant effect of treatment ($F_{(1,45)}$=3.62 p=.064) on reference memory trials on Day 2, with xanthohumol-treated mice having lower cumulative proximities than controls (Fig. 4.3A) There was a significant overall effect of age on probe trials ($F_{((1,45)}$=6.4, p=.015), with old mice having higher average proximities than young, but no effect of treatment ($F_{(1,45)}$=1.3, p=.26; Fig. 4.3B). The reversal platform trials did not show any significant effect of treatment ($F_{(1,44)}$=.03, p =.86) or age ($F_{(1,44)}$=2.23, p=.14). There was no significant main effect of age ($F_{(1,45)}$=1.5, p=.22) or treatment ($F_{(1,45)}$=2.72, p=.11) during the reversal probe trial, but there was a significant interaction between age and treatment ($F_{(1,45)}$=6.22, p=.016). A closer examination revealed a significant treatment effect in the young mice (p=.01), but not the old (p =.54), with the xanthohumol-treated young mice having a significantly lower average proximity during the reversal probe trial

than the young controls (Fig. 4.3C). There was no significant effect of age ($F_{(1,45)}$=.18, p =.67) or treatment ($F_{(1,45)}$=..01, p=.92) on cumulative proximity in the cued trials (young control (mean±SEM; 853±142 cm), young treatment (1085±166 cm), old control (1170±161 cm), old treatment (905±139 cm).

Xanthohumol is known to increase beta-oxidation, leading to increased mitochondrial respiration (Kirkwood et al., 2013). The average swim speed of each group was compared in order to account for the possibility of a treatment-induced increase in mobility. There was no significant main effect of age ($F_{(1,45)}$=1.32, p=.26) or treatment ($F_{(1,45)}$=1.49, p=.23) on average swim speed in place trials (Fig. 4.3D).

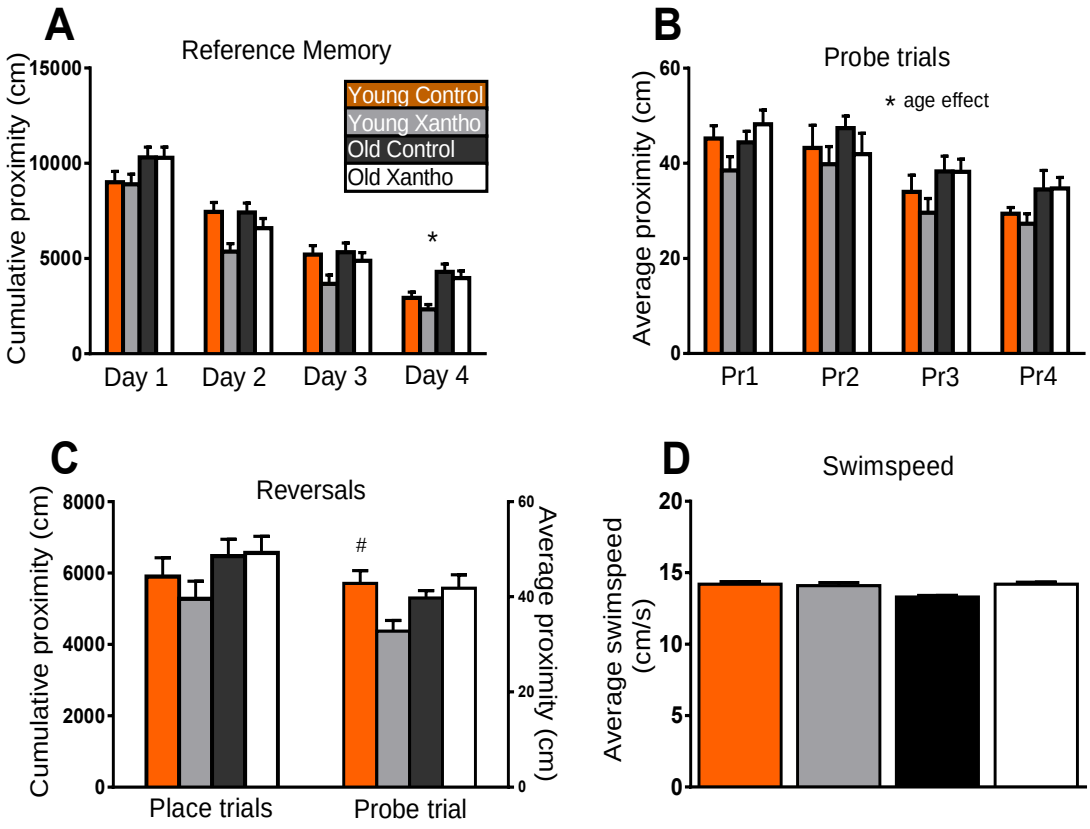

Figure 4.3. Behavioral testing. Behavioral performances shown for place (A) and probe (B) trials for reference memory and reversal trials for cognitive flexibility (C). Xanthohumol treatment was effective in enhancing performance in young mice in reversal probe trials (C). Old mice performed worse than young in probe trials (B) and on Day4 in place trials (A). A significant treatment effect was evident in young mice during reversal probe trials (C). There was no effect of age or treatment on swim speed in place trials (D). * p<.05 for difference between young and old. # p<.0001 for young control vs. young treated. (ANOVA and Fisher's PLSD). N=12-13. Data = mean +/- SEM. Pr1-4, probe trial number.

When performance in the first two days of place and probe trials and in the reversal trials from this study were compared to previous studies, with at least two days of reference memory testing (Brim et al., 2013; Zamzow et al., 2013), a difference in the proximity scores of the young controls was noted. The control groups in this study were then statistically compared to controls averaged across two previous studies (59 young, 70 old), designated as lab standard (Std)(see Methods). There was a significant effect of study on place ($F_{(1,150)}$=9.53, p=.002) and probe ($F_{(1,150)}$=10.98, p=.001) trials and a significant interaction between age and study ($F_{(1,150)}$=11.14, p=.001) in place and probe ($F_{(1,150)}$=9.87, p=.002) trials. Significantly higher proximity scores were seen in young control mice from this study in place trials and in probe trials, as compared to the lab standard scores (Fig. 4.4).

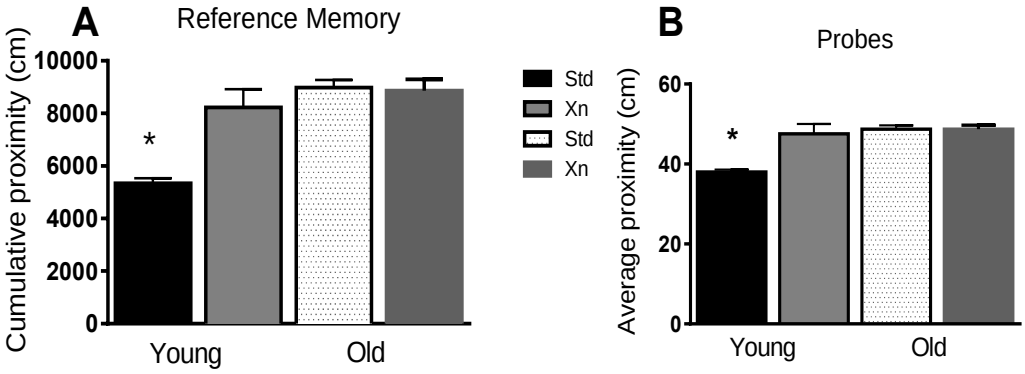

Figure 4.4. Comparison of behavioral data between studies. Significantly higher cumulative proximities were seen in young control mice from this study (Xn) as compared to previous studies in the lab (Std) in an examination of the first 2 days of place (A) and probe (B) trials for spatial reference memory* denotes p<.01 for difference between the present study and previous studies in the lab. Data = mean +/- SEM. N = 12-70.

Palmitate and palmitoyl-CoA concentrations

Palmitate is the precursor to palmitoyl-CoA and palmitoyl-CoA is the substrate needed for protein palmitoylation. Reducing the concentration of palmitate may, theoretically, lead to a reduction in protein palmitoylation. Xanthohumol is effective in increasing beta-oxidation in the livers of rodents, thereby lowering plasma fatty acids (Legette et al., 2013). In order to assess the ability of xanthohumol to reduce palmitate in this study, plasma and brain samples were evaluated by LC-MS/MS. There was a significant effect

of age ($F_{(1,28)}$=10.93, p=.002; Fig. 4.5A) and treatment ($F_{(1,28)}$=6.14, p=.01) on plasma palmitate. Old individuals had less plasma palmitate than young and xanthohumol-treated mice showed lower plasma palmitate than controls (Fig. 4.5A).

Examination of the relative percentage of palmitate in total fatty acids in the frontal cortex and hippocampus of mice yielded no significant main effect of age ($F_{(1,56)}$=.04, p=.84) or treatment ($F_{(1,56)}$=.84; p=.36), but there was a significant effect of brain region ($F_{(1,56)}$=83, p<.0001) and a significant interaction between age and brain region ($F_{(1,56)}$=8.38, p=.005; Fig. 4.5B). The relative percentage of palmitate was significantly higher overall in the frontal cortex, as compared to the hippocampus, and within the old hippocampus, as compared to young (p=.04; Fig. 4.5B). However, palmitate was nearly significantly lower in the frontal cortex of old mice, as compared to young (p=.058; Fig. 4.5B).

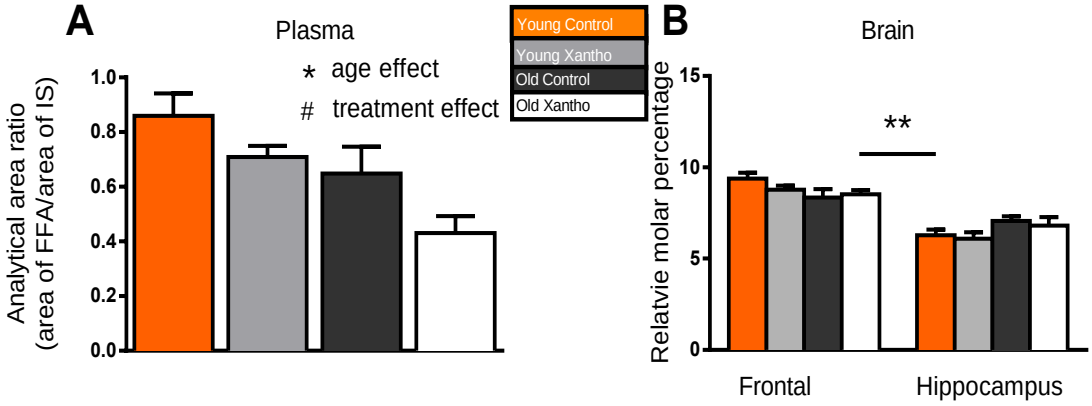

Figure 4.5. Relative amounts of palmitate in plasma and brain. A) Xanthohumol-treated mice had significantly lower plasma palmitate across ages and old mice had lower plasma palmitate than young across treatments. B) The molar percentage of palmitate was unaffected by treatment in the frontal cortices and the hippocampi of young and old mice. ** denotes p < .0001 for difference between frontal cortices and hippocampi.* denotes p<.01 for difference between ages. # denotes p<.05. Data = mean +/- SEM. N =8. FFA=free fatty acids; IS=internal standard.

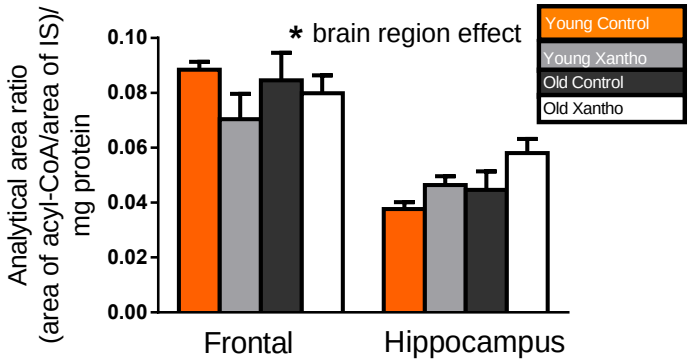

Figure 4.6. Palmitoyl-CoA levels in frontal cortex and hippocampus. Xanthohumol treatment did not affect palmitoyl-CoA levels in the frontal cortex or hippocampus of mice (ANOVA and Fisher's PLSD). FFA= free fatty acids; IS=internal standard. Data = mean +/- SEM. N =8.

Next, the relative amount of palmitoyl-CoA was measured in the frontal cortex and hippocampus from each mouse. There was no significant main effect of age ($F_{(1,56)}$=..66, p =.42) or treatment ($F_{(1,56)}$=.45, p=..51), but there was a significant effect of brain region ($F_{(1,56)}$=64, p<.0001) in palmitoyl-CoA (Fig. 4.6). When the regional differences in brain palmitoyl-CoA were examined, the frontal cortex was found to have a significantly higher level of palmitoyl-CoA than the hippocampus (Fig. 4.6).

Protein palmitoylation

Previous evidence from our lab (Zamzow et al., 2012) demonstrated that protein palmitoylation was disturbed in the frontal cortices of old mice. Specifically, the percentage of GluN2B, GluN2A, Fyn, and PSD95 that were palmitoylated was greater in the frontal cortices, but not the hippocampi, of old mice. Xanthohumol treatment was applied in order to determine if it could modify the palmitoylation status of proteins in the frontal cortices of old mice. There were significant main effects of age on the percentage of palmitoylated proteins for PSD-95 ($F_{(1,22)}$=105, p<.0001; Fig. 4.7A), Fyn ($F_{(1,18)}$=40, p<.0001; Fig. 4.7B), GluN2B ($F_{(1,28)}$=63, p<.0001; Fig. 4.7C), and GluN2A ($F_{(1,28)}$=106,p<.0001; Fig. 4.7D) in the frontal cortex. For each protein, there were significantly more palmitoylated proteins in the frontal cortex of old mice than the young (Fig. 4.7). There was a significant effect of treatment in the percentage of palmitoylated GluN2A in the frontal cortex, with xanthohumol treatment being associated with an increase in palmitoylation of GluN2A across ages ($F_{(1,28)}$=6.4 ,p<.017; Fig. 4.7D). There were no significant effects of treatment on the other proteins in the frontal cortex

(p =.26-.89; Fig. 4.7). There were no significant effects of age (p=.14-.65) or treatment (p=.15-.72) on the palmitoylation status of proteins in the hippocampus (Fig. 4.7).

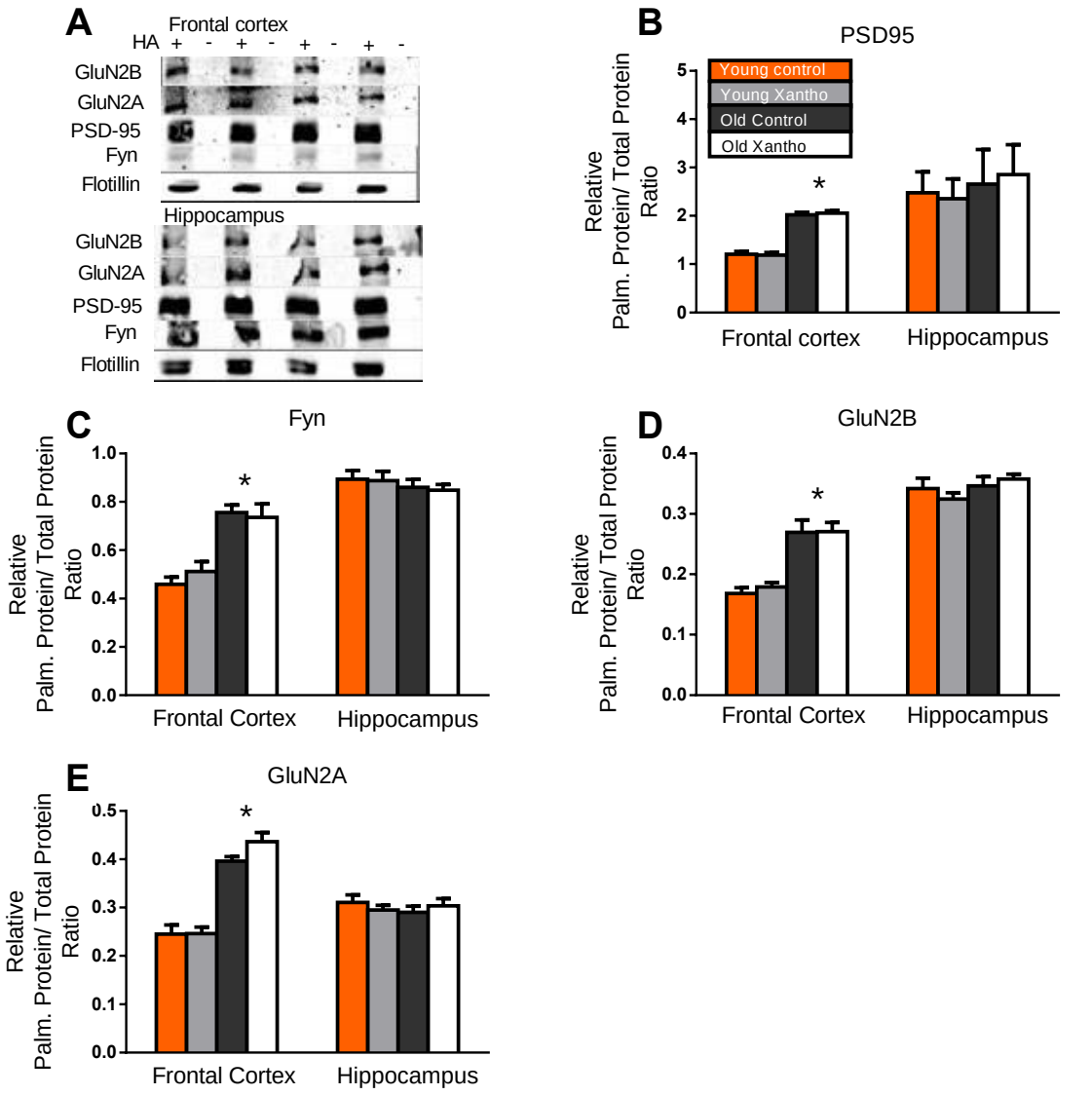

Figure 4.7. Protein palmitoylation. A significant age-related increase in the relative percentage of (B) PSD95, (C) Fyn, (D) GluN2B and (E) GluN2A that were palmitoylated in the frontal cortices, but not the hippocampi of mice. A representative blot (A) of palmitoylated proteins. * denotes p < .0001 for difference between young and old mice (ANOVA and Fisher's PLSD). Data = mean +/- SEM. N =6-8. HA=hydroxylamine.

Discussion

In this study, young and old mice were treated with xanthohumol for 8 weeks. Xanthohumol improved cognitive flexibility in the young treated mice, as compared to age-matched controls. Xanthohumol was able to lower palmitate in the plasma in both young and old mice. Regional comparisons of palmitate and palmitoyl-CoA in the brain revealed significantly higher levels of each molecule in the frontal cortex versus the hippocampus. Relative protein palmitoylation levels were also increased significantly in the frontal cortex with increasing age, but there were no aging changes in the hippocampus. Xanthohumol treatment was unable to reduce palmitoylation levels in any brain region or age of mouse.

There was a significant decline with increased age in spatial reference memory and cognitive flexibility, when data was averaged across treatments, similar to previous findings in C57BL/6 mice (Brim et al., 2013; Zamzow et al., 2013) and other species (Magnusson et al., 2010). Xanthohumol was not effective in significantly reversing these effects in the aged mice. Xanthohumol did improve cognitive flexibility in the young mice and showed a trend for enhancing spatial learning in young and old mice. However, this appeared to be mostly due to the young mice on the control diet performing similar to old controls and worse than young controls previously studied our lab (Brim et al., 2013; Zamzow et al., 2013) and the xanthohumol reversing this effect. We were able to show worse performance in reference memory in the young controls in this study. We were not able to directly compare the reversal probe trials between this study and our previous studies, because previously we only performed 2 days of reference memory testing before conducting the reversal trials. Animals in this study had two more days of learning of the original platform location, so the reversal trials were not directly comparable. However, the fact that young controls in this study performed similarly to old controls in both reversal probes and in place trials averaged over Days 1 and 2 in this study, suggests that control young in this study performed worse than expected in reversal probes too.

The primary difference among the studies, in which the behavioral results were compared, was the diet. The diets for the studies that were combined to provide a lab standard were standard chow diets based on the NIH-31 formulation (Barnard et al., 2009), while the base formula for this study was AIN-93G. The NIH-31 formulation contains whole foods from animal protein and grains that are rich in phytoestrogens. The

AIN-93G-based diet used in this study was formulated from synthesized compounds and used corn oil instead of soy oil, rendering the diet free of most phytoestrogens. While the effects of soy phytoestrogens on improving spatial memory have been the most prominent in female ovariectomized rodents (Luine et al., 2006), male mice treated with the phytoestrogen daidzein were less susceptible to anxiety than control mice (Zeng et al., 2010). It is possible that the stress of swimming in the water maze may have been exacerbated by the lack of phytoestrogens in the diet of the young control mice. The fact that xanthohumol could reverse this deficiency with respect to cognitive flexibility for spatial memory confirms the importance of phytochemicals in the diet for cognitive function (Rendeiro et al., 2009). The effects of stress on spatial memory are much greater in young male mice than in aged male mice (Bowman et al., 2006). It may be that the poor basal performances already seen in aged mice in the Morris water maze were less affected by an additional mild stressor like a lack of phytoestrogens in the diet.
The NIH-31 chow diet and xanthohumol AIN-93G-based diet differ in the base ingredients. The AIN-93G diet is a synthetic diet that uses casein as a protein source and cellulose as filler for bulk. The NIH-31 chow diet is composed of whole grains and fishmeal. One of the effects of altering the diet in a significant way is a change in the composition of the gut microbiota. A comparison of a synthetic versus a whole food diet in mice found significant differences in the population of the gut flora (McCracken et al., 2001). While the study of the relationships between microbiota and memory is a burgeoning field, one study found that supplementing a normal chow diet with probiotics improved spatial memory in rats (Davari et al., 2013). Xanthohumol, however, does not affect the gut microbiota in rats (Hanske et al., 2005), indicating that if the brain-gut axis were disturbed, xanthohumol would likely have no effect.
This study revealed that several different problems may arise when mice are switched from their normal chow diet to a synthetic defined diet. In addition, the mice in this study did not receive the full-intended dosage of xanthohumol. The xanthohumol daily dosage was calculated based on the average daily intake for the C57BL/6 mouse on a normal chow diet (Bachmanov et al., 2002). Mice in this study consumed roughly 67% of what was expected, thereby exposing them to a lower daily intake of xanthohumol. Xanthohumol has been shown to be safe at up to 1000 mg/kg body weight/day, so increasing the dosage is quite feasible (Dorn et al., 2010). A larger dosage of

xanthohumol in a whole food chow diet may be able to have a significant effect on spatial memory in aged mice.

The significant effect of treatment on plasma palmitate in the old mice was not matched in the brains of old or young mice. There was no treatment effect in either the frontal cortex or hippocampus of either age group. There was, however, a significant difference between brain regions in palmitate as a percentage of total fatty acids, with palmitate constituting a higher percentage in the frontal cortex than in the hippocampus. Because there is little *de novo* fatty acid synthesis in the brain, lipids must be imported across the blood-brain barrier (Hamilton and Brunaldi, 2007). The first step after crossing the membrane is esterification to acyl-CoA. In this study, we showed that there was a significant regional, but not age or treatment, difference in the steady-state levels of palmitoyl-CoA, with a greater amount present in the frontal cortex. The resting pool of palmitoyl-CoA in either brain region may not be related to efficiency of palmitate crossing the blood-brain barrier. It may be that downstream metabolism varies between the two brain regions. Too much acyl-CoA has a detergent-like effect so there may be a limit to how much acyl-CoA a cell can hold (Brecher, 1983). An analysis into the rate of fatty acid acylation in the brain showed that there is an age-related increase in arachidonyl-CoA formation in both the frontal cortex and hippocampus (Terracina et al., 1992). Although the authors were unable to note any age-related differences in palmitoyl-CoA formation, it may be that revisiting the experiment with modern equipment could reveal some differences. It is important to note that we also found no age-related differences in the pools of arachidonyl-CoA in either the frontal cortex or the hippocampus (data not shown). It is also important to note that both arachidonyl-CoA and palmitoyl-CoA are synthesized by the same enzyme acyl-CoA synthetase 6 (ACSL6) (Van Horn et al., 2005). Two isoforms of ACSL6 exist, with one having a lower affinity for ATP. Because the aging brain is deficient in ATP (Dorszewska, 2013), it may be that the isoform that has a lower affinity for ATP is upregulated in old mice, compensating for the possibility of a loss of activity due to lower levels of ATP. This may explain why we were unable to see any aging differences in palmitoyl-CoA pools in either the frontal cortex or hippocampus.

There was a significant increase in the levels of protein palmitoylation in the frontal cortex, but not the hippocampus, of old mice. Treatment with xanthohumol was unable to affect protein palmitoylation levels in either the young or old mice. Protein palmitoylation

is integral to neuronal development and plasticity (Fukata and Fukata, 2010), but depalmitoylation is equally as important as it allows proteins to cycle off of membranes thereby modulating a signal (Conibear and Davis, 2010). Palmitoylaton of PSD-95 and the *N*-methyl-D-aspartate receptor (NMDAR) subunits GluN2A and 2B will increase when activation of the NMDAR is diminished allowing the proteins to remain on the synaptic membrane (Hayashi et al., 2009; Noritake et al., 2009). Palmitoylation of the GluR1 subunit of the α-amino-3-hydroxy-5-methyl-4-isoxazolepropionic acid receptor (AMPAR) will also increase when the NMDAR is blocked, but unlike the NMDAR GluN2 subunits, palmitoylation interferes with AMPAR insertion into the synaptic membrane decreasing LTP (Lin et al., 2009). Synaptic vesicle fusion dysfunction occurs when synaptic proteins are not properly depalmitoylated (Kim et al., 2008). It may be that decreased synaptic activity in the aged frontal cortex is associated with persistent anchoring of some synaptic proteins to plasma membranes leading to a loss of LTP and pruning of dendritic arbors.

Although the spatial memory of the aged mice in this study was not significantly improved, there was a significant reduction in plasma palmitate in the treatment group. There was, however, no treatment-induced change in the palmitoylation status of GluN2A, GluN2B, PSD-95 or Fyn. Treating pancreatic β-cells with palmitate can induce greater protein palmitoylation, leading to cell death (Baldwin et al., 2012). The concentration of palmitate used to treat the β-cells was far greater than normal physiological levels. The approximately 30% reduction of plasma palmitate in the old mice was not enough to affect protein palmitoylation. It may be physiologically impossible to safely lower palmitate enough to affect protein palmitoylation.

Previous work has indicated that xanthohumol may be effective in treating metabolic syndrome (Kirkwood et al., 2013). Metabolic syndrome has been associated with age-related deficits in memory (Watts et al., 2013). There was no significant effect of xanthohumol on swim speed or spatial memory in the old mice. This is suggestive, but not definitive, that xanthohumol had little effect on metabolic rate.

Flavanoids are important for cognition. They have been shown to be neuroprotective (Dajas et al., 2013) and good for spatial memory in young and old mice (Rendeiro et al., 2009; Spencer, 2010).Soy isoflavones are also beneficial to memory (Lee et al., 2005). Xanthohumol is a prenylated calconoid that is a part of the flavonoid family. Treatment with xanthohumol has been shown to be neuroprotective in stroke-induced rats (Yen et

al., 2012). Recent evidence found that derivatives of xanthohumol can induce neurite growth in mouse neuronal cells (Oberbauer et al., 2013). In this study we were able to demonstrate that dietary intake of xanthohumol improved cognitive flexibility in young mice on a flavanoid-deficient diet and lowered plasma palmitate in young and old mice. A combination of a diet rich in soy isoflavones supplemented with a higher concentration of xanthohumol could still prove to be beneficial to spatial learning in aged mice.

Conclusion

The NMDAr is pivotal in LTP and learning and memory (Morris, 2013; Nicoll and Roche, 2013). The NMDAr is also vulnerable to the effects of aging (Magnusson et al., 2010). Of the NMDAr subunits, GluN2B has displayed the greatest effect on memory. Overexpression of the subunit in mice results in improved learning scores over wild-type mice (Tang et al., 1999; Wang et al., 2009; Cui et al., 2011). Among the NMDAr subunits, GluN2B shows the greatest decline with age in the frontal cortex (Ontl et al., 2004; Magnusson et al., 2007; Zhao et al., 2009). There are also significant age-related declines in the hippocampus (Magnusson et al., 2002). Increasing expression levels of GluN2B in either the hippocampus or frontal cortex in aged mice improved spatial memory (Brim et al., 2013).

It is interesting to note that the GluN2A/GluN2B ratio increased with age, but it didn't correlate with poorer learning scores in aged mice. Data has shown that triheteromeric NMDAr predominate in the adult rodent brain (Rauner and Kohr, 2011). The physiology of this type of receptor is dictated by the GluN2A subunit (Hansen et al., 2014). Evidence has shown that GluN2A is needed for memory consolidation (Ge et al., 2010). In this thesis GluN2A subunits did not decrease with age in either the hippocampus or the frontal cortex. These data suggest that GluN2A expression may not be detrimental to learning and memory and the age-related deficiencies in memory may be attributed to factors other than GluN2A expression.

There was a significant correlation between PSD-95/GluN2B ratios and poorer learning. PSD-95 is predominantly localized on the synaptic membrane, (Xu, 2011), but the increased association of GluN2B with PSD-95 did not enhance spatial reference memory in this study. A new report has found an additional binding site for PSD-95 on GluN2A and GluN2B C-terminal tails and implies that the ratio of PSD-95 to GluN2 subunit may not be 1:1, but, because PSD-95 can dimerize, could be as high as 4:1 (Cousins and Stephenson, 2012). The age-related decline in GluN2B expression in the synaptic membrane in frontal cortex may result in more molecules of PSD-95 binding to each GluN2B subunit than is seen in younger animals.

An increased GluN2B/GIPC association was correlated with poorer learning. GIPC binds to proteins via its PDZ domain. Evidence shows that it is able to bind to GluN1, GluN2A, and GluN2B subunits (Yi et al., 2007). Because it competes for the same binding site as PSD-95, GIPC binding to the ESDV site may be an indication that PSD-95 is binding to

the alternate site on GluN2B. Indeed, the fact that high levels of GIPC/GluN2B and PSD-95/GluN2B correlate to poorer learning supports this theory.

There was a significant increase in p1472 in the TxP from the frontal cortex of old mice with good reference learning. There was also a decrease in p1336 in the TxP from the frontal cortex of old mice with poor reference learning. Calpain-mediated cleavage of GluN2B was increased in the frontal cortex, but not the hippocampus of old mice with good reference memory. There were significant increases in Fyn levels in Txp from frontal cortex and hippocampus and in hippocampal TxS fractions from bad learners. Finally, the palmitoylation status of NMDAr proteins increased with age in the frontal cortex, but not the hippocampus.

The phosphorylation of Y1472 is able to deter binding of AP-2 allowing PSD-95 to bind (Lavezzari et al., 2003). This permits the NMDAr to remain on the synaptic membrane. Evidence also indicates that blockade of the NMDAr increases p1472 (Ai et al., 2013). The binding of NMDA to the glutamate binding site in age rodents showed greater declines in the frontal cortex than in the hippocampus (Magnusson et al., 2010). The increased p1472 found on synaptic membranes in the frontal cortex of old mice with good reference memory may help compensate for lowered activation of the receptor. There was a decreased amount of p1336 in the synaptic fraction from the frontal cortex of old mice with bad reference memory. There was no change between the young and old mice with good reference memory. We found that the 115 kDa GluN2B cleavage product was located in the TxS fraction, indicating a peri-/extrasynaptic localization. There was a significant group-related increase in cleaved GluN2B only in the TxS from the frontal cortex. This suggests that there may be an increase in p1336 in the frontal cortex of aged mice with good reference memory. Because calpain cleavage of GluN2B subunits is fairly rapid (Guttmann et al., 2001), it may be that subunits with p1336 are unable to accumulate on synaptic membranes. It is interesting to note that calpain activity was increased in the frontal cortex and hippocampus, as witnessed by the calpain autolysis and PSD-95 cleavage products.

The relative levels of protein palmitoylation increased in an age-dependent manner in the frontal cortex, but not the hippocampus of mice. GluN2A, GluN2B, Fyn, and PSD-95 all saw age-related increases in palmitoylation regardless of reference memory status. Palmitoylation of the C-terminus of GluN2 subunits promotes phosphorylation of tyrosine residues, specifically p1472 on GluN2B (Hayashi et al., 2009). We saw a significant rise

in p1472 in the TxP from the frontal cortex for old mice with good reference memory, while levels of p1336 remained similar to young. It is not known if p1336 is affected by palmitoylation of GluN2B. The C-terminus of the GluN2B subunit undergoes calpain-mediated cleavage initiated by p1336 (Wu et al., 2007). Because there was an increase 115 kDa calpain-mediated cleavage product of GluN2B in the same group, increased palmitoylation may have increased levels of p1336 as well. The hippocampal groups did not see the same rise in p1472 or cleaved GluN2B lending further evidence to a role of palmitoylation in promoting modification of GluN2B subunits beyond p1472.

PSD-95 palmitoylation was significantly increased in an age-dependent manner. Palmitoylation of PSD-95 clusters the protein on synaptic membranes (El-Husseini Ael et al., 2002). Our data, however, showed no change in PSD-95 levels in the TxP from either the frontal cortex or hippocampus. Data indicates that mutating the N-terminal cysteine residues responsible for the palmitoylation of PSD-95 does not eliminate association with the synaptic membrane (Topinka and Bredt, 1998). Palmitoylation of PSD-95 is required for the protein to dimerize (Xu et al., 2008). The increased levels of palmitoylation in the frontal cortex may lead to increased dimerization, which may in turn increase binding to the non-ESDV site on GluN2B. This may explain why an increase in GluN2B/PSD-95 and GluN2B/GIPC in the frontal cortex of old mice are simultaneously correlated with poor memory. GIPC may bind to an unoccupied ESDV site when PSD-95 dimerizes and binds to the non-ESDV site.

There was also a group-related increase in the palmitoylation of APT1 in the frontal cortex, but not hippocampus. Recent evidence has found that APT1 acts like a gatekeeper by residing on the Golgi apparatus to control excess palmitoylation of proteins, including APT1 (Vartak et al., 2014). Increased palmitoylation of APT1 would indicate that dynamic shuttling on and off of Golgi membranes may be diminished with age in the frontal cortex. Stimulation of the NMDAr is responsible for the rapid depalmitoylation of GluN2 subunits (Hayashi et al., 2009), PSD-95 (El-Husseini Ael et al., 2002), and the α-Amino-3-hydroxy-5-methyl-4-isoxazolepropionic acid receptor (AMPAr) (Hayashi et al., 2005). This suggests a link between the NMDAr and APT1. Because many proteins are affected by calcium influx through the NMDAr, it would stand to reason that calcium may activate APT1. However, data has shown that calcium levels in both the frontal cortex and hippocampus are increase with age (Murchison and Griffith, 1998; Hajieva et al., 2009). This suggests that APT1 should have increased activation in

aged brains, not unlike the type of age-related increase in activity of calpains shown in this study. That was not observed; therefore APT1 may be activated by some other mechanism, possibly protein interaction. The crystal structure of APT1 suggests that the molecule is a dimer *in vivo* (Devedjiev et al., 2000). It would be interesting to know if the dimer promotes or inhibits activity and if that is affected by age.

Intervention with the flavonoid xanthohumol had mixed results. There was no effect on memory in the old mice, but the young mice saw some improvement in cognitive flexibility and trend towards reference memory improvement. Treatment with xanthohumol did not affect palmitate, palmitoyl-CoA, or protein palmitoylation in the brain of young or old mice. There was, however, a brain region difference for both palmitate and palmitoyl-CoA. There was a treatment effect in palmitate plasma levels in the old mice.

Xanthohumol has been shown to be neuroprotective and derivatives of xanthohumol promote neurite growth (Yen et al., 2012; Oberbauer et al., 2013). Xanthohumol has been shown to combat the effects of metabolic syndrome (Kirkwood et al., 2013; Legette et al., 2013). Metabolic syndrome has been linked to cognitive decline in the elderly (Watts et al., 2013). It stands to reason that xanthohumol would have some positive effect on cognition. Some flaws in the study may explain the poor results. The learning scores in the young mice were significantly worse than those of control mice in the Magnusson lab standard. The only difference among the studies was the type of chow. This study used a defined diet devoid of any flavonoids or whole foods. Revisiting this study with normal chow supplemented with xanthohumol at higher doses may improve learning in the old mice. It may also be that old mice were at an age beyond intervention. Beginning the study in 18 month old mice may lead to a better outcome.

This study raises several questions about possible mechanisms of action in the aged frontal cortex. Fyn expression increased in synaptic membranes from the frontal cortex of old mice, but it also increased in the hippocampus. This suggests that some other mechanism may be involved. Phosphorylation of Fyn activates the kinase, while phosphorylation of STEP61 in the KIM domain deactivates the phosphatase (Braithwaite et al., 2006; Trepanier et al., 2012). Exploring the phosphorylation status with age of Fyn and STEP61 could give further insight into molecular regulation in the aged brain. It is also interesting to note that not all proteins are palmitoylated to the same extent in the aged frontal cortex. Flotillin palmitoylation does not appear to change with age

(Bhattacharyya et al., 2013). Because the palmitoylation of AMPA receptors prevents their insertion into the synaptic membrane, it would be interesting to see if AMPA palmitoylation changes with age (Hayashi et al., 2005). An experiment that may shed some light on the aging effects of palmitoylation in the frontal cortex and hippocampus would be a “palmitoylome” that uses mass spec and an –omics approach to analyze protein palmtoylation in young and old mice. This would give a broader picture of how palmitoylation could affect the functionality of brain tissue.

The studies presented here demonstrate how GluN2B localization may be affected by age. The key may be diminished activity of the thioesterase APT1. A reduction in activity would explain the increased number of GluN2, Fyn, and PSD-95 molecules that palmitoylated in the aged frontal cortex. There are two clusters of cysteines that undergo palmitoylation on GluN2B subunits (Fig. 5.1). Hayashi et al. demonstrated that cysteine cluster 1 was essential for phosphorylation of tyrosine 1472 on GluN2B, but cluster 2 was not essential (Hayashi et al., 2009). What is not known is if an increase in the palmitoylation of cluster 2 would lead to any effects on protein interactions with GluN2B such as decreased phosphorylation or binding to PSD-95. There were two distinct populations of old mice: one with good reference memory and one with bad reference memory (Fig. 5.2). For the old mice with good reference memory, palmitoylation in the frontal cortex may be adaptive by increasing p1472, thus allowing for a longer residence time of GluN2B-containing receptors on the synaptic membrane. At the same time there may be an increase in p1336, leading to more calpain-mediated cleavage of GluN2B and an enrichment of GluN2B-containing NMDAr on extrasynaptic membranes (Fig. 5.2). The increased number of GluN2B subunits on synaptic membranes seems to have a greater effect on memory than the increased number of cleaved GluN2B subunits residing on extrasynaptic membranes. Data from the first chapter also showed an increased association of PSD-95 with GluN2B was correlated with both age and poor memory. The binding of GIPC to the ESDV site of GluN2B also increased in old mice with poor memory. Because PSD-95 and GIPC compete for the same binding site it stands to reason that PSD-95 must no longer bind to the ESDV site in order for GIPC to bind. PSD-95 can only dimerize when it is palmitoylated (Xu et al., 2008). One of the consequence of the increased number of palmitoylated proteins in the aged frontal cortex may be an increased number of PSD-95 dimers binding to the non-ESDV site on GluN2B, freeing up the ESDV site for GIPC to bind to in the dendrites of old mice with

poor memory (Fig. 5.2C). On the other hand, old mice with good reference memory have more GluN2B subunits with p1472 leading to more PSD-95 binding to the ESDV site (Fig. 5.2B). The key difference between old mice with good and bad memory may be the levels of palmitoylation of cysteine cluster 1 and 2(Fig. 5.2B & C). Because there doesn't appear to be any difference in the number of palmitoylated proteins in old frontal cortices with either good or bad memory, it may be that the cysteine clusters are differentially palmitoylated. Old mice with good memory could have GluN2B subunits with cysteine cluster 1 palmitoylated and cluster 2 depalmitoylated, while the opposite may hold true for old mice with poor memory.

Information here shines a light, not only on NMDAr function, but has farther reaching implications. Because the APP protein also has increase palmitoylation with age, it suggests that palmitoylation of proteins in aged animals may lead to the pathophysiology of Alzheimer's disease (Bhattacharyya et al., 2013). Understanding the mechanisms behind this aberration may be the key not only to healthy aging, but to combating the onset of Alzheimer's disease as well.

Figure 5.1 Posttranslational modification of GluN2 subunits. GluN2A and GluN2B both have several sites for phophorylation of serines and tyrosines on the C-terminal tail. A site for calpain-mediated cleavage occurs around amino acid 1030 on GluN2B and at amino acids 1279 and 1330 on GluN2A. PSD-95 and other MAGUKs bind at the ESDV motif on the GluN2 C-terminus. Two cysteine clusters participate in palmitoylation of GluN2 subunits. Adapted from Collingridge et al. 2013.

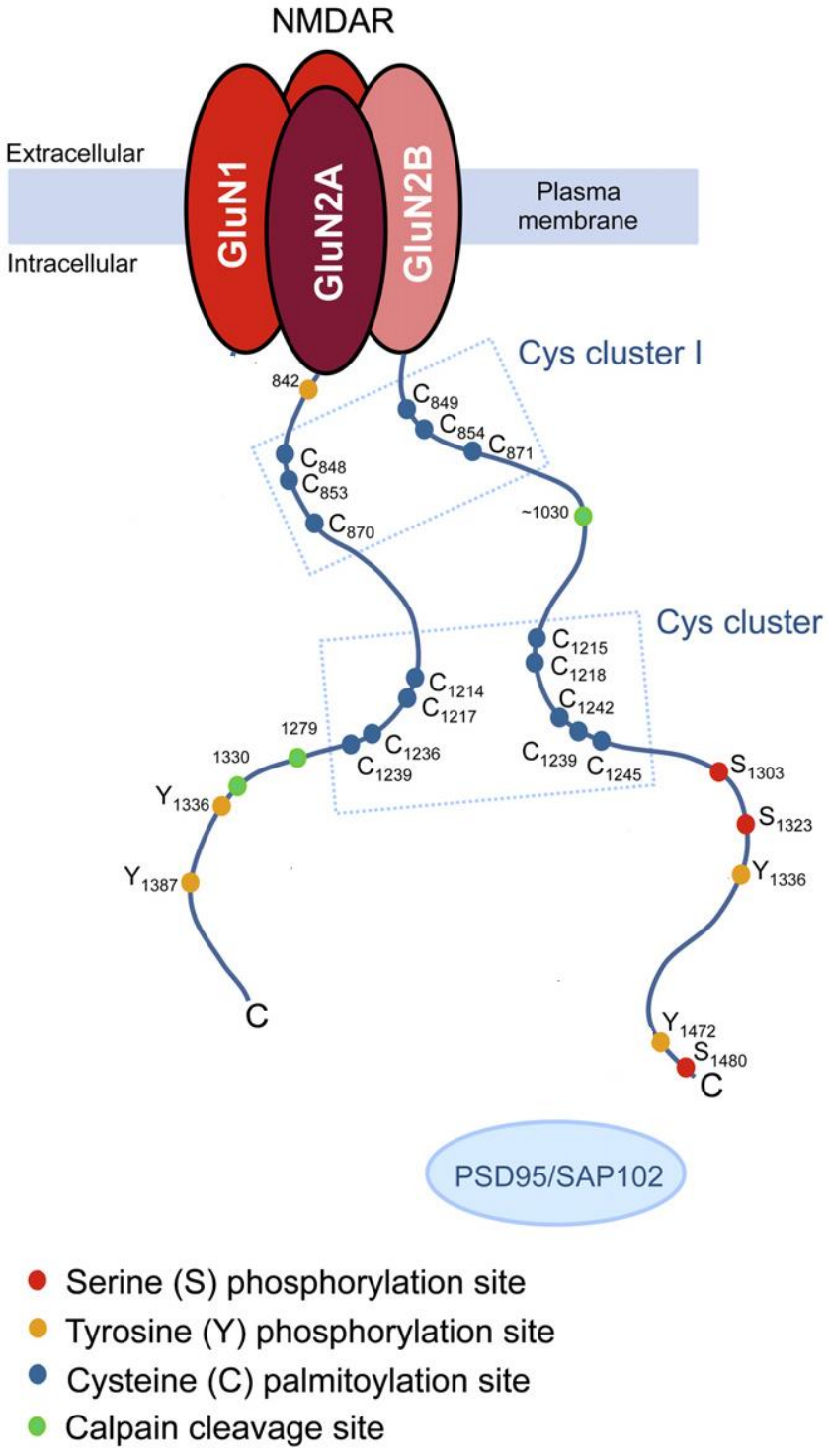
NMDAR
Extracellular
Intracellular
Plasma membrane
GluN1
GluN2A
GluN2B
Cys cluster I
Cys cluster
842
C849
C854
C871
C848
C853
C870
~1030
C1215
C1218
C1242
C1214
C1217
1279
1330
C1236
C1239
C1239
C1245
S1303
S1323
Y1336
Y1336
Y1387
C
Y1472
S1480
C
PSD95/SAP102
Serine (S) phosphorylation site
Tyrosine (Y) phosphorylation site
Cysteine (C) palmitoylation site
Calpain cleavage site

Figure 5.1

Figure 5.2 Overview of the aged dendrite. Old dendrites are separated into two populations: good reference memory (B) and bad reference memory (C). (A) Young dendrites have a higher number of GluN2B-only receptors than old (B & C), but there were more heterotrimeric receptors in old mice. Proteins are able to cycle on and off synaptic membranes in young dendrites (A), but decreased thioesterase (APT1) activity inhibits cycling in old dendrites (B & C).

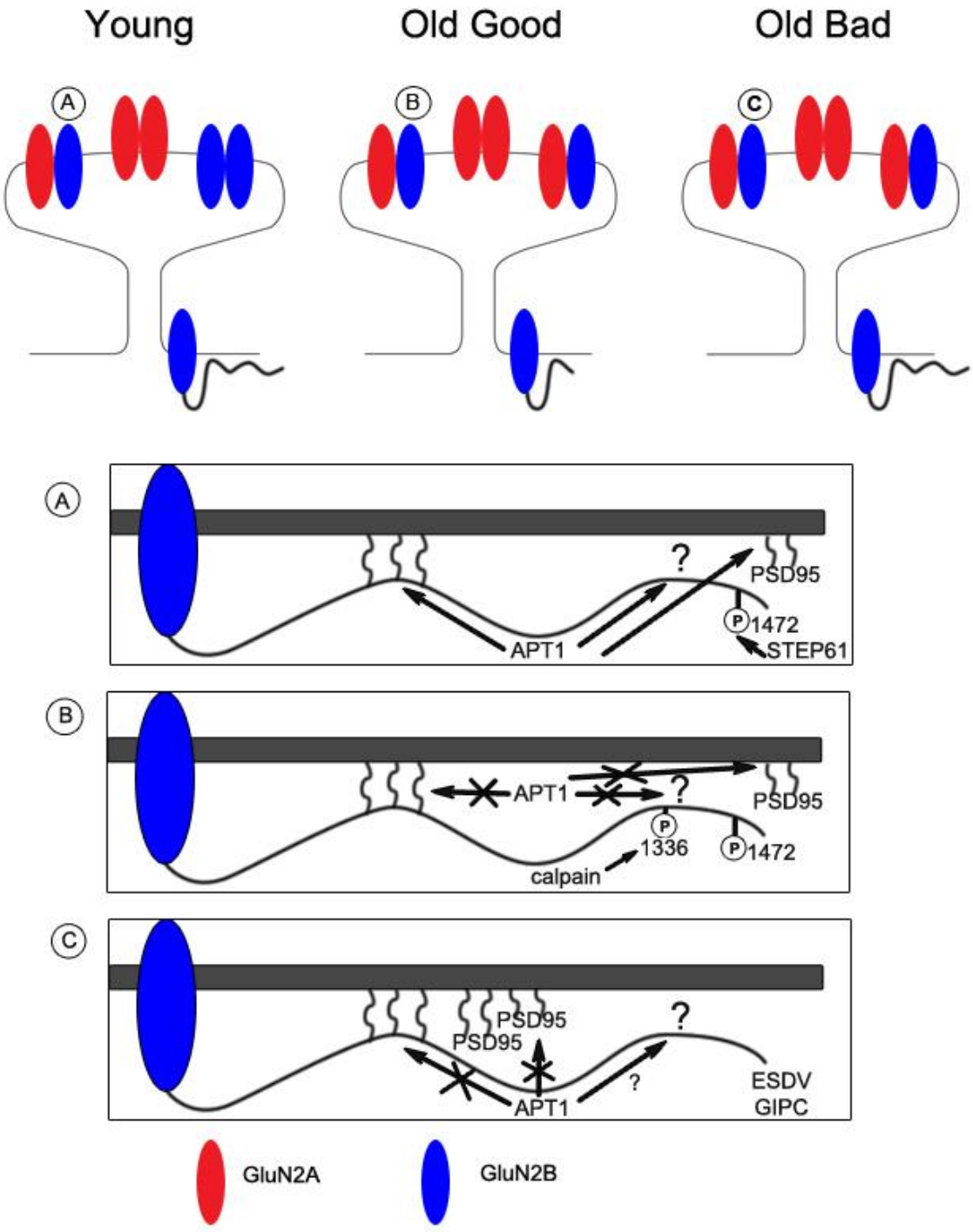
Young
Old Good
Old Bad
A
B
C
A
?
PSD95
P 1472
APT1
STEP61
B
APT1
?
PSD95
P
1336
P 1472
calpain
C
PSD95
PSD95
?
APT1
?
ESDV
GIPC
GluN2A
GluN2B

Figure 5.2

Bibliography

Ai H, Lu W, Ye M, Yang W (2013) Synaptic non-GluN2B-containing NMDA receptors regulate tyrosine phosphorylation of GluN2B 1472 tyrosine site in rat brain slices. Neurosci Bull 29:614-620.

Ando S, Tanaka Y, Toyoda nee Ono Y, Kon K, Kawashima S (2002) Turnover of synaptic membranes: age-related changes and modulation by dietary restriction. J Neurosci Res 70:290-297.

Bachmanov AA, Reed DR, Beauchamp GK, Tordoff MG (2002) Food intake, water intake, and drinking spout side preference of 28 mouse strains. Behav Genet 32:435-443.

Baddeley A (2000) The episodic buffer: a new component of working memory? Trends Cogn Sci 4:417-423.

Baddeley AD, Bressi S, Della Sala S, Logie R, Spinnler H (1991) The decline of working memory in Alzheimer's disease. A longitudinal study. Brain 114 (Pt 6):2521-2542.

Baekkeskov S, Kanaani J (2009) Palmitoylation cycles and regulation of protein function (Review). Mol Membr Biol 26:42-54.

Bai L, Hof PR, Standaert DG, Xing Y, Nelson SE, Young AB, Magnusson KR (2004) Changes in the expression of the NR2B subunit during aging in macaque monkeys. Neurobiol Aging 25:201-208.

Baldwin AC, Green CD, Olson LK, Moxley MA, Corbett JA (2012) A role for aberrant protein palmitoylation in FFA-induced ER stress and beta-cell death. Am J Physiol Endocrinol Metab 302:E1390-1398.

Bard L, Groc L (2011) Glutamate receptor dynamics and protein interaction: lessons from the NMDA receptor. Mol Cell Neurosci 48:298-307.

Barnard DE, Lewis SM, Teter BB, Thigpen JE (2009) Open- and closed-formula laboratory animal diets and their importance to research. J Am Assoc Lab Anim Sci 48:709-713.

Barnes CA (1979) Memory deficits associated with senescence: a neurophysiological and behavioral study in the rat. J Comp Physiol Psychol 93:74-104.

Barnes CA, Nadel L, Honig WK (1980) Spatial memory deficit in senescent rats. Can J Psychol 34:29-39.

Barria A, Malinow R (2002) Subunit-specific NMDA receptor trafficking to synapses. Neuron 35:345-353.

Bhattacharyya R, Barren C, Kovacs DM (2013) Palmitoylation of amyloid precursor protein regulates amyloidogenic processing in lipid rafts. J Neurosci 33:11169-11183.

Bowman RE, Maclusky NJ, Diaz SE, Zrull MC, Luine VN (2006) Aged rats: sex differences and responses to chronic stress. Brain Res 1126:156-166.

Braithwaite SP, Paul S, Nairn AC, Lombroso PJ (2006) Synaptic plasticity: one STEP at a time. Trends Neurosci 29:452-458.

Brandeis R, Brandys Y, Yehuda S (1989) The use of the Morris Water Maze in the study of memory and learning. Int J Neurosci 48:29-69.

Brecher P (1983) The interaction of long-chain acyl CoA with membranes. Mol Cell Biochem 57:3-15.

Brim BL, Haskell R, Awedikian R, Ellinwood NM, Jin L, Kumar A, Foster TC, Magnusson KR (2013) Memory in aged mice is rescued by enhanced expression of the GluN2B subunit of the NMDA receptor. Behav Brain Res 238:211-226.

Carver JD, Benford VJ, Han B, Cantor AB (2001) The relationship between age and the fatty acid composition of cerebral cortex and erythrocytes in human subjects. Brain Res Bull 56:79-85.

Chung HJ, Huang YH, Lau LF, Huganir RL (2004) Regulation of the NMDA receptor complex and trafficking by activity-dependent phosphorylation of the NR2B subunit PDZ ligand. J Neurosci 24:10248-10259.

Clayton DA, Browning MD (2001) Deficits in the expression of the NR2B subunit in the hippocampus of aged Fisher 344 rats. Neurobiol Aging 22:165-168.

Clayton DA, Grosshans DR, Browning MD (2002) Aging and surface expression of hippocampal NMDA receptors. J Biol Chem 277:14367-14369.

Collingridge GL, Volianskis A, Bannister N, France G, Hanna L, Mercier M, Tidball P, Fang G, Irvine MW, Costa BM, Monaghan DT, Bortolotto ZA, Molnar E, Lodge D, Jane DE (2013) The NMDA receptor as a target for cognitive enhancement. Neuropharmacology 64:13-26.

Conibear E, Davis NG (2010) Palmitoylation and depalmitoylation dynamics at a glance. J Cell Sci 123:4007-4010.

Cooke SF, Bliss TV (2006) Plasticity in the human central nervous system. Brain 129:1659-1673.

Coultrap SJ, Bickford PC, Browning MD (2008) Blueberry-enriched diet ameliorates age-related declines in NMDA receptor-dependent LTP. Age (Dordr) 30:263-272.

Cousins SL, Stephenson FA (2012) Identification of N-methyl-D-aspartic acid (NMDA) receptor subtype-specific binding sites that mediate direct interactions with scaffold protein PSD-95. J Biol Chem 287:13465-13476.

Cui Y, Jin J, Zhang X, Xu H, Yang L, Du D, Zeng Q, Tsien JZ, Yu H, Cao X (2011) Forebrain NR2B overexpression facilitating the prefrontal cortex long-term potentiation and enhancing working memory function in mice. PLoS One 6:e20312.

Dajas F, Andres AC, Florencia A, Carolina E, Felicia RM (2013) Neuroprotective actions of flavones and flavonols: mechanisms and relationship to flavonoid structural features. Cent Nerv Syst Agents Med Chem 13:30-35.

Dalton GL, Wang YT, Floresco SB, Phillips AG (2008) Disruption of AMPA receptor endocytosis impairs the extinction, but not acquisition of learned fear. Neuropsychopharmacology 33:2416-2426.

Das SR, Magnusson KR (2011) Changes in expression of splice cassettes of NMDA receptor GluN1 subunits within the frontal lobe and memory in mice during aging. Behav Brain Res 222:122-133.

Das SR, Jensen R, Kelsay R, Shumaker M, Bochart R, Brim B, Zamzow D, Magnusson KR (2012) Reducing expression of GluN1(0XX) subunit splice variants of the NMDA receptor interferes with spatial reference memory. Behav Brain Res 230:317-324.

Davari S, Talaei SA, Alaei H, Salami M (2013) Probiotics treatment improves diabetes-induced impairment of synaptic activity and cognitive function: behavioral and electrophysiological proofs for microbiome-gut-brain axis. Neuroscience 240:287-296.

de Brabander JM, Kramers RJ, Uylings HB (1998) Layer-specific dendritic regression of pyramidal cells with ageing in the human prefrontal cortex. Eur J Neurosci 10:1261-1269.

Devedjiev Y, Dauter Z, Kuznetsov SR, Jones TL, Derewenda ZS (2000) Crystal structure of the human acyl protein thioesterase I from a single X-ray data set to 1.5 A. Structure 8:1137-1146.

Dong QP, He JQ, Chai Z (2013) Astrocytic Ca(2+) waves mediate activation of extrasynaptic NMDA receptors in hippocampal neurons to aggravate brain damage during ischemia. Neurobiol Dis 58:68-75.

Dorn C, Bataille F, Gaebele E, Heilmann J, Hellerbrand C (2010) Xanthohumol feeding does not impair organ function and homoeostasis in mice. Food Chem Toxicol 48:1890-1897.

Dorszewska J (2013) Cell biology of normal brain aging: synaptic plasticity-cell death. Aging Clin Exp Res 25:25-34.

Driscoll I, Hamilton DA, Yeo RA, Brooks WM, Sutherland RJ (2005) Virtual navigation in humans: the impact of age, sex, and hormones on place learning. Horm Behav 47:326-335.

Dunah AW, Standaert DG (2001) Dopamine D1 receptor-dependent trafficking of striatal NMDA glutamate receptors to the postsynaptic membrane. J Neurosci 21:5546-5558.

Dyall SC, Michael GJ, Whelpton R, Scott AG, Michael-Titus AT (2007) Dietary enrichment with omega-3 polyunsaturated fatty acids reverses age-related decreases in the GluR2 and NR2B glutamate receptor subunits in rat forebrain. Neurobiol Aging 28:424-439.

el-Husseini Ael D, Bredt DS (2002) Protein palmitoylation: a regulator of neuronal development and function. Nat Rev Neurosci 3:791-802.

El-Husseini Ael D, Schnell E, Dakoji S, Sweeney N, Zhou Q, Prange O, Gauthier-Campbell C, Aguilera-Moreno A, Nicoll RA, Bredt DS (2002) Synaptic strength regulated by palmitate cycling on PSD-95. Cell 108:849-863.

Elias GM, Nicoll RA (2007) Synaptic trafficking of glutamate receptors by MAGUK scaffolding proteins. Trends Cell Biol 17:343-352.

Fan J, Gladding CM, Wang L, Zhang LY, Kaufman AM, Milnerwood AJ, Raymond LA (2012) P38 MAPK is involved in enhanced NMDA receptor-dependent excitotoxicity in YAC transgenic mouse model of Huntington disease. Neurobiol Dis 45:999-1009.

Finkbiner RG, Woodruff-Pak DS (1991) Classical eyeblink conditioning in adulthood: effects of age and interstimulus interval on acquisition in the trace paradigm. Psychol Aging 6:109-117.

Flood DG (1993) Critical issues in the analysis of dendritic extent in aging humans, primates, and rodents. Neurobiol Aging 14:649-654.

Flood DG, Buell SJ, Horwitz GJ, Coleman PD (1987) Dendritic extent in human dentate gyrus granule cells in normal aging and senile dementia. Brain Res 402:205-216.

Fukata Y, Fukata M (2010) Protein palmitoylation in neuronal development and synaptic plasticity. Nat Rev Neurosci 11:161-175.

Gallagher M, Burwell R, Burchinal M (1993) Severity of spatial learning impairment in aging: development of a learning index for performance in the Morris water maze. Behav Neurosci 107:618-626.

Gallagher M, Stocker AM, Koh MT (2011) Mindspan: lessons from rat models of neurocognitive aging. ILAR J 52:32-40.

Gallagher M, Bizon JL, Hoyt EC, Helm KA, Lund PK (2003) Effects of aging on the hippocampal formation in a naturally occurring animal model of mild cognitive impairment. Exp Gerontol 38:71-77.

Gazzaley AH, Thakker MM, Hof PR, Morrison JH (1997) Preserved number of entorhinal cortex layer II neurons in aged macaque monkeys. Neurobiol Aging 18:549-553.

Ge Y, Dong Z, Bagot RC, Howland JG, Phillips AG, Wong TP, Wang YT (2010) Hippocampal long-term depression is required for the consolidation of spatial memory. Proc Natl Acad Sci U S A 107:16697-16702.

Goebel-Goody SM, Davies KD, Alvestad Linger RM, Freund RK, Browning MD (2009) Phospho-regulation of synaptic and extrasynaptic N-methyl-d-aspartate receptors in adult hippocampal slices. Neuroscience 158:1446-1459.
Granon S, Poucet B (1995) Medial prefrontal lesions in the rat and spatial navigation: evidence for impaired planning. Behav Neurosci 109:474-484.
Greaves J, Chamberlain LH (2011) DHHC palmitoyl transferases: substrate interactions and (patho)physiology. Trends Biochem Sci 36:245-253.
Groc L, Choquet D (2006) AMPA and NMDA glutamate receptor trafficking: multiple roads for reaching and leaving the synapse. Cell Tissue Res 326:423-438.
Groc L, Bard L, Choquet D (2009) Surface trafficking of N-methyl-D-aspartate receptors: physiological and pathological perspectives. Neuroscience 158:4-18.
Groc L, Heine M, Cousins SL, Stephenson FA, Lounis B, Cognet L, Choquet D (2006) NMDA receptor surface mobility depends on NR2A-2B subunits. Proc Natl Acad Sci U S A 103:18769-18774.
Guscott MR, Clarke HF, Murray F, Grimwood S, Bristow LJ, Hutson PH (2003) The effect of (+/-)-CP-101,606, an NMDA receptor NR2B subunit selective antagonist, in the Morris watermaze. Eur J Pharmacol 476:193-199.
Guttmann RP, Baker DL, Seifert KM, Cohen AS, Coulter DA, Lynch DR (2001) Specific proteolysis of the NR2 subunit at multiple sites by calpain. J Neurochem 78:1083-1093.
Hajieva P, Kuhlmann C, Luhmann HJ, Behl C (2009) Impaired calcium homeostasis in aged hippocampal neurons. Neurosci Lett 451:119-123.
Hamilton JA, Brunaldi K (2007) A Model for Fatty Acid Transport into the Brain. J Mol Neurosci 33:12-17.
Hanks SD, Flood DG (1991) Region-specific stability of dendritic extent in normal human aging and regression in Alzheimer's disease. I. CA1 of hippocampus. Brain Res 540:63-82.
Hansen KB, Ogden KK, Yuan H, Traynelis SF (2014) Distinct functional and pharmacological properties of Triheteromeric GluN1/GluN2A/GluN2B NMDA receptors. Neuron 81:1084-1096.
Hanske L, Hussong R, Frank N, Gerhauser C, Blaut M, Braune A (2005) Xanthohumol does not affect the composition of rat intestinal microbiota. Mol Nutr Food Res 49:868-873.
Hardingham GE, Bading H (2002) Coupling of extrasynaptic NMDA receptors to a CREB shut-off pathway is developmentally regulated. Biochim Biophys Acta 1600:148-153.
Hardingham GE, Bading H (2010) Synaptic versus extrasynaptic NMDA receptor signalling: implications for neurodegenerative disorders. Nat Rev Neurosci 11:682-696.
Hardingham GE, Fukunaga Y, Bading H (2002) Extrasynaptic NMDARs oppose synaptic NMDARs by triggering CREB shut-off and cell death pathways. Nat Neurosci 5:405-414.
Hayashi T, Rumbaugh G, Huganir RL (2005) Differential regulation of AMPA receptor subunit trafficking by palmitoylation of two distinct sites. Neuron 47:709-723.
Hayashi T, Thomas GM, Huganir RL (2009) Dual palmitoylation of NR2 subunits regulates NMDA receptor trafficking. Neuron 64:213-226.
Horst NK, Laubach M (2009) The role of rat dorsomedial prefrontal cortex in spatial working memory. Neuroscience 164:444-456.
Huang W, Fileta J, Rawe I, Qu J, Grosskreutz CL (2010) Calpain activation in experimental glaucoma. Invest Ophthalmol Vis Sci 51:3049-3054.

Huerta PT, Scearce KA, Farris SM, Empson RM, Prusky GT (1996) Preservation of spatial learning in fyn tyrosine kinase knockout mice. Neuroreport 7:1685-1689.
Husi H, Ward MA, Choudhary JS, Blackstock WP, Grant SG (2000) Proteomic analysis of NMDA receptor-adhesion protein signaling complexes. Nat Neurosci 3:661-669.
Ingram DK (1988) Complex maze learning in rodents as a model of age-related memory impairment. Neurobiol Aging 9:475-485.
Jeyifous O, Waites CL, Specht CG, Fujisawa S, Schubert M, Lin EI, Marshall J, Aoki C, de Silva T, Montgomery JM, Garner CC, Green WN (2009) SAP97 and CASK mediate sorting of NMDA receptors through a previously unknown secretory pathway. Nat Neurosci 12:1011-1019.
Jiang X, Knox R, Pathipati P, Ferriero D (2011) Developmental localization of NMDA receptors, Src and MAP kinases in mouse brain. Neurosci Lett 503:215-219.
Kandel ER (1997) Genes, synapses, and long-term memory. J Cell Physiol 173:124-125.
Kandel ER, Schwartz JH, Jessell TM (2000) Principles of neural science, 4th Edition. New York: McGraw-Hill, Health Professions Division.
Kandel ER, Dudai Y, Mayford MR (2014) The molecular and systems biology of memory. Cell 157:163-186.
Kandel ER, Klein M, Castellucci VF, Schacher S, Goelet P (1986) Some principles emerging from the study of short- and long-term memory. Neurosci Res 3:498-520.
Kasuya F, Kazumi M, Tatsuki T, Suzuki R (2009) Effect of salicylic acid and diclofenac on the medium-chain and long-chain acyl-CoA formation in the liver and brain of mouse. J Appl Toxicol 29:435-445.
Kessels RP, Postma A, Wijnalda EM, de Haan EH (2000) Frontal-lobe involvement in spatial memory: evidence from PET, fMRI, and lesion studies. Neuropsychol Rev 10:101-113.
Keuker JI, Luiten PG, Fuchs E (2003) Preservation of hippocampal neuron numbers in aged rhesus monkeys. Neurobiol Aging 24:157-165.
Kim SJ, Zhang Z, Sarkar C, Tsai PC, Lee YC, Dye L, Mukherjee AB (2008) Palmitoyl protein thioesterase-1 deficiency impairs synaptic vesicle recycling at nerve terminals, contributing to neuropathology in humans and mice. J Clin Invest 118:3075-3086.
Kirkwood JS, Legette LL, Miranda CL, Jiang Y, Stevens JF (2013) A metabolomics-driven elucidation of the anti-obesity mechanisms of xanthohumol. J Biol Chem 288:19000-19013.
Knox R, Zhao C, Miguel-Perez D, Wang S, Yuan J, Ferriero D, Jiang X (2013) Enhanced NMDA receptor tyrosine phosphorylation and increased brain injury following neonatal hypoxia-ischemia in mice with neuronal Fyn overexpression. Neurobiol Dis 51:113-119.
Kong E, Peng S, Chandra G, Sarkar C, Zhang Z, Bagh MB, Mukherjee AB (2013) Dynamic palmitoylation links cytosol-membrane shuttling of acyl-protein thioesterase-1 and acyl-protein thioesterase-2 with that of proto-oncogene H-ras product and growth-associated protein-43. J Biol Chem 288:9112-9125.
Kuehl-Kovarik MC, Magnusson KR, Premkumar LS, Partin KM (2000) Electrophysiological analysis of NMDA receptor subunit changes in the aging mouse cortex. Mech Ageing Dev 115:39-59.
Kuhla A, Blei T, Jaster R, Vollmar B (2011) Aging is associated with a shift of fatty metabolism toward lipogenesis. J Gerontol A Biol Sci Med Sci 66:1192-1200.

Kurup P, Zhang Y, Venkitaramani DV, Xu J, Lombroso PJ (2010) The role of STEP in Alzheimer's disease. Channels (Austin) 4:347-350.

Kutsuwada T, Sakimura K, Manabe T, Takayama C, Katakura N, Kushiya E, Natsume R, Watanabe M, Inoue Y, Yagi T, Aizawa S, Arakawa M, Takahashi T, Nakamura Y, Mori H, Mishina M (1996) Impairment of suckling response, trigeminal neuronal pattern formation, and hippocampal LTD in NMDA receptor epsilon 2 subunit mutant mice. Neuron 16:333-344.

Lavezzari G, McCallum J, Lee R, Roche KW (2003) Differential binding of the AP-2 adaptor complex and PSD-95 to the C-terminus of the NMDA receptor subunit NR2B regulates surface expression. Neuropharmacology 45:729-737.

Lee HK (2006) Synaptic plasticity and phosphorylation. Pharmacol Ther 112:810-832.

Lee JM, Ross ER, Gower A, Paris JM, Martensson R, Lorens SA (1994) Spatial learning deficits in the aged rat: neuroanatomical and neurochemical correlates. Brain Res Bull 33:489-500.

Lee YB, Lee HJ, Sohn HS (2005) Soy isoflavones and cognitive function. J Nutr Biochem 16:641-649.

Legette L, Ma L, Reed RL, Miranda CL, Christensen JM, Rodriguez-Proteau R, Stevens JF (2012) Pharmacokinetics of xanthohumol and metabolites in rats after oral and intravenous administration. Mol Nutr Food Res 56:466-474.

Legette L, Karnpracha C, Reed RL, Choi J, Bobe G, Christensen JM, Rodriguez-Proteau R, Purnell JQ, Stevens JF (2014) Human pharmacokinetics of xanthohumol, an antihyperglycemic flavonoid from hops. Mol Nutr Food Res 58:248-255.

Legette LL, Luna AY, Reed RL, Miranda CL, Bobe G, Proteau RR, Stevens JF (2013) Xanthohumol lowers body weight and fasting plasma glucose in obese male Zucker fa/fa rats. Phytochemistry 91:236-241.

Li H, Thompson VF, Goll DE (2004) Effects of autolysis on properties of mu- and m-calpain. Biochim Biophys Acta 1691:91-103.

Liao GY, Wagner DA, Hsu MH, Leonard JP (2001) Evidence for direct protein kinase-C mediated modulation of N-methyl-D-aspartate receptor current. Mol Pharmacol 59:960-964.

Lin DT, Makino Y, Sharma K, Hayashi T, Neve R, Takamiya K, Huganir RL (2009) Regulation of AMPA receptor extrasynaptic insertion by 4.1N, phosphorylation and palmitoylation. Nat Neurosci 12:879-887.

Linder ME, Deschenes RJ (2007) Palmitoylation: policing protein stability and traffic. Nat Rev Mol Cell Biol 8:74-84.

Liu XY, Chu XP, Mao LM, Wang M, Lan HX, Li MH, Zhang GC, Parelkar NK, Fibuch EE, Haines M, Neve KA, Liu F, Xiong ZG, Wang JQ (2006) Modulation of D2R-NR2B interactions in response to cocaine. Neuron 52:897-909.

Low CM, Wee KS (2010) New insights into the not-so-new NR3 subunits of N-methyl-D-aspartate receptor: localization, structure, and function. Mol Pharmacol 78:1-11.

Lu X, Rong Y, Baudry M (2000) Calpain-mediated degradation of PSD-95 in developing and adult rat brain. Neurosci Lett 286:149-153.

Luine V, Attalla S, Mohan G, Costa A, Frankfurt M (2006) Dietary phytoestrogens enhance spatial memory and spine density in the hippocampus and prefrontal cortex of ovariectomized rats. Brain Res 1126:183-187.

Lyons-Warren A, Lillie R, Hershey T (2004) Short- and long-term spatial delayed response performance across the lifespan. Dev Neuropsychol 26:661-678.

Magnusson KR (1998a) The aging of the NMDA receptor complex. Front Biosci 3:e70-80.

Magnusson KR (1998b) Aging of glutamate receptors: correlations between binding and spatial memory performance in mice. Mech Ageing Dev 104:227-248.
Magnusson KR (2000) Declines in mRNA expression of different subunits may account for differential effects of aging on agonist and antagonist binding to the NMDA receptor. J Neurosci 20:1666-1674.
Magnusson KR (2001) Influence of diet restriction on NMDA receptor subunits and learning during aging. Neurobiol Aging 22:613-627.
Magnusson KR (2012) Aging of the NMDA receptor: from a mouse's point of view. Future Neurol 7:627-637.
Magnusson KR, Nelson SE, Young AB (2002) Age-related changes in the protein expression of subunits of the NMDA receptor. Brain Res Mol Brain Res 99:40-45.
Magnusson KR, Kresge D, Supon J (2006) Differential effects of aging on NMDA receptors in the intermediate versus the dorsal hippocampus. Neurobiol Aging 27:324-333.
Magnusson KR, Brim BL, Das SR (2010) Selective Vulnerabilities of N-methyl-D-aspartate (NMDA) Receptors During Brain Aging. Front Aging Neurosci 2:11.
Magnusson KR, Scruggs B, Zhao X, Hammersmark R (2007) Age-related declines in a two-day reference memory task are associated with changes in NMDA receptor subunits in mice. BMC Neurosci 8:43.
Magnusson KR, Scruggs B, Aniya J, Wright KC, Ontl T, Xing Y, Bai L (2003) Age-related deficits in mice performing working memory tasks in a water maze. Behav Neurosci 117:485-495.
Malenka RC, Bear MF (2004) LTP and LTD: an embarrassment of riches. Neuron 44:5-21.
Markham JA, Juraska JM (2002) Aging and sex influence the anatomy of the rat anterior cingulate cortex. Neurobiol Aging 23:579-588.
McCracken VJ, Simpson JM, Mackie RI, Gaskins HR (2001) Molecular ecological analysis of dietary and antibiotic-induced alterations of the mouse intestinal microbiota. J Nutr 131:1862-1870.
McLay RN, Freeman SM, Harlan RE, Kastin AJ, Zadina JE (1999) Tests used to assess the cognitive abilities of aged rats: their relation to each other and to hippocampal morphology and neurotrophin expression. Gerontology 45:143-155.
Merrill DA, Chiba AA, Tuszynski MH (2001) Conservation of neuronal number and size in the entorhinal cortex of behaviorally characterized aged rats. J Comp Neurol 438:445-456.
Migaud M, Charlesworth P, Dempster M, Webster LC, Watabe AM, Makhinson M, He Y, Ramsay MF, Morris RG, Morrison JH, O'Dell TJ, Grant SG (1998) Enhanced long-term potentiation and impaired learning in mice with mutant postsynaptic density-95 protein. Nature 396:433-439.
Miller GA (1956) The magical number seven plus or minus two: some limits on our capacity for processing information. Psychol Rev 63:81-97.
Milner B, Squire LR, Kandel ER (1998) Cognitive neuroscience and the study of memory. Neuron 20:445-468.
Milnerwood AJ, Gladding CM, Pouladi MA, Kaufman AM, Hines RM, Boyd JD, Ko RW, Vasuta OC, Graham RK, Hayden MR, Murphy TH, Raymond LA (2010) Early increase in extrasynaptic NMDA receptor signaling and expression contributes to phenotype onset in Huntington's disease mice. Neuron 65:178-190.
Mitchell RW, On NH, Del Bigio MR, Miller DW, Hatch GM (2011) Fatty acid transport protein expression in human brain and potential role in fatty acid transport across human brain microvessel endothelial cells. J Neurochem 117:735-746.

Moffat SD, Zonderman AB, Resnick SM (2001) Age differences in spatial memory in a virtual environment navigation task. Neurobiol Aging 22:787-796.
Mogensen J, Pedersen TK, Holm S, Bang LE (1995) Prefrontal cortical mediation of rats' place learning in a modified water maze. Brain Res Bull 38:425-434.
Morris R (1984) Developments of a water-maze procedure for studying spatial learning in the rat. J Neurosci Methods 11:47-60.
Morris RG (2013) NMDA receptors and memory encoding. Neuropharmacology 74:32-40.
Morris RG, Garrud P, Rawlins JN, O'Keefe J (1982) Place navigation impaired in rats with hippocampal lesions. Nature 297:681-683.
Morris RG, Anderson E, Lynch GS, Baudry M (1986) Selective impairment of learning and blockade of long-term potentiation by an N-methyl-D-aspartate receptor antagonist, AP5. Nature 319:774-776.
Moser E, Moser MB, Andersen P (1993) Spatial learning impairment parallels the magnitude of dorsal hippocampal lesions, but is hardly present following ventral lesions. J Neurosci 13:3916-3925.
Muller WE, Stoll S, Scheuer K, Meichelbock A (1994) The function of the NMDA-receptor during normal brain aging. J Neural Transm Suppl 44:145-158.
Murchison D, Griffith WH (1998) Increased calcium buffering in basal forebrain neurons during aging. J Neurophysiol 80:350-364.
Nakazawa T, Komai S, Tezuka T, Hisatsune C, Umemori H, Semba K, Mishina M, Manabe T, Yamamoto T (2001) Characterization of Fyn-mediated tyrosine phosphorylation sites on GluR epsilon 2 (NR2B) subunit of the N-methyl-D-aspartate receptor. J Biol Chem 276:693-699.
Nath R, Raser KJ, Stafford D, Hajimohammadreza I, Posner A, Allen H, Talanian RV, Yuen P, Gilbertsen RB, Wang KK (1996) Non-erythroid alpha-spectrin breakdown by calpain and interleukin 1 beta-converting-enzyme-like protease(s) in apoptotic cells: contributory roles of both protease families in neuronal apoptosis. Biochem J 319 (Pt 3):683-690.
Nguyen TH, Paul S, Xu Y, Gurd JW, Lombroso PJ (1999) Calcium-dependent cleavage of striatal enriched tyrosine phosphatase (STEP). J Neurochem 73:1995-2001.
Nicoll RA, Malenka RC (1999) Expression mechanisms underlying NMDA receptor-dependent long-term potentiation. Ann N Y Acad Sci 868:515-525.
Nicoll RA, Roche KW (2013) Long-term potentiation: peeling the onion. Neuropharmacology 74:18-22.
Noritake J, Fukata Y, Iwanaga T, Hosomi N, Tsutsumi R, Matsuda N, Tani H, Iwanari H, Mochizuki Y, Kodama T, Matsuura Y, Bredt DS, Hamakubo T, Fukata M (2009) Mobile DHHC palmitoylating enzyme mediates activity-sensitive synaptic targeting of PSD-95. J Cell Biol 186:147-160.
Nyffeler M, Zhang WN, Feldon J, Knuesel I (2007) Differential expression of PSD proteins in age-related spatial learning impairments. Neurobiol Aging 28:143-155.
Oberbauer E, Urmann C, Steffenhagen C, Bieler L, Brunner D, Furtner T, Humpel C, Baumer B, Bandtlow C, Couillard-Despres S, Rivera FJ, Riepl H, Aigner L (2013) Chroman-like cyclic prenylflavonoids promote neuronal differentiation and neurite outgrowth and are neuroprotective. J Nutr Biochem 24:1953-1962.
Olton DS (1977) Spatial memory. Sci Am 236:82-84, 89-94, 96, 98.
Ontl T, Xing Y, Bai L, Kennedy E, Nelson S, Wakeman M, Magnusson K (2004) Development and aging of N-methyl-D-aspartate receptor expression in the prefrontal/frontal cortex of mice. Neuroscience 123:467-479.

Pakkenberg B, Gundersen HJ (1997) Neocortical neuron number in humans: effect of sex and age. J Comp Neurol 384:312-320.
Pancani T, Anderson KL, Brewer LD, Kadish I, DeMoll C, Landfield PW, Blalock EM, Porter NM, Thibault O (2013) Effect of high-fat diet on metabolic indices, cognition, and neuronal physiology in aging F344 rats. Neurobiol Aging 34:1977-1987.
Paoletti P, Neyton J (2007) NMDA receptor subunits: function and pharmacology. Curr Opin Pharmacol 7:39-47.
Paoletti P, Bellone C, Zhou Q (2013) NMDA receptor subunit diversity: impact on receptor properties, synaptic plasticity and disease. Nat Rev Neurosci 14:383-400.
Parsons MP, Raymond LA (2014) Extrasynaptic NMDA receptor involvement in central nervous system disorders. Neuron 82:279-293.
Passafaro M, Sala C, Niethammer M, Sheng M (1999) Microtubule binding by CRIPT and its potential role in the synaptic clustering of PSD-95. Nat Neurosci 2:1063-1069.
Paul CM, Magda G, Abel S (2009) Spatial memory: Theoretical basis and comparative review on experimental methods in rodents. Behav Brain Res 203:151-164.
Pearce JM, Roberts AD, Good M (1998) Hippocampal lesions disrupt navigation based on cognitive maps but not heading vectors. Nature 396:75-77.
Pelkey KA, Askalan R, Paul S, Kalia LV, Nguyen TH, Pitcher GM, Salter MW, Lombroso PJ (2002) Tyrosine phosphatase STEP is a tonic brake on induction of long-term potentiation. Neuron 34:127-138.
Prybylowski K, Chang K, Sans N, Kan L, Vicini S, Wenthold RJ (2005) The synaptic localization of NR2B-containing NMDA receptors is controlled by interactions with PDZ proteins and AP-2. Neuron 47:845-857.
Rapp PR, Gallagher M (1996) Preserved neuron number in the hippocampus of aged rats with spatial learning deficits. Proc Natl Acad Sci U S A 93:9926-9930.
Rauner C, Kohr G (2011) Triheteromeric NR1/NR2A/NR2B receptors constitute the major N-methyl-D-aspartate receptor population in adult hippocampal synapses. J Biol Chem 286:7558-7566.
Rendeiro C, Spencer JP, Vauzour D, Butler LT, Ellis JA, Williams CM (2009) The impact of flavonoids on spatial memory in rodents: from behaviour to underlying hippocampal mechanisms. Genes Nutr 4:251-270.
Rhodes MG (2004) Age-related differences in performance on the Wisconsin card sorting test: a meta-analytic review. Psychol Aging 19:482-494.
Riedel G, Micheau J, Lam AG, Roloff EL, Martin SJ, Bridge H, de Hoz L, Poeschel B, McCulloch J, Morris RG (1999) Reversible neural inactivation reveals hippocampal participation in several memory processes. Nat Neurosci 2:898-905.
Roche KW, Standley S, McCallum J, Dune Ly C, Ehlers MD, Wenthold RJ (2001) Molecular determinants of NMDA receptor internalization. Nat Neurosci 4:794-802.
Rodrigues SM, Schafe GE, LeDoux JE (2001) Intra-amygdala blockade of the NR2B subunit of the NMDA receptor disrupts the acquisition but not the expression of fear conditioning. J Neurosci 21:6889-6896.
Rowe WB, Blalock EM, Chen KC, Kadish I, Wang D, Barrett JE, Thibault O, Porter NM, Rose GM, Landfield PW (2007) Hippocampal expression analyses reveal selective association of immediate-early, neuroenergetic, and myelinogenic pathways with cognitive impairment in aged rats. J Neurosci 27:3098-3110.

Sanz-Clemente A, Matta JA, Isaac JT, Roche KW (2010) Casein kinase 2 regulates the NR2 subunit composition of synaptic NMDA receptors. Neuron 67:984-996.
Sanz-Clemente A, Gray JA, Ogilvie KA, Nicoll RA, Roche KW (2013) Activated CaMKII couples GluN2B and casein kinase 2 to control synaptic NMDA receptors. Cell Rep 3:607-614.
Sato I, Obata Y, Kasahara K, Nakayama Y, Fukumoto Y, Yamasaki T, Yokoyama KK, Saito T, Yamaguchi N (2009) Differential trafficking of Src, Lyn, Yes and Fyn is specified by the state of palmitoylation in the SH4 domain. J Cell Sci 122:965-975.
Scherr PA, Albert MS, Funkenstein HH, Cook NR, Hennekens CH, Branch LG, White LR, Taylor JO, Evans DA (1988) Correlates of cognitive function in an elderly community population. Am J Epidemiol 128:1084-1101.
Scheuer K, Stoll S, Paschke U, Weigel R, Muller WE (1995) N-methyl-D-aspartate receptor density and membrane fluidity as possible determinants of the decline of passive avoidance performance in aging. Pharmacol Biochem Behav 50:65-70.
Schwenk RW, Holloway GP, Luiken JJ, Bonen A, Glatz JF (2010) Fatty acid transport across the cell membrane: regulation by fatty acid transporters. Prostaglandins Leukot Essent Fatty Acids 82:149-154.
Sharma S, Rakoczy S, Brown-Borg H (2010) Assessment of spatial memory in mice. Life Sci 87:521-536.
Shi L, Adams MM, Linville MC, Newton IG, Forbes ME, Long AB, Riddle DR, Brunso-Bechtold JK (2007) Caloric restriction eliminates the aging-related decline in NMDA and AMPA receptor subunits in the rat hippocampus and induces homeostasis. Exp Neurol 206:70-79.
Singh-Manoux A, Kivimaki M, Glymour MM, Elbaz A, Berr C, Ebmeier KP, Ferrie JE, Dugravot A (2012) Timing of onset of cognitive decline: results from Whitehall II prospective cohort study. BMJ 344:d7622.
Snyder EM, Nong Y, Almeida CG, Paul S, Moran T, Choi EY, Nairn AC, Salter MW, Lombroso PJ, Gouras GK, Greengard P (2005) Regulation of NMDA receptor trafficking by amyloid-beta. Nat Neurosci 8:1051-1058.
Sonntag WE, Bennett SA, Khan AS, Thornton PL, Xu X, Ingram RL, Brunso-Bechtold JK (2000) Age and insulin-like growth factor-1 modulate N-methyl-D-aspartate receptor subtype expression in rats. Brain Res Bull 51:331-338.
Spencer JP (2010) The impact of fruit flavonoids on memory and cognition. Br J Nutr 104 Suppl 3:S40-47.
Spencer WD, Raz N (1995) Differential effects of aging on memory for content and context: a meta-analysis. Psychol Aging 10:527-539.
Stephenson FA, Cousins SL, Kenny AV (2008) Assembly and forward trafficking of NMDA receptors (Review). Mol Membr Biol 25:311-320.
Stevens JF, Page JE (2004) Xanthohumol and related prenylflavonoids from hops and beer: to your good health! Phytochemistry 65:1317-1330.
Stiffler MA, Grantcharova VP, Sevecka M, MacBeath G (2006) Uncovering quantitative protein interaction networks for mouse PDZ domains using protein microarrays. J Am Chem Soc 128:5913-5922.
Strack S, McNeill RB, Colbran RJ (2000) Mechanism and regulation of calcium/calmodulin-dependent protein kinase II targeting to the NR2B subunit of the N-methyl-D-aspartate receptor. J Biol Chem 275:23798-23806.
Tang YP, Shimizu E, Dube GR, Rampon C, Kerchner GA, Zhuo M, Liu G, Tsien JZ (1999) Genetic enhancement of learning and memory in mice. Nature 401:63-69.

Tchkonia T, Morbeck DE, Von Zglinicki T, Van Deursen J, Lustgarten J, Scrable H, Khosla S, Jensen MD, Kirkland JL (2010) Fat tissue, aging, and cellular senescence. Aging Cell 9:667-684.

Terracina L, Brunetti M, Avellini L, De Medio GE, Trovarelli G, Gaiti A (1992) Arachidonic and palmitic acid utilization in aged rat brain areas. Mol Cell Biochem 115:35-42.

Tezuka T, Umemori H, Akiyama T, Nakanishi S, Yamamoto T (1999) PSD-95 promotes Fyn-mediated tyrosine phosphorylation of the N-methyl-D-aspartate receptor subunit NR2A. Proc Natl Acad Sci U S A 96:435-440.

Topinka JR, Bredt DS (1998) N-terminal palmitoylation of PSD-95 regulates association with cell membranes and interaction with K+ channel Kv1.4. Neuron 20:125-134.

Tovar KR, McGinley MJ, Westbrook GL (2013) Triheteromeric NMDA receptors at hippocampal synapses. J Neurosci 33:9150-9160.

Trepanier CH, Jackson MF, MacDonald JF (2012) Regulation of NMDA receptors by the tyrosine kinase Fyn. FEBS J 279:12-19.

Turner DA, Deupree DL (1991) Functional elongation of CA1 hippocampal neurons with aging in Fischer 344 rats. Neurobiol Aging 12:201-210.

Uttal DH (1996) Angles and distances: children's and adults' reconstruction and scaling of spatial configurations. Child Dev 67:2763-2779.

Uttal DH, Fisher JA, Taylor HA (2006) Words and maps: developmental changes in mental models of spatial information acquired from descriptions and depictions. Dev Sci 9:221-235.

Van Horn CG, Caviglia JM, Li LO, Wang S, Granger DA, Coleman RA (2005) Characterization of recombinant long-chain rat acyl-CoA synthetase isoforms 3 and 6: identification of a novel variant of isoform 6. Biochemistry 44:1635-1642.

VanGuilder HD, Yan H, Farley JA, Sonntag WE, Freeman WM (2010) Aging alters the expression of neurotransmission-regulating proteins in the hippocampal synaptoproteome. J Neurochem 113:1577-1588.

VanGuilder HD, Farley JA, Yan H, Van Kirk CA, Mitschelen M, Sonntag WE, Freeman WM (2011) Hippocampal dysregulation of synaptic plasticity-associated proteins with age-related cognitive decline. Neurobiol Dis 43:201-212.

Vartak N, Papke B, Grecco HE, Rossmannek L, Waldmann H, Hedberg C, Bastiaens PI (2014) The autodepalmitoylating activity of APT maintains the spatial organization of palmitoylated membrane proteins. Biophys J 106:93-105.

Venkitaramani DV, Moura PJ, Picciotto MR, Lombroso PJ (2011) Striatal-enriched protein tyrosine phosphatase (STEP) knockout mice have enhanced hippocampal memory. Eur J Neurosci 33:2288-2298.

Vitureira N, Goda Y (2013) Cell biology in neuroscience: the interplay between Hebbian and homeostatic synaptic plasticity. J Cell Biol 203:175-186.

Wan J, Roth AF, Bailey AO, Davis NG (2007) Palmitoylated proteins: purification and identification. Nat Protoc 2:1573-1584.

Wang D, Cui Z, Zeng Q, Kuang H, Wang LP, Tsien JZ, Cao X (2009) Genetic enhancement of memory and long-term potentiation but not CA1 long-term depression in NR2B transgenic rats. PLoS One 4:e7486.

Washbourne P, Bennett JE, McAllister AK (2002) Rapid recruitment of NMDA receptor transport packets to nascent synapses. Nat Neurosci 5:751-759.

Watts AS, Loskutova N, Burns JM, Johnson DK (2013) Metabolic syndrome and cognitive decline in early Alzheimer's disease and healthy older adults. J Alzheimers Dis 35:253-265.

West MJ, Coleman PD, Flood DG, Troncoso JC (1994) Differences in the pattern of hippocampal neuronal loss in normal ageing and Alzheimer's disease. Lancet 344:769-772.

Wu HY, Lynch DR (2006) Calpain and synaptic function. Mol Neurobiol 33:215-236.

Wu HY, Hsu FC, Gleichman AJ, Baconguis I, Coulter DA, Lynch DR (2007) Fyn-mediated phosphorylation of NR2B Tyr-1336 controls calpain-mediated NR2B cleavage in neurons and heterologous systems. J Biol Chem 282:20075-20087.

Xiong XD, Chen GH (2010) Research progress on the age-related changes in proteins of the synaptic active zone. Physiol Behav 101:1-12.

Xu W (2011) PSD-95-like membrane associated guanylate kinases (PSD-MAGUKs) and synaptic plasticity. Curr Opin Neurobiol 21:306-312.

Xu W, Schluter OM, Steiner P, Czervionke BL, Sabatini B, Malenka RC (2008) Molecular dissociation of the role of PSD-95 in regulating synaptic strength and LTD. Neuron 57:248-262.

Yashiro K, Philpot BD (2008) Regulation of NMDA receptor subunit expression and its implications for LTD, LTP, and metaplasticity. Neuropharmacology 55:1081-1094.

Yen TL, Hsu CK, Lu WJ, Hsieh CY, Hsiao G, Chou DS, Wu GJ, Sheu JR (2012) Neuroprotective effects of xanthohumol, a prenylated flavonoid from hops (Humulus lupulus), in ischemic stroke of rats. J Agric Food Chem 60:1937-1944.

Yetimler B, Ulusoy G, Celik T, Jakubowska-Dogru E (2012) Differential effect of age on the brain fatty acid levels and their correlation with animal cognitive status in mice. Pharmacol Biochem Behav 103:53-59.

Yi Z, Petralia RS, Fu Z, Swanwick CC, Wang YX, Prybylowski K, Sans N, Vicini S, Wenthold RJ (2007) The role of the PDZ protein GIPC in regulating NMDA receptor trafficking. J Neurosci 27:11663-11675.

Zamzow DR, C.M. D, D.B. J, K.R. M, (2012) The palmitoylation state of NMDA receptor-associated proteins in the aged mouse brain. In: Society for Neuroscience Meeting. New Orleans.

Zamzow DR, Elias V, Shumaker M, Larson C, Magnusson KR (2013) An increase in the association of GluN2B containing NMDA receptors with membrane scaffolding proteins was related to memory declines during aging. J Neurosci 33:12300-12305.

Zehethofer N, Pinto DM, Volmer DA (2008) Plasma free fatty acid profiling in a fish oil human intervention study using ultra-performance liquid chromatography/electrospray ionization tandem mass spectrometry. Rapid Commun Mass Spectrom 22:2125-2133.

Zeng S, Tai F, Zhai P, Yuan A, Jia R, Zhang X (2010) Effect of daidzein on anxiety, social behavior and spatial learning in male Balb/cJ mice. Pharmacol Biochem Behav 96:16-23.

Zhang J, Petit CM, King DS, Lee AL (2011) Phosphorylation of a PDZ domain extension modulates binding affinity and interdomain interactions in postsynaptic density-95 (PSD-95) protein, a membrane-associated guanylate kinase (MAGUK). J Biol Chem 286:41776-41785.

Zhao MG, Toyoda H, Lee YS, Wu LJ, Ko SW, Zhang XH, Jia Y, Shum F, Xu H, Li BM, Kaang BK, Zhuo M (2005) Roles of NMDA NR2B subtype receptor in prefrontal long-term potentiation and contextual fear memory. Neuron 47:859-872.

Zhao X, Rosenke R, Kronemann D, Brim B, Das SR, Dunah AW, Magnusson KR (2009) The effects of aging on N-methyl-D-aspartate receptor subunits in the synaptic membrane and relationships to long-term spatial memory. Neuroscience 162:933-945.

Zheng CY, Seabold GK, Horak M, Petralia RS (2011) MAGUKs, synaptic development, and synaptic plasticity. Neuroscientist 17:493-512.